

Comparison of the *in vitro* effect of two-dimensional and three-dimensional polycaprolactone polymers on cell morphology, viability and cytotoxicity

by

Tenille Steynberg

21176851

Submitted in fulfillment of part of the requirements for the degree

Masters of Science (Physiology)

in the Faculty of Health Sciences

University of Pretoria

Feb 2010

Collaboration:

Biosciences and Materials Science and Manufacturing (MSM), Divisions
of the Council for Scientific and Industrial Research (CSIR)

Supervisor: Prof AM Joubert

Co-supervisor: Dr A Idicula

Summary

Engineered tissue arrives from applying both life sciences and engineering. Polymers which illustrate both biocompatibility and resorbability, such as polycaprolactone (PCL), are particularly attractive. The aim was to assess cytocompatibility on both two-dimensional (2D) PCL disks and three-dimensional (3D) PCL solid and PCL hollow microspheres using human uterine mixed leiomyosarcoma (SKUT-1) and hamster ductus deferens leiomyosarcoma (CRL-1701) cell lines. The possibility of PCL cytotoxicity, and whether pre-conditioning the samples with DMEM + 10% FCS would improve cell attachment were investigated. Cellular morphology and changes in cell cycle progression were analysed during time intervals of 24 h, 72 h and 5 days. A metabolic assay assessed cytotoxicity of the following extracts: i) control medium, ii) PCL disk medium extract and iii) PCL microsphere extracts during the time frames of 24 h, 72 h, 5 day, 1 month and 1 year. SKUT cells cultured in disk and microsphere extracts between the 24 h and 5 day time periods displayed statistically increased metabolic activity, though this activity decreased significantly on the 1 month and 1 year extracts. The CRL-1701 cells displayed metabolic activities comparable to the controls when cultured on the 24 h to 5 day extracts, activity increased significantly on the 1 month extracts and decreased significantly on the 1 year extracts. Scanning electron microscopy illustrated an increase in cell density when cells were allowed to attach on the pre-conditioned disks. After 5 days, cells showed spindle-shaped morphologies, closely following the contours of the microspheres, indicative of high focal adhesion. Both cell lines migrated inside the hollow microspheres, indicating that they may benefit from the sheltered environment. SKUT cell cycle on the microspheres illustrated a G₁/0 block at 72 h and recovered after 5 days. The CRL-1701 cells remained in G₁/0 block throughout the 5 day culture period. This block could indicate a senescent phenotype, which could elude towards cellular migration and potential contractile abilities. This *in vitro* study suggests that hollow microspheres allow for further cell expansion with a sheltered environment to protect cells from sheer stress experienced *in vivo*.

Keywords: Polymers, polycaprolactone, cytotoxicity, microspheres, morphologies, phenotype

Acknowledgements

I dedicate this dissertation to my family, for their constant support, love and encouragement. Thank you for always being able to make me laugh when I least expected it!

My heartfelt thanks to the following people:

- Professor Annie Joubert, my supervisor, for her patience, words of wisdom and professional support. I thank her for funding my project's cell culture maintenance and experimental work.
- Dr Anu Idicula, my co-supervisor, for a different perspective on things and for her unwavering support.
- The CSIR – Sean Moolman, for arranging financial support both for the experimental work and for my personal use; Avashnee Chetty for her valuable advice; Wim Richter for sharing and expanding polymer concepts; Kersch Naidoo and Kim Easton for the development of the polymers.
- Professor Dirk van Papendorp, head of the Department of Physiology, for allowing me to make use of the facilities of the department.
- Allan and Chris at the Microscopy unit of Pretoria University, for their enthusiastic assistance.

I hereby acknowledge with thanks to the financial help (bursary) from the CSIR for the duration of my studies. Information in the publications and any conclusions which have been drawn are those of the researcher alone and are not necessarily of the CSIR.

Table of Contents

Summary	i
Acknowledgements	ii
List of Figures	viii
List of Tables	x
List of Abbreviations	xi
Graphical representations of Schemes	
Chapter 1	1
Literature Review	1
1.1 Tissue engineering.....	1
1.1.1 Roles of cells in tissue engineering.....	1
1.1.2 Role of growth factors in tissue engineering.....	2
1.2 Polymers in tissue engineering.....	5
1.2.1 Non-degradable and non-resorbable polymers.....	5
1.2.2 Biodegradable and resorbable polymers	5
1.2.2.1a: PCL.....	6
1.2.2.1b: PCL applications.....	6
1.2.3 Cytotoxicity assessment of these polymers.....	7
1.2.4 Viability of cells on polymer scaffolds.....	8
1.3 The ECM.....	9
1.4 Smooth muscle cell (SMC) regeneration.....	12
1.4.1 The function of SMCs.....	12
1.4.2 The structure of SMCs	12
1.4.3 The need for SMC regeneration	14
1.5 The pathogenesis of GERD.....	14
1.5.1 Causes of GERD.....	14
1.5.2 Symptoms of GERD	15
1.5.3 Barrett’s esophagus (BE)	16
1.5.4 Current treatments of GERD.....	17
1.5.4.1 Complimentary lifestyle modifications.....	17
1.5.4.2 First line treatment	18
1.5.4.2a Antacids as a first line treatment of GERD	18
1.5.4.2b Foaming agents as a first line treatment of GERD	18
1.5.4.2c Histamine ₂ (H ₂) blockers as a first line treatment of GERD	18
1.5.4.2d Proton pump inhibitors (PPIs) as a first line treatment of GERD.....	19
1.5.4.3 Surgical interventions.....	19
1.5.4.3a Endoscopic suturing	19
1.5.4.3b Fundoplication	20

1.5.4.4	Implantation procedures as intervention in GERD	20
1.5.4.4a	Hydrogels	20
1.5.4.4b	Microstimulator implants.....	20
1.6	The investigative route for tissue engineering applications.....	21
1.6.1	2D models and 3D models for <i>in vitro</i> analysis of tissue engineering applications	21
1.6.1.1	Hydrogels as 3D models for cell growth.....	21
1.6.1.2	3D polymer models	21
1.6.2	Cell culturing methods to emulate tissue formation	22
1.6.2.1	Static versus dynamic cell culturing techniques	22
1.6.3	<i>In vitro</i> investigation of cancerous SMCs cultured on 2D and 3D PCL polymers.....	23
1.6.3.1	Cell line selection.....	23
1.6.3.2	Investigation of the effect of PCL polymers on the cell lines	24
1.6.4	Rationale for <i>in vitro</i> investigation	25
1.7	Aim	25
1.8	Risks/problems associated with the intended investigative route	26
1.8.1	Cell line related problems	26
1.8.2	Risks of predicting the <i>in vitro</i> investigation effects to <i>in vivo</i> tissue engineering.....	26
Chapter 2	28
Materials and Methods	28
2.1	Materials.....	28
2.1.1	Cell lines.....	28
2.1.2	PCL polymers	28
2.1.2.a:	2D model	28
2.1.2. b:	3D model	28
2.1.3	Other reagents.....	29
2.2	Methods.....	29
2.2.1	General cell culture maintenance.....	29
2.2.2	General experimental setup	30
2.3	Analytical experimental protocols.....	31
2.3.1	Cytotoxicity studies	31
2.3.1.1	Pre-incubation of polymer:	31
2.1.2.2	Extraction of pre-incubated medium:.....	32
2.3.2	Cell viability assessment of cells grown on degradation extracts	32
2.3.2.1	Cell viability assessment by assessing metabolic activity using the MTT assay	32
2.3.2.1a	Principle of the assay	32

2.3.2.1b Materials	33
2.3.2.1c Methods	33
2.3.2.2 Cell viability assessment using the PI/HO assay	33
2.3.2.2a Principle of the assay	33
2.3.2.2b Materials	34
2.3.2.2c Methods	34
2.3.3 Cell attachment studies	35
2.3.3.1 Cell attachment density assessment using Scanning Electron Microscopy (SEM).....	35
2.3.3.1a Principle of method	35
2.3.3.1b Materials	35
2.3.3.1c Methods	35
2.3.4 Cell cycle analysis	36
2.3.4.1 Cell cycle analysis using flow cytometry	36
2.3.4.1a Principle of method	36
2.3.4.1b Materials	37
2.3.4.1c Method.....	37
2.3.4.2 Determination of cells in S-phase using Click-iT™ EdU flow cytometry kit	37
2.3.4.2a Principle of method	37
2.3.4.2b Materials	38
2.3.4.2c Methods	38
2.3.5 Assessment of cell attachment characteristics.....	39
2.3.5.1 Assessment of cell morphology using SEM.....	39
2.3.5.1a Principle of the method.....	39
2.3.5.1b Materials	39
2.3.5.2 Assessment of cell cytoskeleton using the phalloidin staining technique.....	40
2.3.5.2a Principle of the staining technique	40
2.3.5.2b Materials	40
2.3.5.2c Method.....	40
2.3.6 Assessment of cells grown on PCL models in 3D format using confocal microscopy	41
2.3.6.1a Principle of the method.....	41
2.3.6.1b Microscope and materials	41
2.3.6.1c Method.....	42
2.3.7 Statistics	42

Chapter 3.....43

Results43

3.1 Determination of the effect of PCL degradation extracts by assessing cell viability	43
3.1.1 Assessment of cell viability by the determination of metabolic activity using the quantitative MTT assay	43
3.1.2 pH assessment of degradation extracts	45

3.1.3 Assessment of cell viability by the determination of membrane integrity using the qualitative PI/HO assay	46
3.2 The benefits of pre-conditioning PCL polymers for 24 hrs in complete medium ..	50
3.2.1 Qualitative SEM data of SKUT and CL-1701 cells grown on PCL disks which were pre-conditioned in PBS, partial medium and complete medium	50
3.3 Analysis of the cell cycle	53
3.3.1 Determination of the cell cycle characteristics of SKUT and CRL-1701 cell lines when grown in a time dependant manner on the PCL polymer using Flow cytometry	53
3.3.1a SKUT cell cycle progression	53
3.3.1b CRL-1701 cell cycle progression	54
3.3.2 Quantitative analysis of SKUT and CRL-1701 cells within the S phase of the cell cycle after 5 days in culture on the PCL polymer.....	61
3.4 Studies to assess the cell morphology of SKUT and CRL-1701 cells grown on 2D and 3D models of the PCL polymer	64
3.4.1 Cell morphology, attachment, and growth characteristics using SEM.....	64
3.4.2 Studies to determine the morphology of the cells grown on 2D and 3D PCL models as determined by Phalloidin staining.....	72
3.5 The assessment of SKUT and CRL-1701 grown for 5 days on the 2D 3D PCL models using confocal microscopy	74
3.5.1 Illustration of the SKUT and CRL-1701 cells grown for 5 days on the control and PCL disk surfaces	74
3.5.2 3D video images of the SKUT and CRL-1701 cells grown for 5 days on the PCL solid microspheres and the PCL ported microspheres.....	78
Chapter 4.....	80
Discussion	80
Chapter 5.....	87
Conclusion	87
References	88

List of figures

Figure 1: Schematic diagram illustrating the process of tissue engineering.....	4
Figure 2: Survival of the anchorage dependent cells relies on a high degree of focal adhesion to a substrate.....	10
Figure 3: The aetiology of Barrett's Esophagus.....	17
Figure 3.1.1: SKUT cell metabolic activities when cultured for 24 hrs on PCL degradation extracts.....	44
Figure 3.1.2: CRL-1701 cell metabolic activities when cultured for 24 hrs on PCL degradation extracts.....	45
Figure 3.1.3.1: PI/HO fluorescent staining illustrating cell viability and phases in the cell cycle of SKUT cells.....	48
Figure 3.1.3.2: PI/HO fluorescent staining illustrating cell viability and phase in the cell cycle of the CRL-1701 cells.....	49
Figure 3.2.1.1: Qualitative SEM micrographs illustrating SKUT cells attached for 24 hrs on PCL disk surface.....	51
Figure 3.2.1.2: Qualitative SEM micrographs illustrating CRL-1701 cells attached for 24 hrs on PCL disk surface.....	52
Figure 3.3.1.1: Flow cytometric analysis illustrating percentage of SKUT cells cycling through the G ₀ /1, S and G ₂ /M phases of the cell cycle after 24 hrs proliferation.....	56
Figure 3.3.1.2: Flow cytometric analysis illustrating percentage of SKUT cells cycling through the G ₀ /1, S and G ₂ /M phases of the cell cycle after 72 hrs proliferation.....	57
Figure 3.3.1.3: Flow cytometric analysis illustrating percentage of SKUT cells cycling through the G ₀ /1, S and G ₂ /M phases of the cell cycle after 5 days proliferation.....	58
Figure 3.3.1.4.: Flow cytometric analysis illustrating percentage of CRL-1701 cells after 24 hrs cycling through the G ₀ /1, S and G ₂ /M phases of the cell cycle.....	59
Figure 3.3.1.5: Flow cytometric analysis illustrating percentage of CRL-1701 cells after 72 hrs cycling through the G ₀ /1, S and G ₂ /M phases of the cell cycle.....	60

Figure 3.3.1.6: Flow cytometric analysis illustrating percentage of CRL-1701 cells cycling for 5 days through the G ₀ /1, S and G ₂ /M phases of the cell cycle.....	61
Figure 3.3.2.1: Flow cytometric analysis illustrating the incorporation of BrdU into the S phase of the SKUT cells after 5 days of proliferation.....	62
Figure 3.3.2.2: Flow cytometric analysis illustrating the incorporation of BrdU into the S phase of the CRL-1701 cells after 5 days proliferation.....	63
Figure 3.4.1.1: SEM micrographs illustrating SKUT cells attached for 24 hr, 72 hr, and 5 days on the 2D and 3D PCL models.....	68
Figure 3.4.1.2: SEM micrographs illustrating the CRL-1701 cells attached for 24 hr, 72 hr, and 5 days on the 2D and 3D PCL models.....	71
Figure 3.4.2.1: Fluorescent micrographs illustrating SKUT cells stained with phalloidin specific for the α -actin component of the SMC cytoskeleton.....	73
Figure 3.4.2.2: Fluorescent micrographs illustrating CRL-1701 cells stained with phalloidin specific for the α -actin component of the SMC cytoskeleton.....	73
Figure 3.5.1.1a: Confocal image of SKUT cells after being allowed to proliferate on the TCP control for 5 days.....	75
Figure 3.5.1.1b: Confocal image of SKUT cells after being allowed to proliferate on the PCL disk for 5 days.....	76
Figure 3.5.1.2a: Confocal image of CRL-1701 after being allowed to proliferate on the TCP control for 5 days.....	77
Figure 3.5.1.2b: Confocal image of CRL-1701 after being allowed to proliferate on the PCL disk for 5 days.....	78
Figure 3.5.2.1a 3D confocal image video of the SKUT cells grown for 5 days on PCL solid microspheres.....	(CD) 79
Figure 3.5.2.1b 3D confocal image video of the SKUT cells grown for 5 days on PCL ported microspheres.....	(CD) 79
Figure 3.5.2.2a 3D confocal image video of the CRL-1701 cells grown for 5 days on PCL solid microspheres.....	(CD) 79
Figure 3.5.2.2b 3D confocal image video of the CRL-1701 cells grown for 5 days on PCL ported microspheres.....	(CD) 79

List of tables

Table 1: Small cells with no focal adhesions have a low survival rate.....	11
Table 2: List of physiological and lifestyle practices resulting in symptoms of GERD.....	15
Table 3.1.2: pH determinations of control medium and PCL disk and microsphere extracts.....	46

List of abbreviations

°	Degree
μ	Mircro
AR-S	Alizarin Red-S
ATCC	American Tissue Culture Collection
ATP	Adenosine triphosphate
ATPase	Adenosine triphosphosphate-phosphatase
BE	Barrett's esophagus
BMP-7	Bone morphogenetic protein-7
BSA	Bovine serum albumin
BSP	Bone sialoprotein
C	Celsius
CAPA	Caprolactone
Cdfa 1	Core binding factor a1
CDK	Cyclin Dependent Kinases
CKI	Cyclin-dependent kinase inhibitor
CO2	Carbon dioxide
Coll 1	Type 1 collagen
COX-2	Cyclo-oxygenase-2
CRL-1701	Syrian hamster ductus deferens leiomyosarcoma cell line
CSIR	Council for Scientific and Industrial Research
CV	Crystal violet
2D	Two-dimentional
3D	Three-dimensional
DCM	Dichloromethane
D-MEM	Dulbecco's minimum essential medium eagle
DMSO	Dimethyl sulfoxide
DNA	Deoxyribonucleic acid
ECs	Endothelial cells
ECM	Extracellular matrix
EDTA	Ethylenediaminetetraacetic acid
EdU	5-ethyl-2'-deoxyuridine
ELISA	Enzyme-Linked ImmunoSorbent Assay

ERD	Erosive reflux disease
F	Filamentous
FAs	Focal adhesions
FCS	Fetal calf serum
FITC	Fluorescein isothiocyanate
FGF	Fibroblast growth factor
G	Globular
GI	Gastrointestinal
GER	Gastroesophageal reflux
GERD	Gastroesophageal reflux disease
H ₂	Histamine ₂
H&E	Haematoxylin and Eosin
HB-EGF	Heparin binding epidermal growth factor like growth factor
HeNe	Helium Neon
HEPES	4-(2-hydroxyethyl)-1-piperazineethanesulfonic acid
HGF	Hepatocyte growth factor
HO	Hoechst
IGF-1	Insulin-like growth factor-1
IMS	Implantable microstimulators
LES	Lower esophageal sphincter
M	Meter
Mm	Milimeter
mmHg	Milimeter Mercury
MSM	Materials Science and Manufacturing
MTT	3-(4, 5-Dimethylthiazol-2-yl)-2, 5-diphenyltetrazolium bromide
nm	Nanometer
NaOH	Sodium hydroxide
NERD	Nonerosive or negative-endoscopy reflux disease
OC	Osteocalcin
OP	Osteopontin
PBS	Phosphate buffered saline
PCL	Poly (L-lactide- <i>co</i> -caprolactone)
PDGF-BB	Platelet-derived growth factor-BB
PE	Polyethylene

PGA	Polyglycolic acid
PI	Propidium iodide
PLAGA	Poly (lactide-co-glycolide)
PLCL	Poly (lactide-co- ϵ -caprolactone)
PLGA	Poly (DL-lactic-co-glycolic acid)
PLLA	Poly- L-lactide acid
PPIs	Proton pump inhibitors
pRb	Retinoblastoma
PVA	Poly vinyl alcohol
RGD	Arginine-glycine-aspartate
RNA	Ribonucleic acid
rpm	Rotations per minute
SEM	Scanning electron microscopy
Si-HPMC	Silated hydroxypropylmethylcellulose
SMCs	Smooth muscle cells
SKUT-1	Human uterine mixed leiomyosarcoma cell line
TCA	Tricarboxylic acid
TCP	Tissue culture plate
TEM	Transmission electron microscopy
TNF	Tumor necrosis factor
TNF α	Tumor necrosis factor alpha
Tris	Hydroxymethylaminomethane
UV	Ultraviolet
VEGF	Vascular endothelial growth factor
VSM	Vascular smooth muscle
VSMCs	Vascular smooth muscle cells
WST-1	4-[3-(4-Iodophenyl)-2-(4-nitrophenol) 2H-5-tetrazolo]-1, 3-benzene disulfonate
Wt	Wild type

Graphical representations of Schemes

Graphics were compiled using Word shapes and tables.
Confocal images are played using Word Media Player.

Chapter 1

Literature Review

1.1 Tissue engineering

Every year, over 8 million surgical procedures are performed annually in the United States to treat the millions of Americans who experience organ failure or tissue loss. During 1996, only 20,000 donor organs were available for 50,000 patients in need [1].

The Tissue Engineering Society was founded by Drs. Charles and Joseph Vacanti in Boston Massachusetts in 1994. Dr. Charles Vacanti defined tissue engineering as ‘a science devoted to the generation of new tissue by employing the principles of engineering in combination with the application of certain biologic principles’ [2]. It is the science of replacing or bulking of damaged or diseased tissue and requires the use of cells, growth factors, and biomaterials individually or in combination to regenerate or replace lost tissue [3]. This science affords great potential for providing living tissue replacement and promises to minimize reliance on the appropriate donor constituents [4]. In other words, tissue engineering ultimately aims to produce functional tissue substitutes by combining biologically active cells with suitable artificial materials [5].

Human tissue from human donors cannot meet the increasing demands for repair and renewal of worn out or injured tissue. Alternatives exist in using related living and trans-species transplantation. However, problems such as disease transfer and ethical dilemmas accompany these options. Tissue engineering provides a new option that aims to meet these increasing demands by utilizing novel cell culture methods *in vitro* to ultimately provide tissue replacements *in vivo* [6].

1.1.1 Roles of cells in tissue engineering

When aiming to produce tissue, the cell type one chooses becomes crucial as they need to be effective when cultured *in vitro* and must be able to withstand an initially hypoxic environment when implanted [2]. The cells used in tissue engineering may be one of the

following: autologous, allogeneic, or xenogeneic. Autologous cells are obtained from the specific individual into whom they will later be reimplanted. This approach avoids the issues of immunogenicity/rejection and transmission of disease. Such autologous cells however pose the limitation of harvest or donation in advance of need, together with following *in vitro* culture expansion, imparting both technical and time constraints [6]. Allogeneic cells originate from an individual of the same species but are other than the recipient, such as cadaveric organ transplantation and human blood transfusions [6]. Xenogeneic cells are derived from a species different to that of the recipient. Both allogeneic and xenogeneic cells preserve the potential advantage of being cultured and constructed in advance of need, their use however raise important issues of disease transmission, immunogenicity and ethical concerns [6].

Most mature cells have a limited capacity to multiply *in vitro*. Some adult stem cells may be pluripotent or ‘committed’ to following a predetermined cellular heritage, whilst all embryonic stem cells however retain the potential to develop into different cell types under the correct conditions [6]. Embryonic stem cells by definition are pluripotent and thus have a greater potential to generate healthier tissue as their potential to differentiate into any cell type is possible when exposed to appropriate growth factors, although this has not been proven conclusively [2].

1.1.2 Role of growth factors in tissue engineering

With the use of various growth factors it is possible to increase the viability and rate of cell growth [7]. The factors are also able to attract specific types of cells to be recruited to the area in the body exposed to the appropriate growth factors. Most phenomenally, growth factors are able to transform one cell type into another [7]. Growth factors have been successfully delivered to specific sites *in vivo* by incorporating them into scaffolds. When using these scaffolds as growth factor delivery systems, growth factors can be incorporated and released in a sustained manner [7]. Growth factors can significantly enhance the chances of new tissue formation.

1.1.3 Role of scaffolds in tissue engineering

Non-load bearing scaffolds are required when replacing or bulking tissue in the body which do not support the body structure. Examples include epithelia, muscle and facial bone and cartilage such as the cheek, nose, and ears.

Load-bearing scaffolds are required when replacing support structures such as vertebrae and all bone tissue. Poly (DL-lactide)/bioglass composite left in phosphate-buffer saline (PBS) for 14 and 28 days formed visible hydroxyapatite domains, the main component of bone. Kazarian *et al.*, have speculated that poly (DL-lactide)/bioglass could be developed for bone tissue engineering scaffolds [8]. Cells derived from rabbit skeletal muscle have been found to differentiate into osteoblast-like cells when exposed to the Bone Morphogenetic Protein-7 (BMP-7) [9]. This was delivered *via* a poly (lactide-co-glycolide) (PLGA) matrix [9].

1.1.4 Scaffolds, cells and growth factors in tissue engineering for *in vivo* transplantation

Scaffolds are often used in order to deliver various growth factors and, thereby becoming protein matrices [9]. The delivery of vascular endothelial growth factor (VEGF) from a biodegradable poly (DL-lactic-co-glycolic acid) (PLGA) which is a copolymer of d,l-lactide and glycolide scaffold was found to enhance neovascularization and bone regeneration in irradiated osseous defects in the calvarium of Fisher rats [7]. Bone formed within VEGF included scaffolds was significantly higher than that within PLGA scaffolds. VEGF was incorporated into these scaffolds using a variation of the gas-foaming fabrication process [7].

The process of tissue engineering involves obtaining a biopsy (if possible) of the relevant tissue from the patient. This tissue is then processed in the lab in order to expand/increase cell number *in vitro*. The cells are either grown statically, as is the norm, or in dynamic rotating vessels. Once cell number is sufficient, the cells are seeded onto an appropriate scaffold where growth factors can be added in order to enhance cell attachment, proliferation, and differentiation. This cell/scaffold complex can either be re-implanted

into the patient immediately or be allowed to proliferate *in vitro* before re-implantation takes place (fig. 1).

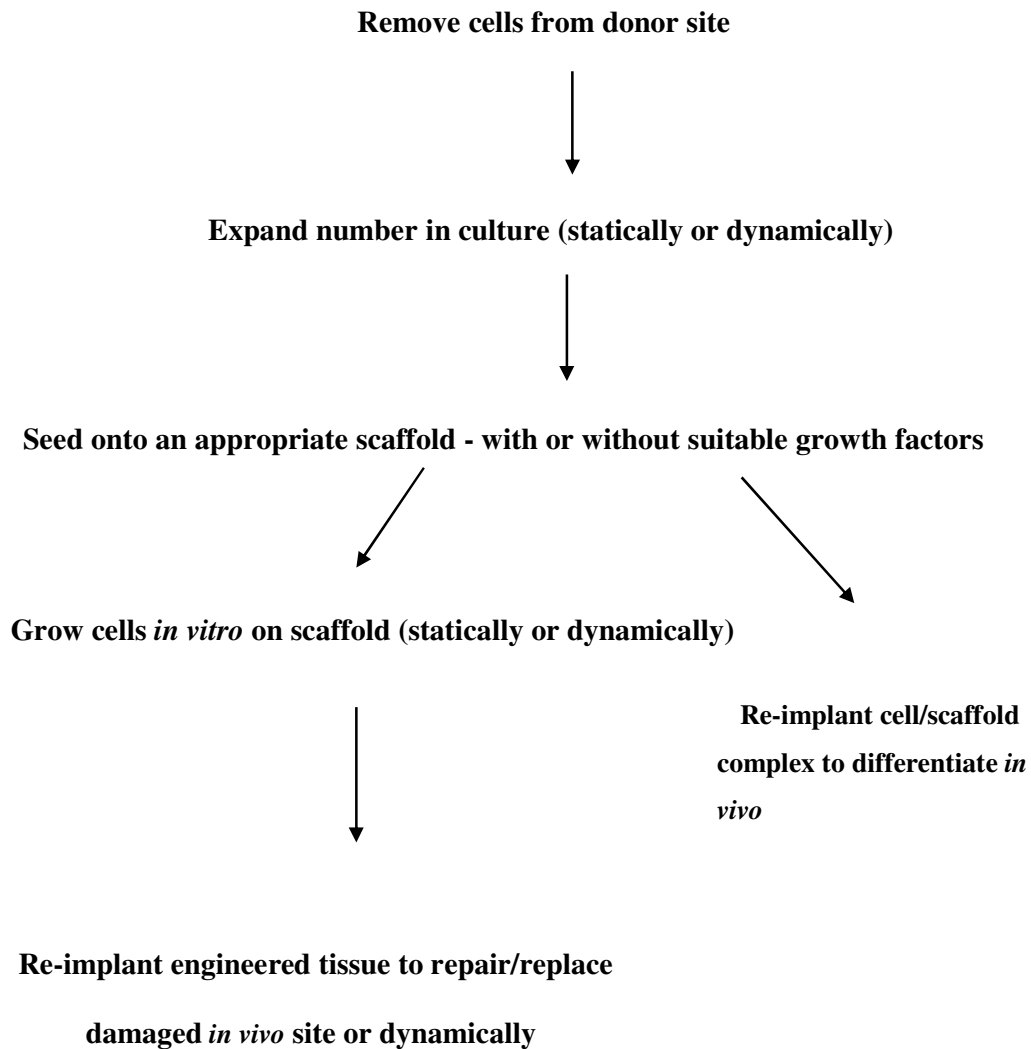


Figure 1: Schematic diagram illustrating the process of tissue engineering. The first step involves ideally harvesting a small number of cells from the patient by means of a biopsy. The cells are then cultured and expanded in numbers *in vitro*. These cells can then be grown within a three-dimensional natural or synthetic scaffold in the presence of appropriate growth (and differentiation) factors either within a static or dynamic environment. If the scaffold, growth factors, and growth conditions are ideal the cells create an actual living tissue that can be used as a replacement tissue to be implanted back into the defective/missing site in the patient. Scaffolds which in due course degrade help to prevent certain risks which can occur in the body with the long-term presence of any foreign material. Autologous cells would be the most suitable to use as this will prevent an immune rejection response to the implanted tissue.

1.2 Polymers in tissue engineering

Polymers used in tissue engineering require that they are biocompatible or evade the body's immune reaction. These polymers are called biomaterials and can act as three-dimensional (3D) scaffolds that enable cells to attach and configure into the required anatomical shape of the tissue [10]. The use of polymer scaffolds can greatly assist in providing a supportive environment for cellular attachment and proliferation and hence aid the regeneration of tissue or restore lost tissue function [10]. Synthetic biodegradable polymers generally offer several advantages over natural materials. These advantages include the ability to change the mechanical properties and degradation kinetics of the material to suit various applications [11]. The type of polymer chosen and its structural compositions play a key role in cellular invasion [4].

1.2.1 Non-degradable and non-resorbable polymers

These polymers are applied mainly when replacing structural tissues in the body that mimic those of cartilage and load-bearing bone. Regardless of the application, a scaffold becomes essential in cell growth, attachment, and tissue formation [10]. The scaffold provides support and a structural framework.

Hydrogels can both be used both within tissue engineering applications as well as growing cells *in vitro* within a 3D organization [12]. This is a widely used application in tissue engineering as natural hydrogels are easily obtainable. Examples include collagen, gelatine, fibrin, agarose and chitosan. However, there remains risk of infection in clinical applications along with batch variation [12].

1.2.2 Biodegradable and resorbable polymers

When a polymer breaks down into its monomeric constituents, it may be absorbed by the body. Such degradable polymers are called biodegradable or resorbable polymers [8]. The development of biodegradable and resorbable polymers is an attractive proposition as they provide a polymer scaffold that degrades with time. They break down into smaller fragments and as a result lose their structural strength [13]. The body's own cells are able to replace the polymer as it degrades. Whereby, the scaffolds assist and enhance the

body's natural healing process, and once a polymer has degraded, the degradation products that are resorbed into the body should optimally not result in harmful or toxic effects. Toxicity occurs when the solvents used to manufacture the polymers leach out as the polymer degrades. These solvents may alter the pH out of the physiological range. Examples of non-toxic polymers that resorb are poly (DL-lactide) [8], polyglycolic acid (PGA), poly- L-lactide acid (PLLA) [14], poly (3-hydroxybutyrate) [15], poly (glycolic acid) [11] and poly (L-lactide-co-caprolactone) (PCL) [16]. The resorbed polymer are non-toxic as the degradation products may be natural products normally found in the body such as lactic acid, as is the case of PLLA [14] and PCL [16] degradation.

1.2.2.1a: PCL

PCL is widely used as biodegradable polyester for medical applications because of its known biocompatibility and degradability [17]. The degradation product, lactic acid, can be metabolized by the body *via* the tricarboxylic acid (TCA) cycle [18]. Some reports suggest that this degradation product could cause an unsuitable microenvironment and may not be ideal for tissue growth due to the decrease in pH elicited by lactic acid levels rising [10]. However, as PCL's degradation rate spans over more than a year, it becomes ideal for applications where a long-term scaffold or support is needed [19]. The slow degradation rate may cause relatively small local pH changes; however, even a small decrease in pH can have a detrimental effect on the cells [14].

1.2.2.1b: PCL applications

PCL is widely used in orthopaedic applications and in dentistry as it exhibits structural capabilities compared to that of bone tissue [20]. Ideally, the scaffold should degrade as new bone matrix is formed and should exhibit the same mechanical and biological properties of its' natural counterpart [4].

Zhu *et al.* (2003) found the biodegradable membrane of PCL modified with fibronectin and collagen was able to support both epithelial and smooth muscle cells from porcine esophageal cultures [16]. This provides an example of how crucial a matrix is initially available to support cellular attachment, the shape of the tissue formed as well as how degradability enhances the chances of vascular formation to the new tissue. The ability to

form tissue consisting of both the smooth muscle and epithelial layers can ultimately be used in esophageal tissue applications [20].

Studies have shown implants of PCL microspheres to induce low neutrophil activation and inflammation during the early days after implantation. These negative effects disappeared after 3 months [21]. This suggests that PCL elicits only a low grade immune response and implicates PCL as a highly biocompatible long-term polymer implant. Hutmacher *et al.* (2003) found 4.5 month-old PCL implants within pig and rabbit models formed thin capsules of fibrous tissue. There was however only a minimal fibrotic reaction with promising vascular network formation. Along with these findings it was also discovered that the PCL scaffold in a rabbit model was also able to withstand wound contraction forces for over an 8-week period [22]. This suggests that the PCL polymer may be able to withstand the shear stress experienced *in vivo* without the risk of the polymer collapsing.

1.2.2.2 Other polymers

The biodegradable mesh of PGA was seeded with myoblasts. Over a 6-week period, well vascularized neo-muscle-like tissue had begun to form [23]. Other examples of the use of biodegradable microspheres include the use of PLLA microspheres for human chondrocyte expansion [24]. A PCL microparticle-dispersed PLGA was investigated as a possible injectable urethral bulking agent [25]. The latter achieved much success when injected subcutaneously into a hairless mouse and was found to elicit surrounding tissue blood vessel formation, good biocompatibility, injectability and volume retention potential [25]. The microspheres have an increased surface area for cells to proliferate without having to create bulky polymers which run the risk for fibrous encapsulation and rejection when explanted *in vivo*.

1.2.3 Cytotoxicity assessment of these polymers

Cytotoxic effects of polymers can be assessed by means of how prevalent apoptosis is in a culture of cells when grown on these surfaces. Apoptosis, whether it occurs physiologically or is a materialization of a pathological condition, is an active and regulated mode of cell death [26]. The regulation consists of several check-points at

which a variety of interacting molecules either serves to promote or prevents the offset of apoptosis [27].

The term homo-phase apoptosis has been used to define apoptosis which occurs in the same phase of the cycle in which the cells were initially exposed to the apoptosis triggering agent [28]. During homo-phase apoptosis, the cells remain arrested at a particular phase, or pass through it slowly and die without progressing into the next phase of the cell cycle. Because homo-phase apoptosis is difficult to determine, the term homo-cycle apoptosis, was proposed by Halicka *et al.*, (1997) in order to indicate apoptosis which occurs in the same cell cycle in which the cells were initially exposed to the cytotoxic agent, though without specifying the cell cycle phase [28]. This means that the cells die either before or during the first mitosis after induction of the damage. The term post-mitotic apoptosis was put forward to define apoptosis which occurs in the cell cycle(s) following the one in which the cells were initially exposed to the harmful agent [28].

A cell metabolic assay performed on chondrocytes loaded on PGA/PLLA composites and PLLA revealed that at concentrations above 2mg/ml, the glycolic degradation product exerted a more cytotoxic effect than that of the lactic acid [14]. These cytotoxic effects however were not attributed to acidity alone, as was revealed by pH equilibration [20].

1.2.4 Viability of cells on polymer scaffolds

When using biomaterials, adhesion of cells is an important consideration. In studying the cells' contact with the material surface, one is able to establish whether the contacts formed are general or confined to concentrated regions of the cell. Close contacts could allude to strong adhesion, as opposed to those where the cell is not closely associated with the surface alluding to weak adhesion [29]. It has been accepted that cells respond to physicochemical stimuli such as chemical and topographical changes [30]. It is important to combine the appropriate biomaterial and cytokine growth factors for tissue regeneration. In order to improve cell attachment and bring forth a higher seeding effectiveness, polymer surface engineering may be performed. This usually involves enriching the polymer surface with extracellular matrix (ECM) components. These components build a structural network of proteins on the polymer surface which assist in the strength of attachment and viability of the cells when initially seeded on to the

surface. When explanted *in vivo* the healing process causes many changes to occur in cellular and ECM composition, as well as in the morphology of the cells involved [31]. Smooth muscle cell (SMC) response to growth factors is influenced to a large extent by their local environment along with the composition of the ECM [32].

1.3 The ECM

Major components of the ECM of collagen and fibronectin. These proteins contain the arginine-glycine-aspartate (RGD) motif [16]. Anchorage-dependent cells bind to the RGD motif ensuring correct spatial conformation and survival of the anchorage dependent cells [33]. At the end of the cells' cytoskeletal actin fibres, concentrated integrin receptors of the ECM are recruited from a series of reactions. The integrin sites found at the ends of the actin fibres are forceful structures and are referred to as "focal adhesions" (FAs) [33], [34]. FAs concentrated along the perimeter of the cell assist greatly in cell attachment [35]. Vinculin, paxillin and talin are examples of membrane associated cytoskeletal proteins which when mature, are 2 - 5 μm^2 and are "dash" shaped [35]. These cytoskeletal proteins act as linkers between the integrin receptors and the cytoplasmic actin cytoskeleton (fig. 2). The integrin receptors then form a link between the membranes of the nucleus and cell organelles, as well as various cell enzymes. These links influence both structural and signaling molecules involved in cell proliferation, apoptosis, cell migration, and other important functions such as cell contraction [35]. Studies have postulated that the forces encouraged on the cell cytoskeleton by the process of cellular alignment are conveyed to the nucleus. This in turn causes a rearrangement of the centromeres, which may even affect gene expression [29].

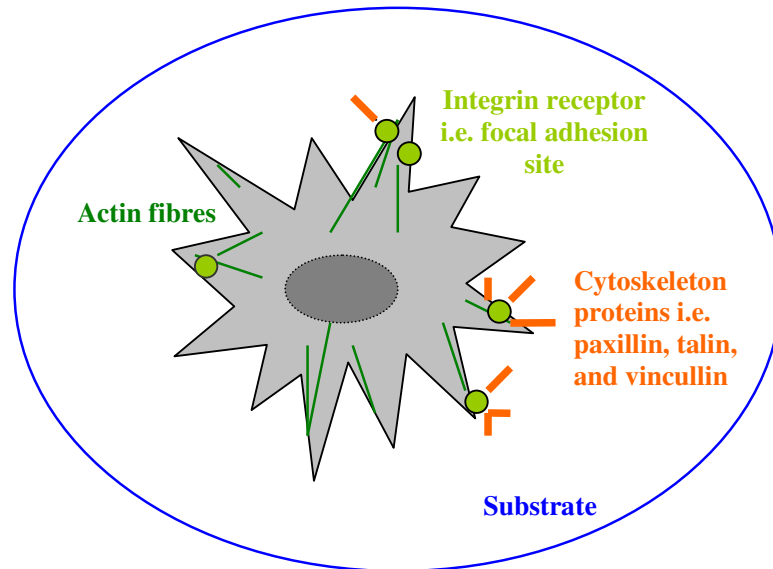
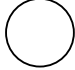
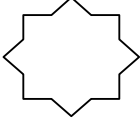
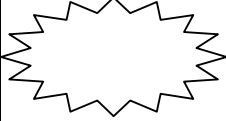


Figure 2: Survival of the anchorage dependent cells relies on a high degree of focal adhesion to a substrate. At the end of the cells' cytoskeletal actin fibres, concentrated integrin receptors of the ECM are recruited. Vincullin, paxillin and talin are examples of membrane associated cytoskeletal proteins which act as linkers between the integrin receptors and the cytoplasmic actin cytoskeleton.

The size, shape, number, and distribution of FAS, as well as the shape of the cell cytoplasm for example, the spreading area, predict the ability of anchorage dependant cells to migrate, proliferate, and differentiate [35]. Small, round cells with no FAs have a low survival and proliferation rate. These small cells also lack the ability to migrate and differentiate [35]. Cells which have an intermediate amount of adhesions and are spread out on the substrate surface display high viability, migration, and proliferation properties, but do not have the ability to differentiate [35]. High and long FAs allow cells to become flattened and spread out on the substrate surface. This in turn allows high FA cells the ability to differentiate and remain highly viable, however their ability to migrate and proliferate are compromised (table 1) [35].

Table 1: Small cells with no FAs have a low survival rate. Those cells with an intermediate amount of FAs and spreading display high viability, migration and proliferation ability, though not much differentiation. High FAs allow cells to differentiate and remain highly viable but to sacrifice on migration and proliferation [Adapted from 35].

	<u>Slight/None</u> Cell is round, small and has no FAs 	<u>Intermediate</u> Cell is flattened in the substrate with a few FAs 	<u>High</u> Cell is flattened and spread out with many, long FAs 
Cell spreading			
Viability	↓	↑	↑
Migration	↓	↑	↓
Proliferation	↓	↑	↓
Differentiation	↓	↓	↑

Cell cycle progression is prompted due to the organization of the cell cytoskeleton and the formation of focal adhesions [34]. Cells which are migrating and differentiating will not undergo active mitosis, but rather remain senescent within the $G_{0/1}$ phase. Whereas those cells which are proliferating, i.e. mitosis, will illustrate a cell cycle mainly within the S and G_2/M phases. This can be explained molecularly as the adhesion of cells to the ECM is a direct stimulant for the expression of cyclin D1 or the cyclin-dependant kinase (CDK) inhibitor (CKI) p27^{kip1} proteins [35]. The localization of CKI within the cell nucleus plays a key role in the control of cell cycle progression [36]. The presence of CKI p27^{kip1} has been noted to have an inhibitory effect on cell motility [37]. This has been illustrated particularly in smooth muscle cells [38] which have altered phenotypes according to their state within the cell cycle progression.

1.4 Smooth muscle cell (SMC) regeneration

1.4.1 The function of SMCs

Smooth muscle is present in a vast array of human tissues and assists in the maintenance of normal function of the cardiovascular, gastrointestinal, reproductive, and urinary systems [39]. They are mainly located within the walls of blood vessels, lining the organs of the GI tract (the stomach wall, surrounding the intestine, in the various sphincters) and in the uterus [40]. Their presence within these organs is vital for normal bodily functions and helps separate the different bodily compartments from each other. Their cellular flexibility is important both for regular differentiation and maturation of gastrointestinal smooth muscle, and also plays a significant role in a variety of gastrointestinal diseases [40]. SMCs and α -actin filaments are oriented in the circumferential direction and have the physiological function of contracting and dilating the circumference of blood vessels, suggesting that the SMCs are more sensitive to changes in circumferential than axial strain [39].

1.4.2 The structure of SMCs

Smooth muscle cells are non-striated and elongated cells that range between 20 and 500 μ m in length [40]. They have noticeable sarcomeres and stain positively for α -smooth muscle actin [41]. It has been illustrated, however, that the elastic properties of SMCs is not only attributed to the amount of actin filaments present, but rather also due to the cell's distribution and organisation [42]. The primary function of the highly specialised smooth muscle cell is to contract and relax [43]; this involuntary movement takes place within the walls of the organs within which they are present [44]. Although based on a sliding-filament mechanism similar to that of striated muscles, contraction of smooth muscle is regulated by pharmacomechanical, as well as by electromechanical coupling mechanisms [45].

Growth factors involved in smooth muscle proliferation and angiogenesis consist of the following: hepatocyte growth factor (HGF), platelet-derived growth factor-BB (PDGF-BB), vascular endothelial growth factor (VEGF), insulin like growth factor-1 (IGF-1) and

heparin binding epidermal growth factor like growth factor (HB-EGF) [46], [47]. Fibroblast growth factor (FGF)-2 is a potent mitogen for SMCs and endothelial cells (ECs) [48].

In adults, SMCs are terminally differentiated cells which express cytoskeletal marker proteins like smooth muscle α -actin and smooth muscle myosin heavy chains, and contract in response to chemical and mechanical stimuli [49]. SMCs are able to alternate between two morphologically separate phenotypes, namely synthetic and mature. This phenomena is also exhibited *in vitro* [46]. The synthetic SMC phenotype produces a wide range of ECM proteins and growth factors making it highly proliferative, migratory and spindle shaped, though is non-contractile. In contrast, mature SMCs proliferate less, are non-migratory and do not have the classic spindle shape. They are however, highly contractile [46].

It has been illustrated that arterial smooth muscle cells can convert from a mature (contractile) to a synthetic (non-contractile) phenotype when grown in primary culture on a substrate of fibronectin in serum-free medium [50]. This process was found to rely on integrin signaling as well as major structural reorganization, including the loss of myofilaments and formation of a large secretory apparatus (an extensive rough endoplasmic reticulum and a large Golgi complex) [50], [51]. Herein, the cells lose their contractility function and instead are able to migrate, secrete ECM components, and proliferate in response to growth factor stimulation [51]. Evidence suggests pressure-induced actin polymerization in vascular smooth muscle (VSM) as a mechanism underlying myogenic behaviour [52]. VSM contains a significant amount of unpolymerized globular (G) actin which becomes significantly reduced by an elevation in intravascular pressure. This implies a dynamic nature of actin within VSM and a shift in the filamentous (F) actin: G equilibrium towards F-actin [52]. This actin filament formation in VSM may therefore trigger mechanotransduction. It may also provide additional sites for myosin-actin interaction, enhancing the force production in response to pressure [52].

1.4.3 The need for SMC regeneration

Bulking of SMCs for tissue regeneration is needed particularly in the gastrointestinal (GI) [44] and urinary tracts where defects are commonly found. These include various gastrointestinal diseases, bladder dysfunction, and urinary incontinence [43]. Smooth muscle sphincters include the lower esophageal sphincter (LES), pyloric sphincter, ileocecolic sphincter, internal anal sphincter [44] and urinary sphincter. These sphincters act as one-way valves regulating the flow of gastrointestinal contents. At rest, they remain in a state of tonic contraction and closure [53]. This contractile function diminishes along with the aging process. The incidence of physiological problems of dysphagia, constipation, and incontinence also increase significantly with age. This aging-related dysfunction mostly affects the upper GI tract (particularly the oropharynx and esophagus) and the distal GI tract consisting of the colon and rectum [53]. Being able to restore the lost function would impact greatly on the quality of life of the many patients affected by problems associated with loss of activity of these sphincter muscles. For example, chronic heartburn is symptomatic of gastroesophageal reflux disease (GERD) which is a condition caused by a malfunctioning LES [54].

1.5 The pathogenesis of GERD

GERD is a disease which involves both brief LES relaxations and various abnormalities in the LES [54]. Maintenance of the normal LES tone is crucial to prevent gastric acid reflux [54].

Baáková *et al.* (2004) have found the enzyme phospholipase A₂ present within the circular muscle layer of the LES converts phospholipids in the cell membrane to arachidonic acid. Metabolites of arachidonic acid (prostaglandin F_{2a} and thromboxane A₂) bind to selective receptors on the cell membrane to maintain the LES tone [54]. However, in a patient suffering from GERD an inflammation response is triggered, which alters the normal signal transduction pathway [54].

1.5.1 Causes of GERD

Complete pressure of LES needs to be less than 6 mmHg for the reflux to occur [55]. Transient relaxations and loss in pressure becomes exasperated with the ingestion of fatty

foods, drinking, smoking, various medications, and most importantly, obesity. Most patients with complicated GERD have the impediment of a hiatal hernia [55], [56] (table 2).

Table 2: List of physiological and lifestyle practices resulting in symptoms of GERD. The physiological causes and lifestyle practices which result in or aggravate GERD symptoms [Adapted from 57].

<u>Physiological causes</u>	<u>Lifestyle practices</u>
Obesity	Smoking
Aging	Excessive alcohol consumption
Hiatal hernia	Various medications (anticholinergic agents)
Pregnancy	Fatty, spicy foods
During infancy and early childhood (present as asymptomatic)	Peppermint flavourings
	Caffeine

1.5.2 Symptoms of GERD

The most common symptom of GERD in adults is that of chronic heartburn experienced as a burning sensation in the lower part of the mid-chest, located behind the breast bone, as well as in the mid-abdomen [57]. However, children under the age of 12 (and some adults) do not present with a burning sensation but rather extra-esophageal symptoms which involve the pulmonary system, noncardiac chest pains, as well as ear, nose and throat infections with difficulty in swallowing [57], [58]. Because these children appear happy and healthy, it becomes particularly difficult to diagnose. In young children signs include irritability and arching of the back during or directly after feedings [57]. They also may experience poor growth due to a refusal to feed [57]. It is important to note that occasional reflux *i.e.* gastroesophageal reflux (GER), is not necessarily GERD, and is only classified as a chronic condition if symptoms occur at least twice a week [57]. If GERD persists and is not well controlled, complications such as erosive esophagitis and stricture occur [58]. More importantly, a person runs the risk of developing Barrett's esophagus (BE).

1.5.3 Barrett's esophagus (BE)

This long-term complication of GER (D) has long been established as the premalignant phase for developing the majority of esophageal and gastroesophageal junction adenocarcinomas [60]. The esophagus is normally lined with squamous epithelial cells (fig 3). There exists a rapid rate of epithelial cell turnover within the gastrointestinal tract, attributed to the gastrointestinal stem cell [57]. Frequent exposure of these cells to the stomach acids result in the cells converting into specialised columnar cells (fig. 3). These cells are similar to those found within the stomach lining and are therefore an adaptation of the cells to be able to withstand the low pH of the refluxed acids. These columnar cells are pre-malignant and remain permanently fixed within this phenotype regardless if the GERD condition becomes resolved [58]. Over-exposure of the epithelial esophageal lining by refluxed stomach acid, bile, pepsin and pancreatic enzymes eventually causes BE to develop [52], [59], [60]. BE presents itself as patches of red, irritated, abnormal cells lining the lower esophagus. This process is referred to as intestinal metaplasia [60]. Patches of these transformed cells are present within the lower esophageal region, which strikingly increase the risk of developing esophageal adenocarcinoma [60] (fig. 3).

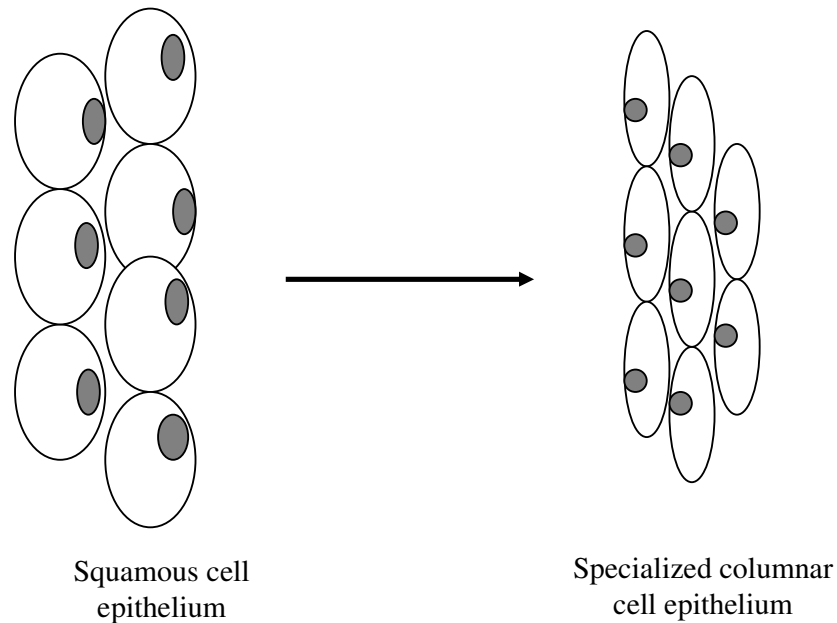


Figure 3: The aetiology of BE: Illustration compiled using Word shapes depicting normal squamous cell epithelium which line the lower esophageal region and become permanently transformed into specialized columnar cell epithelium.

There are no real statistics for how prevalent GERD is in South Africa, though it is thought that sub-Saharan Africa has less people suffering from GERD than in the Western world [60]. Possible reasons for this lower statistic has been attributed to the following factors: the patients may not go to hospitals, endoscopic services are not adequate, and that the average life expectancy of a sub-Saharan is less than that found in industrialized countries [61]. Approximately 10% of Americans experience severe GERD symptoms. From this 10%, if left untreated for five or more years, 5-10% will develop BE. In turn, BE increases the risk of developing esophageal cancer by 30-125-fold [57]. As few as 10% of the people who progress from BE to adenocarcinoma survive past five years [57].

1.5.4 Current treatments of GERD

1.5.4.1 Complimentary lifestyle modifications

- Raising the head of one's bed by about 10 cm. This assists in preventing the stomach acid from rising into the esophagus

- Stop smoking and excessive alcohol intake
- Eating more frequent smaller meals. This reduces the amount of stomach acid produced at a time
- Not consuming food for at least 3 hours before going to bed. Thereby digestion is not taking place while in the supine position
- Eliminating acidic and spicy foods, along with caffeine [57].

1.5.4.2 First line treatment

The first line treatment of GERD is aimed at stopping the stomach acid entering into the esophagus. This is achieved by various drugs which either stop the production of acid or assist the muscles which empty your stomach. These medications are usually very costly and remain as a lifetime therapy [57], [62].

1.5.4.2a Antacids as a first line treatment of GERD

These drugs are available over the counter and are relatively inexpensive; examples include Maalox, Tums and Rennies [57]. These serve to relieve mild symptoms associated with heartburn and GERD and usually use the combination of magnesium, calcium, and aluminium salts, along with the stomach acid neutralizing agents: hydroxide or bicarbonate salts [57]. Side effects include diarrhea (from the magnesium salts) or constipation from the aluminium and calcium salts [63].

1.5.4.2b Foaming agents as a first line treatment of GERD

The over the counter medication, Gaviscon is such a foaming agent. It works by forming a layer above the stomach contents, thereby protecting the esophageal lining from the acid reflux [57]. An advantage of this product is that it is not absorbed by the body and is therefore safe to use during pregnancy [65].

1.5.4.2c Histamine₂ (H₂) blockers as a first line treatment of GERD

These agents work by decreasing the production of acid in the stomach by blocking the H₂ receptors responsible for the release of hydrochloric acid. The drugs include Axid AR, Pepcid AC, and Zantac 75 [57], [62].

Though these drugs are available both in prescription strength and over-the-counter strength, they are only effective in approximately half of the population which suffers from GERD symptoms [57].

1.5.4.2d Proton pump inhibitors (PPIs) as a first line treatment of GERD

Symptomatic treatment includes PPIs which suppress the production of acid in the stomach [62]. Examples include Protonix, Prevacid and Nexium [57]. PPI treatment forms the basis of the primary care of GER (D) and Barrett's esophagus patients. They are more effective than the H₂ blockers and serve not only to relieve the symptoms of everyone who suffers from GERD, but also assist in healing the esophageal lining [57]. However, the treatment is costly and requires a lifetime prescription. Also, most symptomatic GERD patients do not have erosive reflux disease (ERD); this group has been referred to as non-erosive or negative-endoscopy reflux disease (NERD) [65].

1.5.4.3 Surgical interventions

Surgery is only recommended if drug treatment remains ineffective or if the patient is unwilling or unable to continue the therapy. Once the patient has progressed towards high grade dysplasia, the most effective yet controversial treatment is to remove the entire esophagus, known as esophagectomy [62].

Clinicians need to be made aware of these differences in the presentation of this disease [63] and determine whether the patient may be a candidate for surgical intervention. NERD patients have been found to be resistant towards proton pump inhibitors and do not make good candidates for surgery [63].

Many of the surgeries have been standard practice for a few decades; however surgery does not resolve remaining Barrett metaplasia which in turn can lead towards high-grade dysplasia and even cancer [62]. Frequently, surgery results in a high rate of symptom recurrence and also the need for repeat surgeries [62].

1.5.4.3a Endoscopic suturing

Suturing of the gastroesophageal junction has been found to reduce the transient LES reflux along with basal LES pressure. Three methods exist: the Endocinch and NDO

Plicator systems involve creating pleats with stitches in order to strengthen the LES muscle [57]. The Stretta system involves burning tiny incisions with electrodes around the LES; scar tissue forms as the burns heal, thereby strengthening the muscle [57]. This however only results in an insignificant drop in gastroesophageal reflux and the long-term effects are yet to be determined [64].

1.5.4.3b Fundoplication

Fundoplication has been proven to improve symptoms and is the standard surgical intervention for patients of all ages with GERD; however this procedure is extremely invasive and costly along with the risks associated with surgery [65]. Nissen fundoplication involves wrapping the upper part of the stomach around the LES. This method helps strengthen the sphincter, prevent acid reflux and is effective in repairing hiatal hernias [57]. Nissen fundoplication can also be performed laproscopically using a laproscope to make small incisions in the abdomen resulting in a less invasive type of surgery [57]. However, surgical intervention still results in recurrence of symptoms, abnormal pH values and often a need for additional surgery [65].

The trend has moved towards a less invasive approach with the use of injectable gels to bulk up the LES and microstimulator implants which enhance the regeneration of SMCs.

1.5.4.4 Implantation procedures as intervention in GERD

1.5.4.4a Hydrogels

There is promising research into reversible, expandable polyacrylonitrile-based hydrogel prosthesis to augment the LES [12]. These hydrogels, however, will remain as a permanent fixture in the body lending the risk of immunogenic resistance.

1.5.4.4b Microstimulator implants

Implantable microstimulators (IMS) have been used in a variety of medical conditions. The microstimulator can selectively increase the LES pressure and thereby may be useful in the control of GERD [66]. Experiments were performed in three 30 kg dogs where the LES manometry, a 3.3 mm x 28 mm microstimulator (the Bion) was implanted into the LES [66]. After stimulation the resultant LES pressures were 62.1 mm Hg, 35.1 mm Hg

and 26 mm Hg respectively. These recordings were higher than post-implantation baseline levels [66].

1.6 The investigative route for tissue engineering applications

1.6.1 2D models and 3D models for *in vitro* analysis of tissue engineering applications

Until recent years, growing cells *in vitro* has been performed predominantly on tissue culture plastic. Since this limits the cells to only grow in a monolayer, it is known as a 2D model. Limitations of growing cells this way is that many cell types alter their natural phenotypes, morphologies, motilities and differentiated functions [12], [67]. This manifests in the cells' natural morphology and actions being different to how the cells would be when grown *in vitro*. 3D scaffolds however have been found to promote an environment wherein cells can proliferate and produce their own ECM [22]. These 3D constructs also provide a guide for tissue development into the desired structure/organ.

1.6.1.1 Hydrogels as 3D models for cell growth

Hutmacher *et al.* (2003) [22] made use of a 3D bioresorbable synthetic PCL polymer in combination with a fibrin hydrogel. Sufficient chondrocyte cell attachment and morphology was not observed *in vitro*, however, once the seeded constructs were implanted within both pig and rabbit models, islets of cartilage and mineralized tissue formation was observed via phase contrast microscopy and the GIEMSA histological stain [22]. When culturing human osteogenic cells in a silated hydroxypropylmethylcellulose (Si-HPMC)-based hydrogel. The human osteogenic cells within this 3D hydrogel displayed more mature differentiation status than when the same cells were cultured in the plastic two dimensional (2D) model [12].

1.6.1.2 3D polymer models

3D models assist in creating an environment into which cells can migrate, proliferate, and form the basis of 3D tissue. Often the constructs are prepared in the shape of the eventual tissue the researches wish to form.

1.6.2 Cell culturing methods to emulate tissue formation

The problems associated with using normal 2D models are that it is difficult to determine the cells' true behavior as cells do not grow in a monolayer *in vivo*.

Cells and organ structures obtain suitable characteristics in order to withstand the environment they are placed within *in vivo*. Do the cells need to develop into structures that need strength, such as load-bearing bone? Are they subjected to highly acidic environments such as the stomach lining? Mechanical stressors/stimulation also plays a major role in the characteristics the cells will exhibit. These many environmental factors become vitally important when culturing tissue *in vitro* later to be explanted *in vivo*. Therefore, both the operating and environmental conditions need to be optimal and specific for the type of tissue being generated.

1.6.2.1 Static versus dynamic cell culturing techniques

Static and dynamic seeding can be performed on 2D as well as 3D models. The difference comes in the movement of the vessel or medium the culture is maintained in. Static seeding and cultivation would involve seeding cells within a static environment where neither the vessel containing the cells nor the medium surrounding the cells rotates or flows about. Dynamic seeding can take place in many forms, the principle of which is that either the vessels rotates, shakes, moves and/or the medium flows around the vessel, thus mimicking more closely what would occur *in vivo* [70]. Three different combinations of these techniques can be explored: static seeding followed by static cultivation, dynamic seeding followed by static cultivation, and dynamic seeding followed by dynamic cultivation [68]. When growing human dermal fibroblasts, Xiao *et al.* found the dynamic seeding followed by static cultivation to yield higher seeding efficiency/cell number (cells were trypsinized and counted under a haemocytometer) as well as ECM formation (stained with methylene blue and viewed *via* SEM) compared to the other two seeding/cultivation techniques as mentioned above [71]. Dynamic seeding/cultivation took place by using a spinner flask with a non-heated magnetic stirrer at 40 r.p.m (this speed was found to be optimal and did not result in cell damage). The static seeding yielded low seeding efficiency, whereas the dynamic culturing caused the fibroblasts to form aggregates [68]. Dynamic cultivation allows for significant cell expansion. This becomes particularly important when culturing cells where only meager

amounts of donor tissue are available (such as skin grafts from severely burnt patients) [69], [72]. It has been suggested that by imitating the forces experienced by cells *in vivo*, known as shear stress, may enhance not only cell proliferation and ECM synthesis, but also improve the quality of engineered tissue [68]. In particular, SMCs have been observed to benefit from dynamic seeding. Kim *et al.* noted that dynamically seeded SMCs, when compared to statically seeded SMCs, displayed the formation of new tissue which had higher cellularity, a more uniform cell distribution, along with greater deposition of elastin [69].

Though it has been proven that dynamic culturing is superior to that of static culturing with regard to a more natural phenotype and behavioural characteristics of the cells, it was decided to maintain both static culturing and static seeding methods. This will ensure that we are observing and recording the cells' response to 2D and 3D surfaces without the interference of additional factors.

1.6.3 *In vitro* investigation of cancerous SMCs cultured on 2D and 3D PCL polymers

1.6.3.1 Cell line selection

Unfortunately, no cell lines are available for investigating the LES, and there is no animal model to represent GERD. Due to the variation in cell behaviour of primary cell lines, it was decided that the study would utilize cancerous smooth muscle cell lines. The SKUT-1, mixed leiomyosarcoma (human uterine) cell line provided for SMCs originating from the human uterus, an organ which undergoes regular contraction and relaxation as would the LES.

The CRL-1701, leiomyosarcoma (syrian hamster ductus deferens) cell line provided for a pure SMC culture which would undergo shear stress and contractions/relaxations *in vivo*. The cell lines were chosen to explore the influence of the PCL polymer effects *in vitro* which resemble our envisioned application of smooth muscle bulking *in vivo* as closely as possible.

1.6.3.2 Investigation of the effect of PCL polymers on the cell lines

This study therefore chose two smooth muscle carcinoma cell lines (SKUT-1 and CRL-1701). The focus of the investigation is to assess the impact of altering the architecture of the PCL polymer (i.e. from a flat disk, to a solid microsphere as well as a hollow ported microsphere) on the cellular response.

The above mentioned usual route of 2D *in vitro* investigations of the PCL polymer in the form of a flat PCL disk is inconclusive as the spatial organization of the cells cannot be investigated as discussed previously (section 1.6.1). Therefore (i) 3D solid PCL microspheres and (ii) hollow/ported PCL microspheres (both being 100-200 μm in diameter) were implemented. Microspheres aim to provide for a larger surface area of growth and also allow for significant cell expansion. Growth of the cells on the 3D surface will also better represent the motile behavior of the cells as they would *in vivo* since many cell types are known to have altered motility on 3D matrices compared to 2D surfaces [70]. These microspheres (100-200 μm) are small enough to be injected in a surgical environment: this creates potential for tissue regeneration *in vivo* where the filling of irregularly shaped defects is needed [71]. It also ensures a minimally invasive surgical procedure for the patient. In utilizing biodegradable microspheres, side effects such as granuloma formation, embolization and chronic inflammation may be avoided [25].

- (i) Solid microspheres: Due to cells *in vivo* never being further than a few hundred microns from a blood supply, even conservative volumes of engineered tissue has been found to exhibit a central necrosis attributed to the diffusional limit of nutrients and waste products [72]. However, the cells due to its growth only on the surface of the microsphere, lack of nutrient diffusion will not pose a problem.
- (ii) Hollow/ported microspheres: The benefit of the hollow microspheres is that cells are protected within the structure from frictional forces exerted once implanted. Ports also allow for the invasion of a blood supply, thereby preventing cell starvation. In effect, these microspheres will become cell microcarriers which could be implanted in the body and provide a bulking, functional effect [73], [74].

1.6.4 Rationale for *in vitro* investigation

The *in vitro* study has been initiated to determine cytocompatibility, cytotoxicity and cellular morphology on PCL models. Once the study has confirmed the above, animal trials will follow, providing a correlation as to how the application relates to a live model. If these studies are successful, human clinical trials are intended.

SMC-seeded scaffolds were implanted subcutaneously in athymic nude mice to confirm the biocompatibility [74]. Such a high elastic property and proper biocompatibility to SMCs of PLCL scaffolds prepared in this study will be very useful to engineer SM-containing tissues such as blood vessels under mechanically dynamic environments (mechano-active tissue engineering)[74].

1.7 Aim

The aim of this study was to characterise the cellular physiology of two cancerous smooth muscle cell lines (human and hamster) *in vitro* in the presence of a bioresorbable PCL polymer in order to establish its biocompatibility and observe the differences in cell-polymer interactions when cells are cultured on a 2D surface and a 3D surfaces.

We investigated the following:

- 1.7.1 suitability of PCL polymers as an environment for smooth muscle cell attachment and proliferation;
- 1.7.2 cytocompatibility and biocompatibility of the PCL polymer with the smooth muscle cells;
- 1.7.3 nature of the interactions of the cells and the polymer with respect to cell/tissue viability and growth responses when the polymer undergoes degradation with time; and
- 1.7.4 differences of 2D and 3D polymer-cell interactions with regard to cell attachment, growth, viability and degradation responses.

1.8 Risks/problems associated with the intended investigative route

1.8.1 Cell line related problems

There is no animal model or commercially available sphincter smooth muscle cell line for the physiological problem GERD. However, because our main focus was to develop the techniques for investigating smooth muscle cell interactions with PCL polymers, the following cell lines were utilised:

1.8.1.1. SKUT-1, mixed leiomyosarcoma (human uterine)

1.8.1.2 CRL-1701, leiomyosarcoma (syrian hamster ductus deferens)

Leiomyosarcomas are malignant mesenchymal tissue tumours whose histologic characteristics are consistent to those cells of smooth muscle differentiation [75].

1.8.2 Risks of predicting the *in vitro* investigation effects to *in vivo* tissue engineering

The mechanical properties of tissues engineered from cells and polymer scaffolds are significantly lower than the native tissues they replace. In order for the engineered SM tissue to express the contractile phenotype characteristic genes, it becomes crucial to provide both the chemical and mechanical morphogenetic inputs in a realistic three-dimensional environment which mimics that which would be experienced *in vivo* [68].

The engineering tissue would preferably involve obtaining a biopsy from the host (autologous cells), expanding the cells *in vitro* and then seeding them onto a matrix/polymer scaffold and implanting the cell-matrix composite back into the host [76]. Currently it is not known whether non-contractile LES SMCs may be engineered into contractile tissue. Although another study found that there were no phenotypic or functional differences between muscle cells obtained from urodynamically normal or pathological bladders seeded on polyglycolic acid scaffolds [76]. Regardless of the cell

origin (functional or non-functional bladder tissue) they retained their phenotype after implantation *in vivo* [76].

Chapter 2

Materials and Methods

2.1 Materials

2.1.1 Cell lines

2.1.1.1 The SKUT-1 cell line: characterized as mixed leiomyosarcoma derived from the human uterus.

2.1.1.2 The CRL-1701 cell line: characterized as a leiomyosarcoma derived from the syrian hamster ductus deferens.

Both cell lines were obtained from the American Tissue Culture Collection (ATCC) (Maryland, USA).

2.1.2 PCL polymers:

PCL polymer (Caprolactone (CAPA[®]) Thermoplastics) material was obtained from collaborators in Materials Science and Manufacturing (MSM) Division of the Council for Scientific and Industrial Research (CSIR) (Pretoria, South Africa).

2.1.2.a: 2D model: PCL was prepared as flat sheets by placing PCL beads (as originally obtained) into a mould which then were hydraulically pressed at 80°C for 15 min. The sheet was allowed to cool, after which it was pressed for 15 min with a weight above it. The mould was removed and allowed to cool with a 10 kg weight on it. The sheet was then cut into the correct size to fit into 24-well plates.

2.1.2.b: 3D model: Solid PCL microspheres were prepared by dissolving the original PCL beads in dichloromethane (DCM) at 25°C. This was added to 1% w/v poly vinyl alcohol (PVA) in deionised water while magnetically stirring the mixture. The solvent was allowed to evaporate for 3 hrs,

then filtered and rinsed several times. The microspheres were sieved in order to obtain the desired size range between 100 and 200µm.

Both the PCL disks and solid microspheres were gamma-sterilized at 25 kGy at Isotron (Pty) Ltd. (Kempton Park, Johannesburg, SA), followed by 70% ethanol for 30 min, and rinsed thrice in phosphate buffered saline (PBS) prior to testing.

2.1.3 Other reagents:

All chemicals were supplied by Sigma-Aldrich (St. Louis, United States of America) unless specified otherwise. Dulbecco's Modified Eagles Medium (DMEM) with glucose, sodium pyruvate, L-glutamine and heat-inactivated fetal calf serum (FCS) was purchased from The Scientific Group (Johannesburg, South Africa). Penicillin, streptomycin and fungizone were supplied by Sigma-Aldrich (St. Louis, United States of America) and trypsin/versene was obtained from Highveld Biological (Pty) Ltd (Sandringham, South Africa). Sterile cell culture flasks and plates were obtained through Laboratory Equipment Supplies (Germiston, South Africa) and 0.22 µm syringe filters from Aqualytic CC (Irene, South Africa).

2.2 Methods

2.2.1 General cell culture maintenance

Cells were grown in both 25 cm² and 75 cm² tissue culture flasks in a Forma Scientific water-jacketed incubator (Ohio, United States of America) and maintained in a humidified atmosphere at 37°C in 5% CO₂ air. Fresh medium was replaced every 72 hr. The maintenance of both the SKUT-1 and CRL-1701 cell lines consisted of DMEM supplemented with 10% heat-inactivated FCS, penicillin (100 µg/l), streptomycin (100 µg/l), and fungizone (250 µg/l). This is the standard operating procedure for the growth of these cells as stipulated by the ATCC.

Phosphate buffered saline (PBS) consisting of 80 g/l NaCl, 2 g/l KH₂PO₄ and 11.5 g/l Na₂HPO₄.2H₂O was prepared at a ten times concentrated stock solution and stored in 50

ml aliquots at 4°C. When utilized, the PBS was diluted ten times with the pH adjusted to 7.4 with 1 M NaOH and then autoclaved (20 min, 120°C, 15 psi).

The cell culture medium of the cells was replaced with fresh medium every three days or when a drop in pH was observed, as indicated by the phenol red present in the DMEM. When confluent, cells were washed with PBS and subsequently incubated with trypsin/versene (37°C, 5 min). Cells were gently detached from the surface of the cell culture flasks by means of a gentle tap against the palm. The detached cells were resuspended in fresh medium, to be divided into subcultures or used in experiments. Stock suspensions of cells were frozen away at regular intervals in cryovials at -70°C. Cells were frozen in freeze medium which consists of 10% cell culture media, 10% dimethyl sulphoxide (DMSO) and 80% FCS.

Sterile conditions for cell culture maintenance and experiments were maintained at all times. Procedures were carried out in a laminar flow cabinet from Labotec (Midrand, South Africa). All solutions were filter sterilized (0.22 µm pore size) with all glassware and non-sterile equipment being sterilized by autoclaving (20 min, 120°C, 15 psi) before use.

2.2.2 General experimental setup

Tissue culture plate (TCP) surfaces are considered optimal for cell attachment and hence this surface was used as a 100% control [77]. Depending on the type of study 6-, 24-, and 96-well plates were used. PCL disks were synthesised by MSM (CSIR, South Africa) and cut to fit into the wells of 24-well plates. Cells were seeded onto these disks to serve as a 2D experimental setup. For the 3D experiments, 3.237 µg of solid PCL microspheres were weighed off in order to correspond with the surface area of one 24-well size and were placed in individually sterilized glass vials into which the cells were seeded. Cells were harvested for experiments as described previously (section 2.2.1, par. 3) by means of the trypsinization procedure. A 1 ml aliquot of cells was resuspended in medium and counted with the use of a haemocytometer. 20 µl of trypan blue was added to 20 µl of the cell suspension in order to identify viable cells during the cell counting procedure. Viable cells do not take up the trypan blue stain as their cell membranes are intact, whereas dead cells stain dark blue. The dead cells were excluded from the count [78].

Concentration of cells was determined as follows:

Cells/ml = Average count per four squares in haemocytometer chamber (depth = 0.001 m³) x dilution factor x 10⁴. The 1 ml cell suspension was then appropriately diluted with medium in order to obtain the required cell number per experiment.

2.3 Analytical experimental protocols

In the studies using the polymer construct DegraPol[®], a biodegradable block-copolyesterurethane, the following time frames were used to evaluate SMC growth on this polymer: 24 hr, 48 hr, 72 hr and 96 hr [79].

2.3.1 Cytotoxicity studies

The effects of the solvent DMSO present in the PCL solid microspheres was analyzed for cellular cytotoxicity. Since the PCL disks did not undergo the same solvent preparation procedure, it was considered a positive control. 0.1 g PCL disks, solid and ported microspheres were weighed off each and sterilized as described previously (section 2.1.2, par. 4).

2.3.1.1 Pre-incubation of polymer:

The PCL polymers were incubated in 10 ml cell culture medium for the following time periods: 24 hr, 72 hr, 5 day, 1 month and 1 year, to allow for any residual solvent leaching.

2.1.2.2 Extraction of pre-incubated medium:

The medium was subsequently separated from the polymer and used as the experimental medium to conduct a 24 hr metabolic analysis. Medium that did not undergo polymer incubation served as the 100% control.

2.3.2 Cell viability assessment of cells grown on degradation extracts

3-[4, 5 dimethylthiazol-2-yl]-2, 5-diphenyl tetrazolium bromide (MTT) and propidium iodide/ Hoechst 33342 (PI/HO) stains was utilized in order to quantify and qualify cell viability respectively.

2.3.2.1 Cell viability assessment by assessing metabolic activity using the MTT assay

2.3.2.1a Principle of the assay

The MTT assay determines the amount of viable and metabolically active cells by monitoring formazan formation. Changes in cell proliferative activity caused by trophic factors, growth inhibitors, or inducers and inhibitors of apoptosis, may be quantified using the MTT. MTT is reduced to insoluble formazan crystals associated with metabolic activity. Live cells have active mitochondria and therefore the mitochondrial dehydrogenase enzyme would cleave the MTT to form dark purple formazan crystals [80]. The reduction of MTT is primarily due to enzymatic activity within the cell dependent upon the presence of NADH and NADPH [81]. The colour intensity is a direct correlation to the amount of formazan and therefore an indirect correlation to the metabolically active (alive) cells. The colour was spectrophotometrically measured at an absorbance of 570nm (ref. 630nm) [81].

2.3.2.1b Materials

3-[4, 5 dimethylthiazol-2-yl]-2, 5-diphenyl tetrazolium bromide (MTT) and DMSO were purchased from Sigma-Aldrich (St. Louis, United States of America).

2.3.2.1c Methods

SKUT-1 and CRL-1701 cells were trypsinized and seeded at 50 000 cells per well in 96-well plates. Cells seeded in medium that was pre-incubated with the PCL disks or microspheres were compared against medium that was not exposed to PCL disks or microspheres. The fresh medium that was not pre-incubated was considered the optimal and therefore the control. The cells were allowed to attach for 24 hr at 37°C. 20 µl MTT (5 mg/ml in PBS) was added to 200 µl medium in each well and left to incubate at 37°C for 3.5 hr. The supernatant was removed without disturbing the attached cells. Cells were gently washed with 200 µl PBS, after which 200 µl DMSO was added per well and shaken for 1 hr. 100 µl of the supernatant was then removed and transferred to a new 96-well plate to be measured at absorbance 570 nm (reference 630 nm), using an EL_x800 Universal Microplate Reader from Bio-Tek Instruments Inc. (Vermont, United States of America). (All experiments were conducted thrice with n=10) [81].

2.3.2.2 Cell viability assessment using the PI/HO assay

2.3.2.2a Principle of the assay

In order for cells to maintain a steady-state, cell division must be compensated by cell death. This important active process of cell death is known as apoptosis or programmed cell death [82]. A series of molecular and biochemical events are activated as a cell undergoes apoptosis. This leads to its total physical disintegration. Cell dehydration is one of the early events which lead towards cytoplasmic condensation, results in a change in cell shape and size [83]. However, the most characteristic feature of apoptosis is condensation of nuclear chromatin [84]. DNA in condensed, i.e pycnotic, chromatin

show signs of hyperchromasia, which stains strongly with fluorescent dyes. Disintegration of the nuclear envelope follows, with lamin proteins undergoing proteolytic degradation. Finally, nuclear fragmentation (karyorrhexis) takes place [85].

The fluorescent stain PI is impermeable to the intact cell membrane whilst HO is permeable to the intact cell membrane [86]. These properties of the two stains were used to analyze the cells' integrity and therefore conclude its viability or apoptosis. When the cells are stained with PI, the cells that are intact would not stain and the damaged and/or apoptotic cells would stain. The fluorescence in the red visible range is then measured. On the other hand, as HO is permeable, it is able to stain the chromosome of the cells and emits a blue fluorescence. Due to the chromosomes being stained, it is possible to distinguish the different mitotic stages of the cell, which allows the specific cell cycle phase to be distinguished.

2.3.2.2b Materials

Propidium Iodide (PI) and Hoechst 33342 (HO) were purchased from Sigma-Aldrich (St. Louis, United States of America).

2.3.2.2c Methods

SKUT-1 and CRL-1701 cells were trypsinized and seeded at 500 000 cells per well in 6-well plates onto heat-sterilized glass cover slips. Cells incubated with non-PCL exposed medium were used as the 100% control as they would grow within optimal conditions. The experimental setup included cells incubated with the experimental medium extracts obtained from PCL disks or PCL microspheres. The cells were allowed to attach for 24 hr at 37°C. The growth medium was discarded and replaced with PBS in order to rinse the cells. Once the PBS was removed, the cells were stained with 2 ml HO (0.5 µg/ml in PBS) and incubate for 30 min at 37°C. 0.5 ml PI (40 µg/ml in PBS) was added to the HO solution and left for a further 5 min at 37°C. The coverslips were removed and mounted on glass slides in mounting fluid (90% glycerol, 4% N-propyl-gallate, 6% PBS). This assay was visualised under a Zeiss Axiovert200, inverted fluorescence microscope (München, Germany). Photos were taken with a Zeiss AxioCam MRc5 (München, Germany). (All experiments were conducted thrice with n=3) [86].

2.3.3 Cell attachment studies

PCL preconditioning with medium for 24 h was shown to improve cell adhesion [33]. This study demonstrated that it enhances ECM like factors from the medium to deposit on the PCL prior to cell seeding and could therefore improve cell adhesion [33].

Cells cultured on the 2D PCL polymer disk that was treated in DMEM + 10% FCS (now referred to as ‘complete medium’) for 24 hr prior to cell seeding was compared to those cells seeded on PCL disks that did not undergo the pre-incubation. Cells cultured on disks that were treated with DMEM without 10% FCS (now referred to as ‘partial medium’) served as a control in order to rule out the effects of the proteins found in FCS.

2.3.3.1 Cell attachment density assessment using Scanning Electron Microscopy (SEM)

2.3.3.1a Principle of method

Observation of cells by SEM allows visualization of cells and their morphology. SEM allows for the qualitative observation of cellular attachment density [87].

2.3.3.1b Materials

Gluteraldehyde, osmium tetroxide and hexamethyldisilazane were purchased from Sigma-Aldrich (St. Louis, United States of America).

2.3.3.1c Methods

SKUT-1 and CRL-1701 cells were trypsinized and seeded at 100 000 cells per 24-well in 24-well plate. The experimental groups included polymer disks incubated at 37°C in, 1) complete medium (experiment) and 2) partial medium (positive control) for 24 h prior to cell seeding. The negative control was 3) incubated in PBS for 24 h. The cells were allowed to attach for 24 hr at 37°C. Experiments were terminated by rinsing the samples in PBS, to remove non-adherent cells. Cells were then fixed by placing the samples in 2.5 gluteraldehyde in 1.15 M Na/K buffer for 1 hr. The samples were rinsed thrice in 0.15 M

Na/K buffer and immersed in osmium tetroxide for 30 min. Once again the samples were rinsed thrice in 0.15 M Na/K buffer, followed by a graded dehydration in ethanol from 30% through to 100%. The samples were covered in hexamethyldisilazane and left to dry in a desiccator overnight. Samples were then sputter coated in gold and viewed under a JSM 840 Scanning Electron Microscope (JEOL, Tokyo, Japan). (All experiments were conducted thrice with n=3).

2.3.4 Cell cycle analysis

Cell cycle was analyzed when the cells were grown on the 2D models (TCP and PCL disk) and 3D models (PCL solid microsphere and PCL ported microsphere). All experiments were conducted on polymers which had been incubated in complete DMEM for 24 hr prior to seeding. The experiments consisted of the following time periods: 24 hr, 72 hr, and 5 day. 100 000 cells were seeded for 24 hr experiments, 50 000 cells for 72 hr and 25 000 cells for 5 day experiments.

2.3.4.1 Cell cycle analysis using flow cytometry

2.3.4.1a Principle of method

Flow cytometry uses a laser light beam which is projected through a liquid stream that contains cells and when struck by the focused light, emitted signals are detected [88]. These emitted signals are then converted for computational data analysis which provides information about biological/biochemical properties (*i.e.* cell senescence, cell replication) of cellular DNA [88]. Therefore analysis of cells using the flow cytometry technique is a useful technique in determining the progress of cells through the cell cycle (G_1 - S - G_2 - M), and allows for a quantitative ratio of cells actively proliferating versus senescent cells [89].

Changes in morphology of cells undergoing cell death can be detected by analyzing the light scatter signal given during flow cytometry [89]. The manner in which the light is scattered provides information about the cell size and structure [89]. During cell death a cell's ability to scatter light is altered and reflects definite morphological changes such as

cell swelling or shrinkage, breakage of plasma membrane and also signs of apoptosis such as: chromatin condensation, nuclear fragmentation and detaching of apoptotic bodies [89].

2.3.4.1b Materials

RNase A was purchased from Roche Diagnostics, GmbH (Mannheim, Germany) and 99.9% ethanol was from Merck Co. (Munich, Germany).

2.3.4.1c Method

After the appropriate incubation periods of 1) 24 hr, 2) 72 hr and 3) 5 day, the SKUT and CRL-1701 cells attached on the TCP plates, PCL disks, solid microspheres, as well as ported microspheres were washed in ice-cold PBS. Cells were trypsinized from the PCL polymers and resuspended in 200 μ l of PBS/0.1% FCS. While vortexing, 4 ml of ice-cold ethanol was added one drop at a time in order to fixate the cells, and then incubated at 4°C for 1 h. The cell suspension was centrifuged and the cell pellet was obtained. The cell pellet was resuspended in 1 ml PI solution (40 μ g/ml PI and 100 μ g/ml RNaseA). The cells were incubated at 37°C for 1 h and filtered through a 40 – 70 μ m mesh prior to analysis. PI fluorescence which is relative to DNA content per cell was measured with a fluorescence activated cell sorting (FACS) FC500 System flow cytometer (Beckman Coulter South Africa (Pty) Ltd) equipped with an air-cooled argon laser excited at 488nm. Cell debris, particles smaller than apoptotic bodies and cell clumps was removed from further analysis. Data from at least 30 000 cells were analyzed with CXP software (Beckman Coulter South Africa (Pty) Ltd). (All experiments were conducted thrice with n=30) [89].

2.3.4.2 Determination of cells in S-phase using Click-iT™ EdU flow cytometry kit

2.3.4.2a Principle of method

The number of cells within the S phase was quantified and confirmed with further assays involving the Click-iT™ EdU flow cytometry kit. This kit tags cells specifically in the S phase during DNA synthesis by inserting the nucleoside analog, 5-ethyl-2'-deoxyuridine

(EdU) to thymidine. This occurs during active DNA synthesis and is referred to as a “click” reaction due to the copper catalyzed reaction between an azide and an alkyne [90].

2.3.4.2b Materials

Click-iT™ EdU flow cytometry kit obtained from Invitrogen, Molecular Probes (Eugene, Oregon, United States of America).

2.3.4.2c Methods

EdU was added at a final concentration of 10 mM to the SKUT and CRL-1701 cells grown for 5 days on the TCP, PCL disks, solid microspheres and ported microspheres. The incorporation of the EdU was allowed for 2 ½ hrs, after which cells were harvested by trypsinization, washed with 1% bovine serum albumin (BSA) in PBS centrifuged at 10 000rpm to pellet cells. The supernatant was discarded and the cells were resuspended at 1×10^7 cells/ml in 100 µl 1% BSA in PBS. To this cell suspension, 100 µl of Click-iT fixative was added and incubated at room temperature for 15 min in the dark. The cells were once again washed with 3 ml 1% BSA in PBS, centrifuged at 10 000 rpm, the supernatant was removed. The cell pellet was dislodged by resuspending in 100 µl Triton X-100 and incubated for 30 min at room temperature, protected from light. After this, cells were washed in 3 ml 1% BSA in PBS, centrifuged at 10 000rpm, the supernatant was removed. The cell pellet was then resuspended in 500 µl of the Click-iT reaction cocktail consisting of 13.2 ml 1x Click-iT reaction buffer, 300 µl CuSO₄, 75 µl fluorescent dye azide and 1.5 ml of reaction buffer additive. The reaction cocktail was allowed to incubate at room temperature for a further 30 min in the dark. The cells were then washed with 3 ml 1% BSA in PBS, centrifuged at 10 000rpm, the supernatant was removed. The cell pellet was further resuspended in 500 µl 1% BSA in PBS to which 5 µl Ribonuclease A and 2 µl CellCycle 633-red was added and left for a further 15 min at room temp. Flow Cytometric analysis was performed using a Coulter Epic Altra (Beckman Coulter, Miami, FL) flow cytometer, equipped with a water-cooled enterprise laser, as well as an air cooled Red Helium Neon (HeNe) laser. It also has a UV and Argon laser. The Argon laser has an excitation wavelength of 488nm, while the HeNe

laser has an excitation wavelength of 633nm. The CellCycle 633-red has an excitation wavelength of 633/635nm and was detected with a red emission filter at 670/14nm [90].

2.3.5 Assessment of cell attachment characteristics

Cell attachment characteristics were analyzed when the cells were grown directly on the PCL disks, solid microspheres and ported microspheres. All experiments were conducted on polymers which had been incubated in complete medium for 24 hr prior to seeding and cells were incubated for 24 hr, 72 hr and 5 days respectively. 100 000 cells were seeded for 24 hr experiments, 50 000 cells for 72 hr and 25 000 cells for 5 day experiments.

2.3.5.1 Assessment of cell morphology using SEM

2.3.5.1a Principle of the method

Observation of cells by SEM allows for assessment of cellular morphology of cells cultured on the PCL polymer disk (2D model) to be compared to those cells cultured on the PCL microspheres (3D models). Observation of the manner in which these cells attach onto the PCL surfaces allowed the comparison of whether the SMCs retain their characteristic spindle-shaped attachment formation on either of the models. The shapes and distribution of attached cells will also elude as to how the cells differ in attachment on flat and curved surfaces. Morphologically flattened cells are characteristic of adherent cells as opposed to rounded cells, and is an indication of cells attaching well to a particular surface [91]. Cells that attach well have an intact cytoskeleton and filopodia that branch out from the cell body. This is indicative of cells that are migrating, spreading out and proliferating well on the polymer surface [92]. SEM allows for the qualitative observation of cellular attachment and patterns of growth.

2.3.5.1b Materials

All experiments were conducted on polymers which had been pre-incubated in complete medium for 24 h prior to seeding. SKUT-1 and CRL-1701 cells were trypsinized and seeded in 24-well plate on PCL disks, and in glass vials on 0.003237g solid microspheres. The cells were allowed to attach for 1) 24 h, 2) 72 h and 3) 5days at 37°C. The method as described in section 2.3.2.2c was used. Samples were sputter coated in gold and viewed under a JSM 840 Scanning Electron Microscope (JEOL, Tokyo, Japan). (All experiments were conducted thrice with n=3).

2.3.5.2 Assessment of the cell cytoskeleton using the phalloidin staining technique

2.3.5.2a Principle of the staining technique

Phalloidin is a green fluorescent agent which stains the cells' actin filaments responsible for cell shape and attachment. Distribution of the actin filaments around the perimeter of the cell membrane is indicative of high focal adhesions of the cell to the substrate [94]. The amount of actin filaments present gives an indication that the SMCs have retained the correct phenotype [94].

2.3.5.2b Materials

Paraformaldehyde and BSA were supplied by Sigma-Aldrich (St. Louis, United States of America). Triton X-100 was purchased from Merck (Darmstadt, Germany). Alexa Fluor 488 phalloidin was purchased from Invitrogen, Molecular Probes (Eugene, Oregon, United States of America).

2.3.5.2c Method

SKUT-1 and CRL-1701 cells were trypsinized and seeded in glass vials on 0.003237g solid microspheres and 0.003237 ported microspheres. Cells seeded on heat-sterilized glass cover slips served as a 100% control. The cells were allowed to proliferate for 5 days at 37°C. Experiments were terminated by rinsing twice in PBS, this removed any

non-adherent cells. The cells were fixed in 3.7% paraformaldehyde in PBS for 5 min at room temperature and subsequently rinsed thrice in PBS. The cell membranes were permeabilised with 0.1% Triton X-100 in PBS for 5 min and subsequently rinsed thrice in PBS. The cells were then incubated at room temperature for 30 min in 1% BSA in PBS. The BSA was removed and the cells were overlaid with 5 µl Alexa Fluor 488 phalloidin in 200 µl PBS and left to incubate at room temperature for 20 - 30 min. The PCL disks, solid microspheres, the glass cover slips were removed and mounted on glass slides in mounting fluid (90% glycerol, 4% N-propyl-gallate, 6% PBS). This assay was visualised under a Zeiss Axiovert200, inverted fluorescence microscope (München, Germany). Photos were taken with a Zeiss AxioCam MRc5 (München, Germany).

2.3.6 Assessment of cells grown on PCL models in 3D format using confocal microscopy

The optical imaging technique of confocal microscopy allows an increase in contrast of micrographs along with the ability to reconstruct 3D images [93]. The confocal microscope uses a spatial pinhole and point illumination in front of the fluorescent detector which eliminates out-of-focus information [93]. 2D and 3D images are compiled by scanning the specimen over a regular raster, which is the compilation of parallel scanning lines into a rectangular shape [93].

2.3.6.1a Principle of the method

As explained in 2.3.5.2a, cells were stained with phalloidin in order to view the entirety of the cell cytoskeleton.

2.3.6.1b Microscope and materials

The Zeiss confocal laser scanning microscope (LSM) 510 (Jena, Germany) was utilized along with the Zeiss LSM Image Browser software. Paraformaldehyde and BSA were supplied by Sigma-Aldrich (St. Louis, United States of America). Triton X-100 was

purchased from Merk (Darmstadt, Germany). Alexa Fluor 488 phalloidin was purchased from Invitrogen, Molecular Probes (Eugene, Oregon, United States of America).

2.3.6.1c Method

SKUT-1 and CRL-1701 cells were trypsinized and seeded in 24-well plates on glass cover slip controls, PCL disks, and in glass vials on 0.003237g PCL solid microspheres and 0.003237 PCL ported microspheres. Cells were incubated for 5 days on the glass cover slips and PCL disks (2D models), and on the PCL solid microsphere and PCL ported microspheres (3D models). The cells were stained with phalloidin (see section 2.3.4.2c for method). 2D model images were photographed using the Zeiss LSM 510 camera. 3D model images were scanned with the xyz-stack with the Zeiss LSM 510 microscope in order to obtain complete 3D images. These images were compiled into a 3D animation using the Projection option of the Zeiss LSM Image Browser software.

2.3.7 Statistics

Analysis of the data was conducted in consultation with Prof. Becker of the Medical Research Council (MRC), an expert in the field of Biostatistics. All experiments were conducted as a factorial design with treatment at four levels (tissue culture plate, 2D PCL polymer disk, 3D PCL polymer solid microsphere and 3D PCL polymer ported microsphere), time at three levels (24 hours, 72 hours, 5 days) and cells at two levels (SKUT-1, CRL-1701). Data was analysed using appropriate number of variance for this 4x3x2 factorial design with three replicates. A difference was considered statistically significant at $P < 0.05$.

Chapter 3

Results

3.1 Determination of the effect of PCL degradation extracts by assessing cell viability

3.1.1 Assessment of cell viability by the determination of metabolic activity using the quantitative MTT assay

Viability of both the SKUT (fig. 3.1.1) and CRL-1701 (fig. 3.1.2) cell lines remained above 80% during the 24 hr, 72 hr and 5 day exposures to PCL disk and PCL microspheres extracts.

In figure 3.1.1 the SKUT cells displayed a statistically significant increase in metabolic activity, between 120-130% when allowed to proliferate in the PCL medium extracts than what they did on the control medium (medium without PCL exposure). This illustrated that the initial degradation products and any chemical leaching from the PCL remained unharmed towards the cells' viability and therefore did not prove to be cytotoxic. The metabolic activity of the SKUT cell line dropped with statistical significance (80% on the PCL microsphere extract and 65% on the PCL disk extract) when cultured within the 1 month PCL disk and microsphere extracts when compared to the control.

In figure 3.1.2 the CRL-1701 cells cultured within the PCL extracts illustrated the lowered metabolic activities between 80% and 98% when compared to the control medium. This was however only statistically lower when the cells were cultured on the 24 hr PCL disk extract and 5 day PCL microsphere extract. The CRL-1701 cell line displayed the opposite effect seen with the SKUT-1 cells, with an increase in metabolic activity over the control, statistically significant at 120% when cultured in the PCL disk extract and 102% when cultured on the PCL microsphere extract.

Both cell lines displayed similar statistically lower metabolic activities when compared to the control when cultured within the 1 year PCL disk and PCL microsphere extracts (between 40% and 50%).

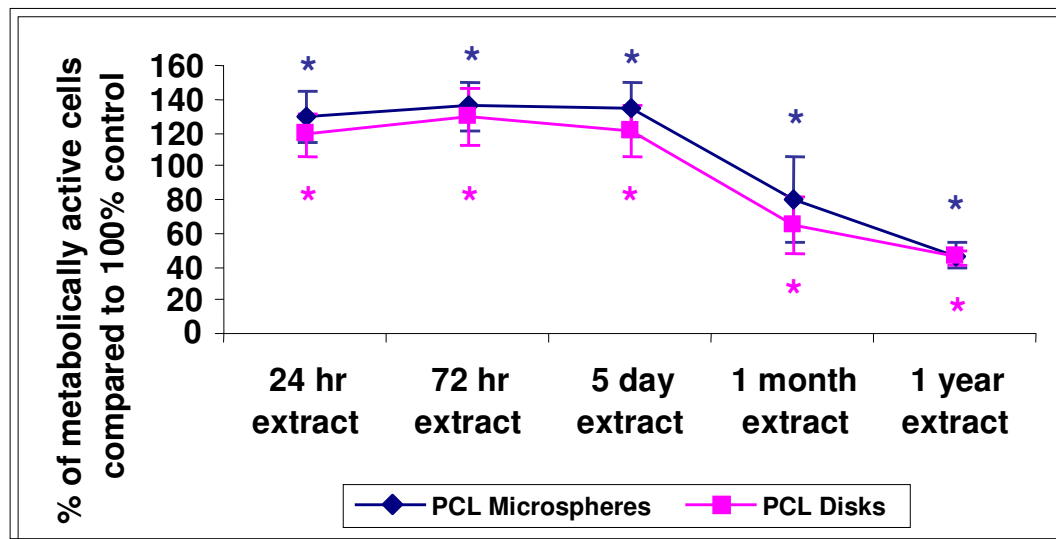


Figure 3.1.1: SKUT cell metabolic activities when cultured for 24 h on PCL degradation extracts. Metabolic activity expressed as a percentage of the control after 24 hr in PCL solid microspheres (dark blue) and PCL disks (pink) extracts. Extracts were prepared for 24 hr, 72 hr, 5 day, 1 month and 1 year time intervals. Cells were cultured for 24 hrs on the PCL-conditioned medium. All experiments were conducted thrice with n=12, the results indicate the overall average. * $P < 0.05$ illustrate statistical significance when comparing PCL disk and PCL microsphere extracts to the control medium.

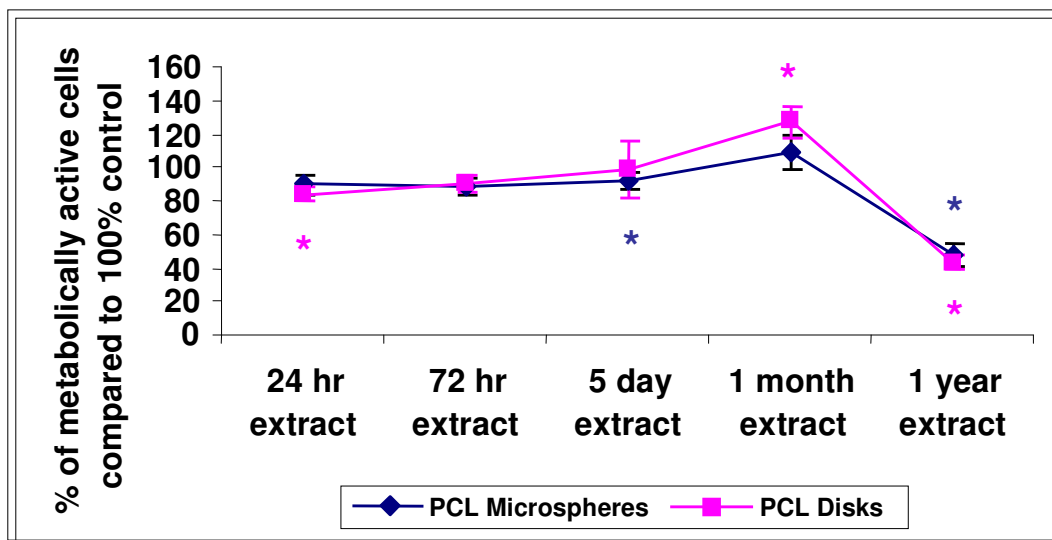


Figure 3.1.2: CRL-1701 cell metabolic activities when cultured for 24 h on PCL degradation extracts. The metabolic activity is expressed as a percentage of the control after 24 hr in PCL solid microspheres (dark blue) and PCL disks (pink) extracts. Extracts were prepared for 24 hr, 72 hr, 5 day, 1 month and 1 year time intervals. Cells were cultured for 24 hrs on the PCL-conditioned medium. All experiments were conducted thrice with n=12, the results indicate the overall average. * $P < 0.05$ illustrate statistical significance when comparing PCL disk and PCL microsphere extracts to the control medium.

3.1.2 pH assessment of degradation extracts

As seen in table 3.1.2 the control medium remained at a constant neutral pH of 7.7 from the 24 hr extract right through to the 1 year long extract. The pH of the PCL microsphere extract declined sooner than the disks' extract, being at 7.6 after 72 hr and 7.5 at 5 days; compared to 7.7 at 72 hr and 7.6 at 5 days. Both the PCL disk and PCL microsphere extracts revealed the same pH at 1 month and 1 year degradation time periods at pH 7.5 and 7.4 respectively.

Table 3.1.2: pH determinations of control medium and PCL disk and microsphere extracts. The control medium remained at a constant pH of 7.7 from 24 hr through to 1 year. The PCL disk and PCL microsphere extracts revealed a similar decline in pH, with both of the extracts resulting in a drop of pH from 7.7 at 24 hr to 7.4 after 1 year.

	24 hr	72 hr	5 days	1 month	1 year
Control medium	7.7	7.7	7.7	7.7	7.7
PCL disk extract medium	7.7	7.7	7.6	7.5	7.4
PCL sphere extract medium	7.7	7.6	7.5	7.5	7.4

3.1.3 Assessment of cell viability by the determination of membrane integrity using the qualitative PI/HO assay

The fluorescent stains PI and HO are impermeable and permeable respectively to the intact cell membrane [80]. Since cell membranes are impermeable to PI, in areas where a red fluorescence is emitted, the cells are damaged and/or apoptotic. HO is permeable to the cell membrane and stains the chromosome of the cells with a blue fluorescence. Chromosomal staining allows the distinguishing of the different mitotic stages of the cell [80].

Metabolic activity determination revealed similar values with both the SKUT and CRL-1701 cell lines across the time frames. However, the cells revealed opposite trends in metabolic activity when cultured on the 1 month extracts: the SKUT cells' metabolic activity significantly declined with both the PCL disk and PCL microsphere extracts compared to the control, whereas the metabolic activity of the CRL-1701 cell line was observed to increase with both the PCL disk (statistically significant) and PCL

microsphere extracts when compared to the control. Therefore the effect of the 1 month degradation extracts was further investigated by means of PI/HO.

The SMC nucleus appears as a long rod-like structure with the staining of the chromosome. The SKUT and CRL-1071 cells grown for 24 hr on the 1 month TCP control medium extractions were exposed to PI/HO and the stained cells are illustrated in figures 3.1.3.1 (a) and 3.1.3.2 (d) respectively. The SKUT cells demonstrated excellent cell viability as no apoptotic or necrotic cells were detected. The cells were observed to be in a uniform distribution of the cell phases, with most of the cells within metaphase, illustrating cell division, and proliferation at 24 hrs post seeding. However, at 24 hrs the CRL-1701 cells displayed only viable cells which were mainly seen to be within interface and prophase, indicative of cellular senescence.

The SKUT and CRL-1071 cells grown for 24 hr on the extracts obtained from the PCL disk in medium are illustrated in figures 3.1.3.1 (b) and 3.1.3.2 (e) respectively. These cells were stained with PI/HO and viewed under a fluorescent microscope. The SKUT and CRL-1701 cells demonstrated excellent cell viability where, again, the cells were observed to be in a uniform distribution of the cell phases, though most of the cells were within interphase and prophase, indicative of cellular senescence.

The SKUT and CRL-1071 cells grown for 24 hr on the 1 month PCL microsphere medium extractions were exposed to PI/HO and the stained cells are illustrated in figures 3.1.3.1 (c) and 3.1.3.2 (f) respectively. The SKUT cells demonstrated excellent cell viability and were observed to be in a uniform distribution of the cell phases, with most of the cells within metaphase and anaphase, illustrating cell division and proliferation. In contrast, the CRL-1701 cells displayed only viable cells which were mainly seen to be within interphase and prophase, indicative of cellular senescence.

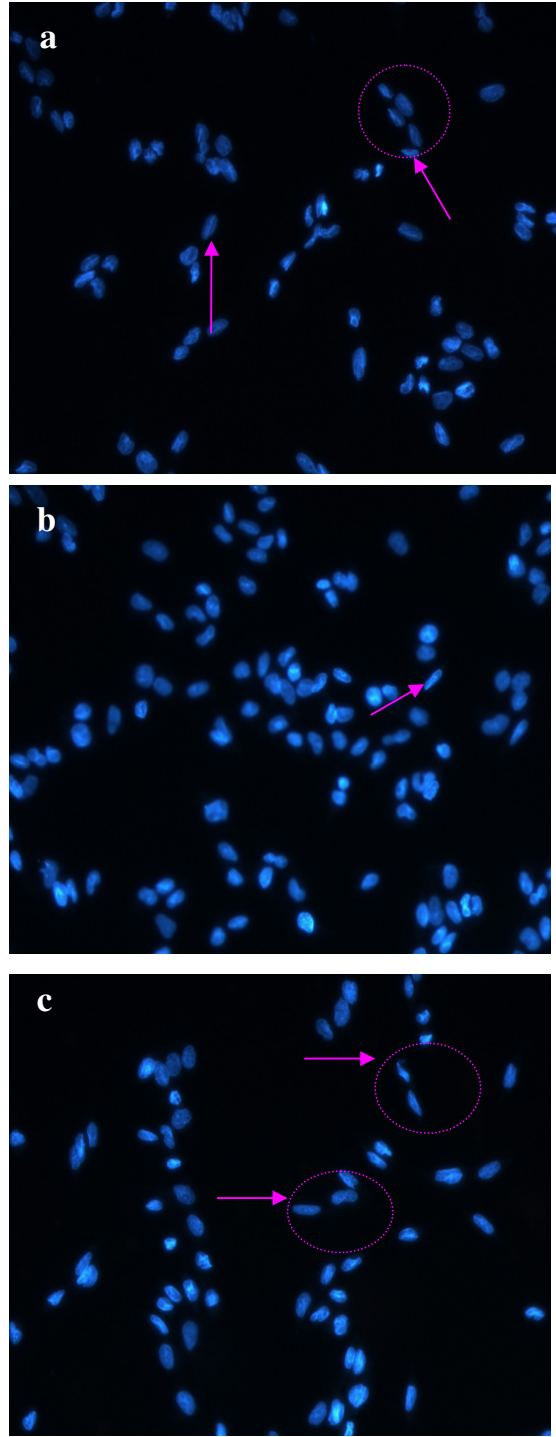


Figure 3.1.3.1 SKUT cell membrane integrity and chromosomal staining when cultured for 24 hr in 1 month TCP (a), PCL disk (b) and PCL microsphere (c) extracts: PI/HO fluorescent staining illustrating cell viability and phases in the cell cycle of SKUT cells. Pink arrows indicate metaphase. Micrographs taken at 100x magnification.

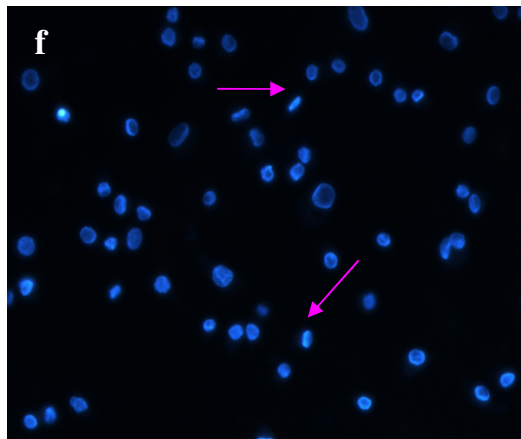
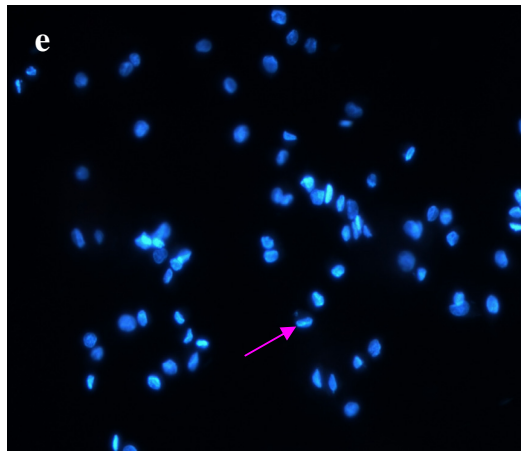
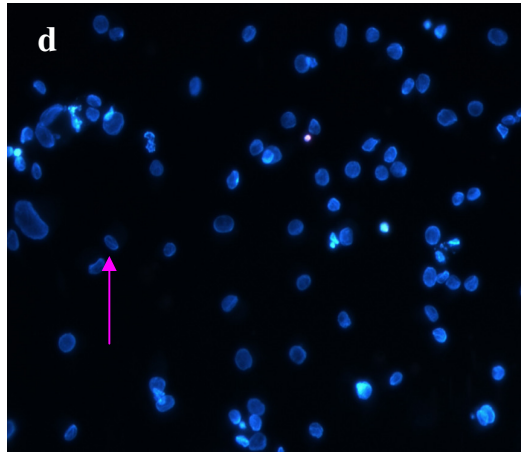


Figure 3.1.3.2 CRL-1701 cell membrane integrity and chromosomal staining when cultured for 24 hr in 1 month TCP (a), PCL disk (b) and PCL microsphere (c) extracts: PI/HO fluorescent staining illustrating cell viability and phase in the cell cycle of the CRL-1701 cells. Pink arrows indicate metaphase. Micrographs taken at 100x magnification.

3.2 The benefits of pre-conditioning PCL polymers for 24 hrs in complete medium

3.2.1 Qualitative SEM data of SKUT and CL-1701 cells grown on PCL disks which were pre-conditioned in PBS, partial medium and complete medium

SKUT cells grown on PCL disks, where the PCL disks were pre-conditioned in the PBS control for 24 hrs, was viewed under SEM. Micrographs were taken at 100x and 500x magnification as seen in figure 3.2.1.1 a and b respectively. SEM views at 100x and 500x magnification respectively of SKUT cells grown on PCL disks, where the PCL disks were pre-conditioned to partial medium and complete medium respectively, are illustrated in figure 3.2.1.1 c & d and figure 3.2.1.1 e & f respectively. Partial medium pre-conditioning was seen to improve cellular attachment density when compared to the PBS control. When the PCL disks were pre-conditioned in complete medium, a notable difference was observed where the SKUT cells attached with a packed cell density.

The SEM micrographs taken at 100x and 500x magnification respectively of CRL-1701 cells grown on PCL disks, where the PCL disks were pre-conditioned for 24 hrs in the PBS control are illustrated respectively in figure 3.2.1.2 g and h. CRL-1701 cells grown on PCL disks viewed under SEM at 100x and 500x magnifications, where the PCL disks were pre-conditioned to partial medium and complete medium respectively are illustrated in figure 3.2.1.2 i & j and figure 3.2.1.2 k & l respectively. The attachment density of the CRL-1701 cells was sparse on PCL disks pre-conditioned in PBS. However, an increased cell attachment density was observed on PCL disks treated partial medium and complete medium. Once again, the PCL disks pre-conditioned in complete medium supported the greater amount of initial cell attachment as qualitatively observed in the cell density.

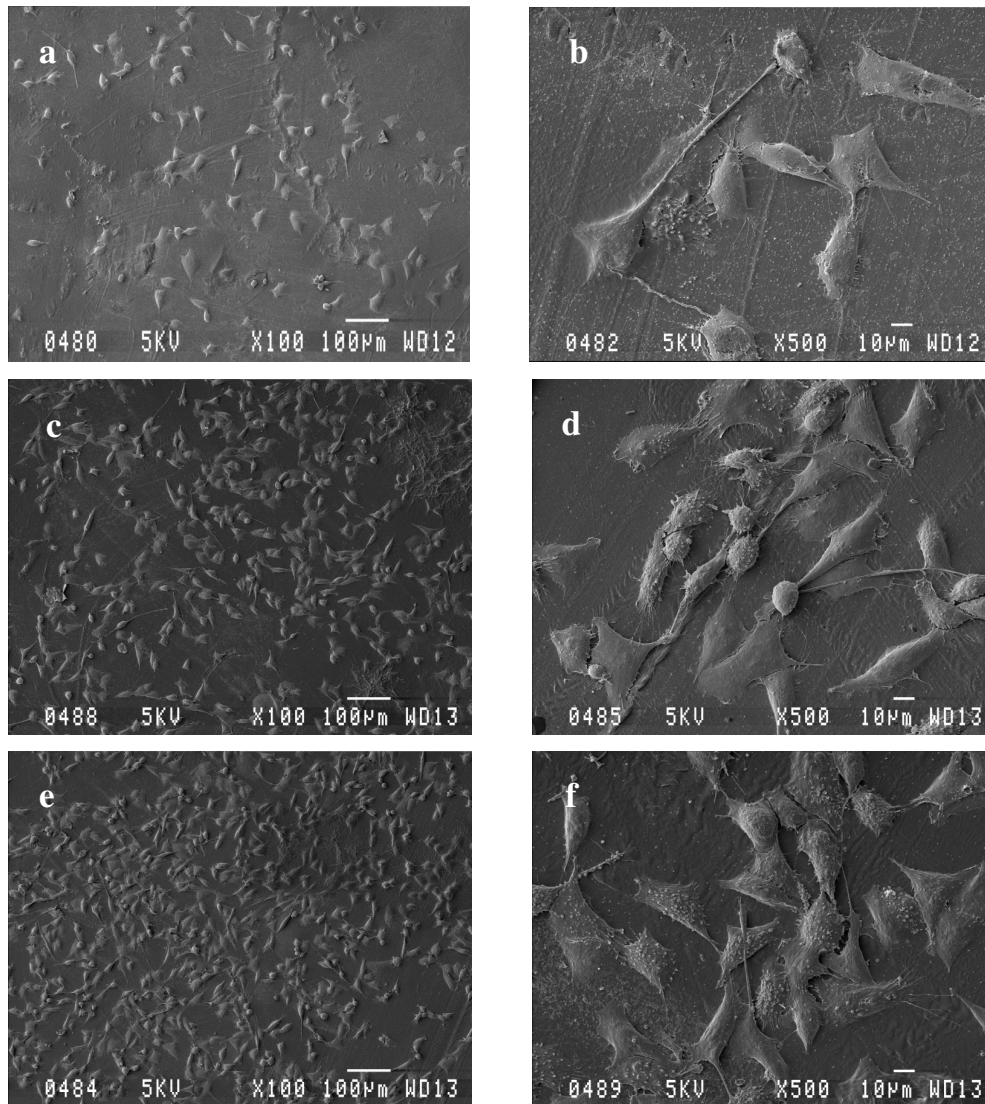


Figure 3.2.1.1: Qualitative SEM micrographs illustrating SKUT cells attached for 24 hrs on PCL disk surface: a and b: Cells grown on PCL disks treated with the PBS control at 100x and 500x magnification respectively. c and d are micrographs of cells attached on PCL disks pre-conditioned with partial medium at 100x and 500x magnifications respectively. e and f : cells attached on PCL disks pre-conditioned in complete medium at 100 and 500x magnifications.

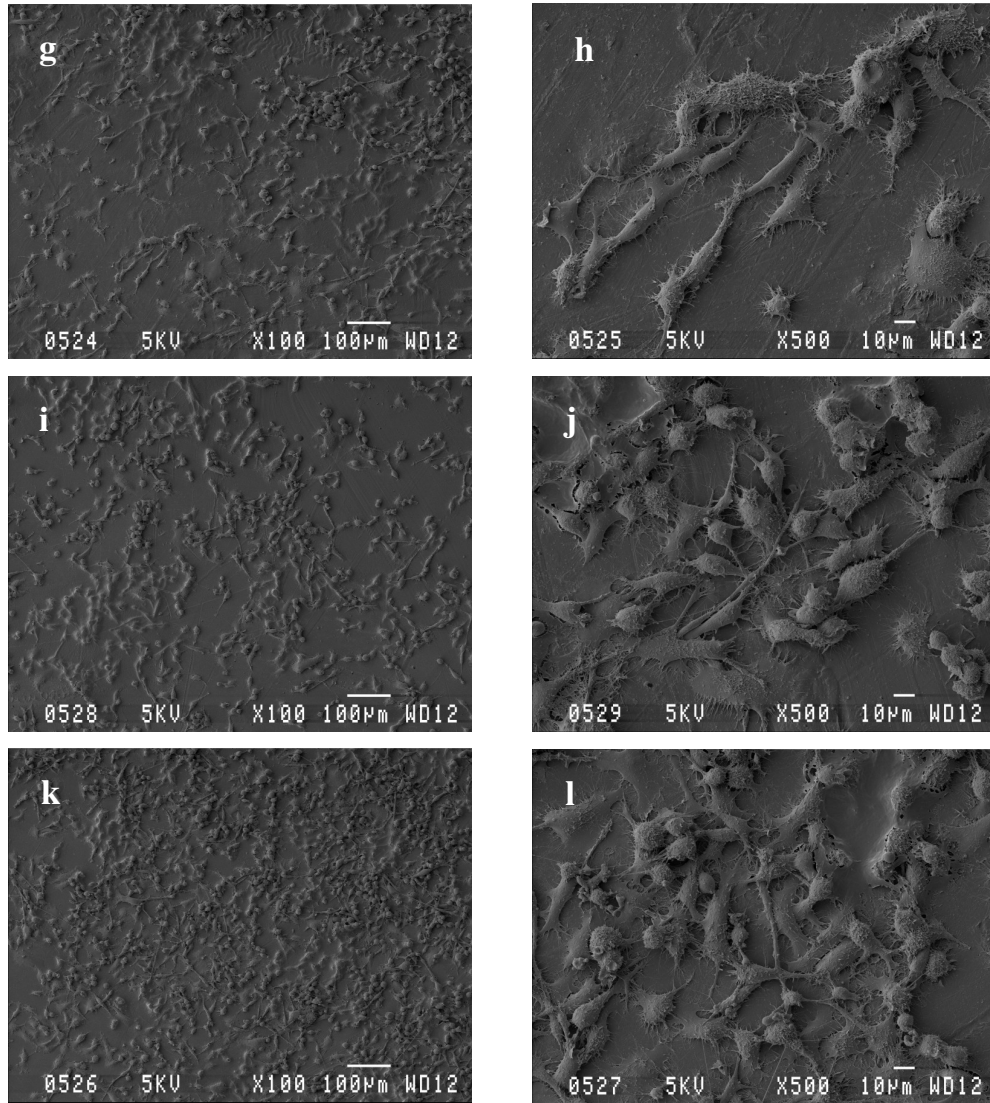


Figure 3.2.1.2: Qualitative SEM micrographs illustrating CRL-1701 cells attached for 24 hrs on PCL disk surface: figures g and h illustrate cells grown on PCL disks treated with the PBS control at 100x and 500x magnification respectively. i and j are micrographs of cells attached on PCL disks pre-conditioned with partial medium at 100x and 500x magnifications respectively. k and l : cells attached on PCL disks pre-conditioned in complete medium at 100 and 500x magnifications.

3.3 Analysis of the cell cycle

3.3.1 Determination of the cell cycle characteristics of SKUT and CRL-1701 cell lines when grown in a time dependant manner on the PCL polymer using flow cytometry

Analysis of cells proliferating using the flow cytometry technique is valuable for determining the progress of cells through the cell cycle (G_1 - S - G_2 - M), and therefore allow for a quantitative ratio amount of cells actively proliferating.

Percentage of SKUT and CRL-1701 cells in the $G_0/1$, S and G_2/M phases on the TCP control, PCL disks (2D model) and PCL solid and ported microspheres (3D models) when allowed to proliferate for 24 hrs, 72 hrs and 5 days are illustrated in figures 3.3.1.1 – 3.3.1.6. The data is reported as the averages of three independent experiments.

3.3.1a SKUT cell cycle progression

When grown on the control TCP, the $G_0/1$ phase remained constant at 50% at 24 hrs, 48% at 72 hrs followed by 52% after 5 days. The S phase was observed to remain stable varying from 24 hrs, 72, hrs and 5 days at 22, 20 and 17% respectively. The cycling cells within the G_2/M phase remained steady from 26% at 24 hrs, followed by 31% at 72 hrs, and finally 27% after 5 days.

When grown on the PCL disk, little variation in cell cycle distribution was observed. The $G_0/1$ phase varied between 58% and 55% at hrs 24 and 72, but rose to 62% on day 5 which was significantly higher than the TCP control. The percentage cells S phase was significantly lower at 17% after 24 hrs which was similar to the control at 72 hrs at 15%, but significantly lower than the control at 10% after 5 days. The G_2/M phase varied between 23% at 24 hrs, 25% after 5 days. This was significantly lower than the control after 72 hrs at 24%.

However, cells grown on the PCL microspheres illustrated a very different trend from those grown on the TCP and PCL disks. The cell cycle distribution was also observed to alter dramatically over the time periods.

When grown on the PCL solid microspheres, cells within the G₀/1 phase were seen to progressively decrease from 61% at 24 hrs (significantly higher than the control), followed by 45% at 72 hrs and 34% (significantly lower than the control and the cells grown on the PCL disk) after 5 days. This was accompanied by a progressive increase in the G₂/M phase from 18% at 24 hrs (significantly lower than the control), followed by 34% at 72 hrs (significantly higher than the PCL disk) and 36% after 5 days, being significantly higher than both the control and the cells grown on the PCL disk). The S phase remained basically the same throughout, ranging from 20%, 19% and 23% (significantly higher than the control) after 24 hrs, 72 hrs and 5 days respectively.

When grown on the PCL ported microspheres, cells within the G₀/1 phase within the first 72 hrs were seen to be significantly elevated when compared to the cells grown on the control as well as the PCL solid microspheres: 71% after 24 hrs and 77% after 72 hrs. This was accompanied by significantly lower S and G₂/M phases once again when compared to the cells grown on the control as well as the PCL solid microspheres. S phase: 12% followed by 10%, G₂/M phase: 14% followed by 12% after 24 hrs and 72 hrs respectively. After 5 days in culture, the cells within the G₀/1 phase reduced to 58% (significantly higher than the cells grown on the PCL solid microspheres, though within the same range as the control), the cells within the S phase increased to 18% and the cell cycling within the G₂/M phase increased to 20%, though this remained significantly lower than both the control and the cells grown on the PCL solid microspheres.

3.3.1b CRL-1701 cell cycle progression

When grown on the TCP control, the G₀/1 phase of the cell cycle remained stable. It ranged between 54% at 24 hrs, 49% at 72 hrs and 56% at 5 days. The S phase continued to drop as culture time progressed from 24 hrs, 72 hrs and 5 days; 22%, 13% and eventually 9% respectively. The G₂/M phase remained relatively high throughout the time periods cultured. The cycling cells ranged from 21% after 24 hrs, 37% after 72 hrs and 34% after 5 days.

Analysis of the CRL-1701 cells grown on the TCP illustrated a highly proliferative rate, as is characterized by this cell line.

As the cells proliferated on the PCL disks, the G₀/1 phase remained steady for 24 and 72 hrs at 75% and 72% respectively, both values being significantly higher than the control. This, however, dropped to 59% on day 5; within the same range as the control. The cell percentage was observed to drop from 15% to 3% (both values being significantly lower than the control) during 24 hrs and 72 hrs respectively during the S phase. The phase rose, however, on day 5 to 10% (significantly higher than the control). The G₂/M proliferative phase increased steadily to 9% at 24 hrs, 23% at 72 hrs (both significantly lower than the control) and 29% at 5 days.

When cultured on the PCL solid microspheres, the G₀/1 ranged between 78% at 24 hrs, 67% at 72 hrs and 77% at 5 days, all values were significantly higher than the control. The S phase went from 11% (significantly lower than the control) and 10% (significantly higher than the cells grown on the PCL disk) at 24 and 72 hrs respectively. A sharp decline of S phase cells at day 5 took them to 3%, being significantly lower than the control and the PCL disk. G₂/M cells varied from 10% at 24 hrs, 23% at 72 hrs and 19% at 5 days, all values being significantly lower than the control in addition with the 19% after 5 days being significantly lower than the cells grown on the PCL disk. The steep decline of cells in the S phase at 72 hrs (3%) may be suggestive of a G₀/1 block.

When cultured on the PCL ported microspheres, the G₀/1 phase remained significantly higher than the control throughout all three time frames. It was also significantly higher to the PCL solid microspheres after 72 hrs. However, this significance dropped to below the PCL solid microspheres after 5 days. The values were as follows: 66% after 24 hrs, 77% after 72 hrs and 72% after 5 days. The cells cycling through the S phase remained significantly lower than the control throughout in addition to being significantly lower than the PCL solid microsphere at the 72 hr time frame: 9% after 24 hrs, 4% after 72 hrs and 3% after 5 days in culture. The G₂/M ranged between 24% at 24 hrs (significantly higher than those on the PCL solid microspheres), 18% at 72 hrs (significantly lower than both the control as well as the PCL solid microspheres) and 22% after 5 days which remained significantly lower than the control.

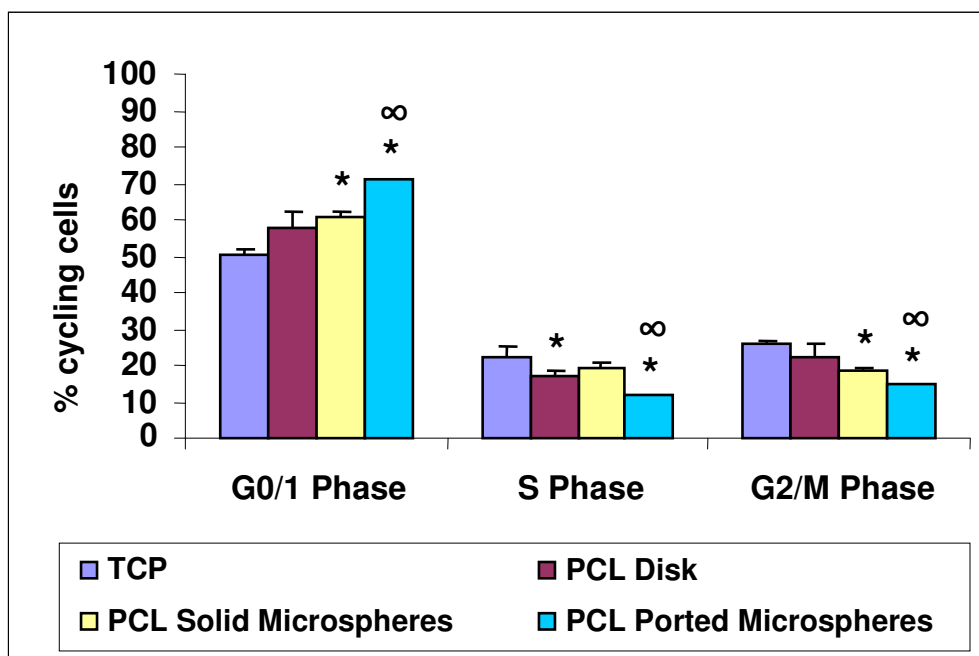


Figure 3.3.1.1: Flow cytometric analysis illustrating percentage of SKUT cells cycling through the G_{0/1}, S and G_{2/M} phases of the cell cycle after 24 hrs proliferation. Cells were allowed to attach for 24 hrs on the TCP (purple bars), PCL disk (maroon bars), PCL solid microspheres (yellow bars) and PCL ported microspheres (blue bars). All experiments were conducted thrice with n=3, the results indicate the overall average. **P*<0.05, comparing PCL disk, solid microspheres and ported microspheres to TCP control, #*P*<0.05 comparing PCL solid microspheres to PCL disk, ∞*P*<0.05 comparing PCL ported microspheres to PCL solid microspheres. Error bars indicate standard deviation.

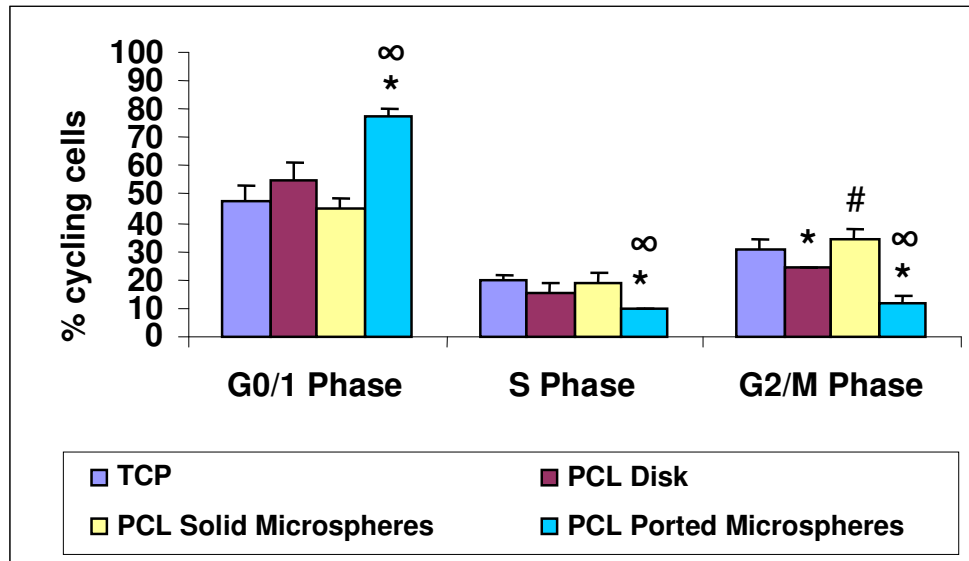


Figure 3.3.1.2: Flow cytometric analysis illustrating percentage of SKUT cells cycling through the G₀/1, S and G₂/M phases of the cell cycle after 72 hrs proliferation: Cells were allowed to grow for 72 hrs on the TCP (purple bars), PCL disk (maroon bars), PCL solid microspheres (yellow bars) and PCL ported microspheres (blue bars). All experiments were conducted thrice with n=3, the results indicate the overall average. **P*<0.05, comparing PCL disk, solid microspheres and ported microspheres to TCP control, #*P*<0.05 comparing PCL solid microspheres to PCL disk, ∞*P*<0.05 comparing PCL ported microspheres to PCL solid microspheres. Error bars indicate standard deviation.

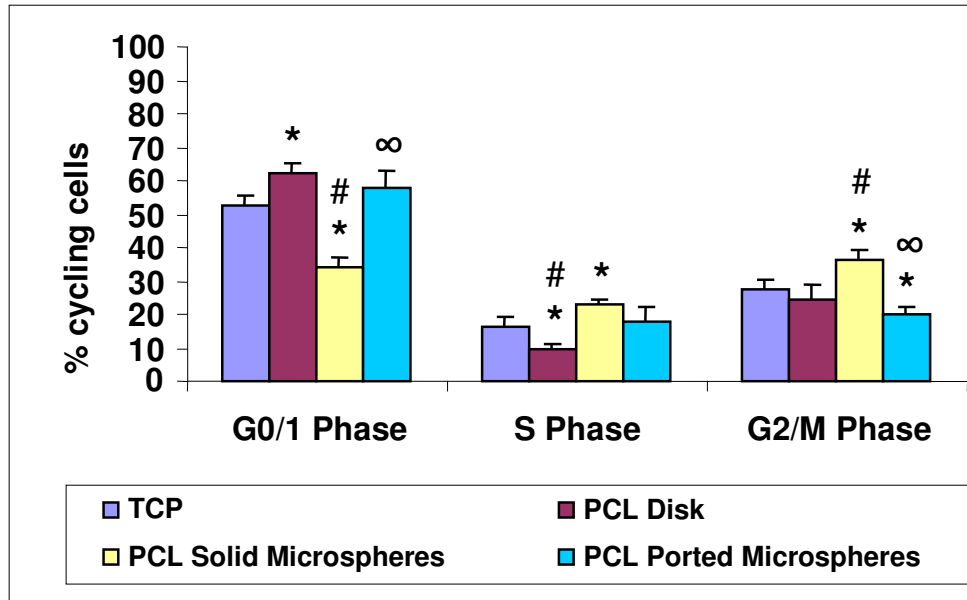


Figure 3.3.1.3: Flow cytometric analysis illustrating percentage of SKUT cells cycling through the G_{0/1}, S and G_{2/M} phases of the cell cycle after 5 days proliferation: Cells were allowed to grow for 5 days on the TCP (purple bars), PCL disk (maroon bars), PCL solid microspheres (yellow bars) and PCL ported microspheres (blue bars). All experiments were conducted thrice with n=3, the results indicate the overall average. **P*<0.05, comparing PCL disk, solid microspheres and ported microspheres to TCP control, #*P*<0.05 comparing PCL solid microspheres to PCL disk, ∞*P*<0.05 comparing PCL ported microspheres to PCL solid microspheres. Error bars indicate standard deviation.

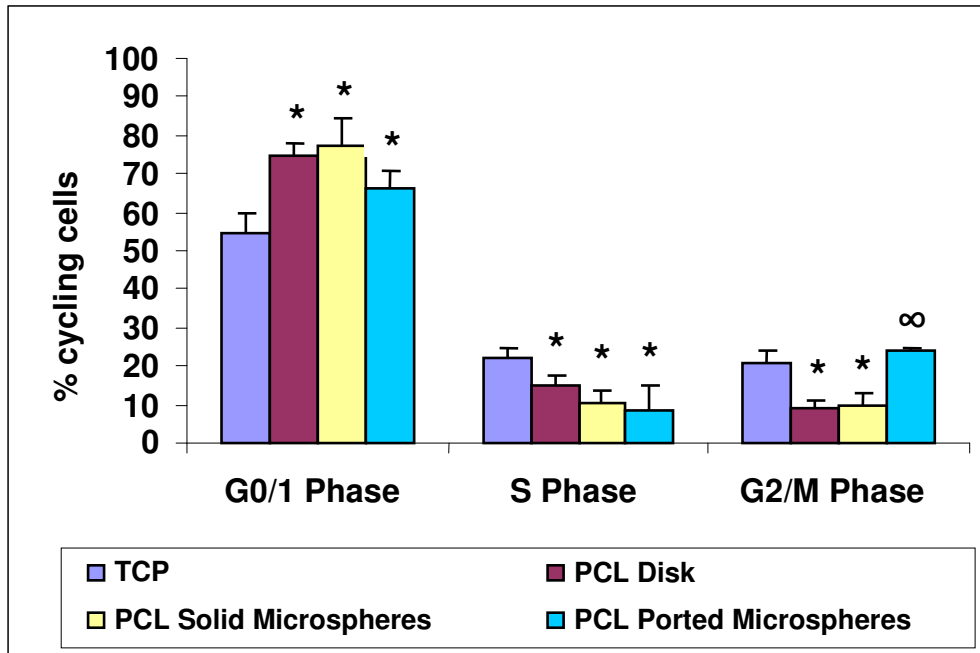


Figure 3.3.1.4.: Flow cytometric analysis illustrating percentage of CRL-1701 cells after 24 hrs cycling through the G_{0/1}, S and G_{2/M} phases of the cell cycle. Cells were allowed to attach for 24 hrs on the TCP (purple bars), PCL disk (maroon bars) PCL solid microspheres (yellow bars) and PCL ported microspheres (blue bars). All experiments were conducted thrice with n=3, the results indicate the overall average. **P*<0.05, comparing PCL disk, solid microspheres and ported microspheres to TCP control, # *P*<0.05 comparing PCL solid microspheres to PCL disk, ∞*P*<0.05 comparing PCL ported microspheres to PCL solid microspheres. Error bars indicate standard deviation.

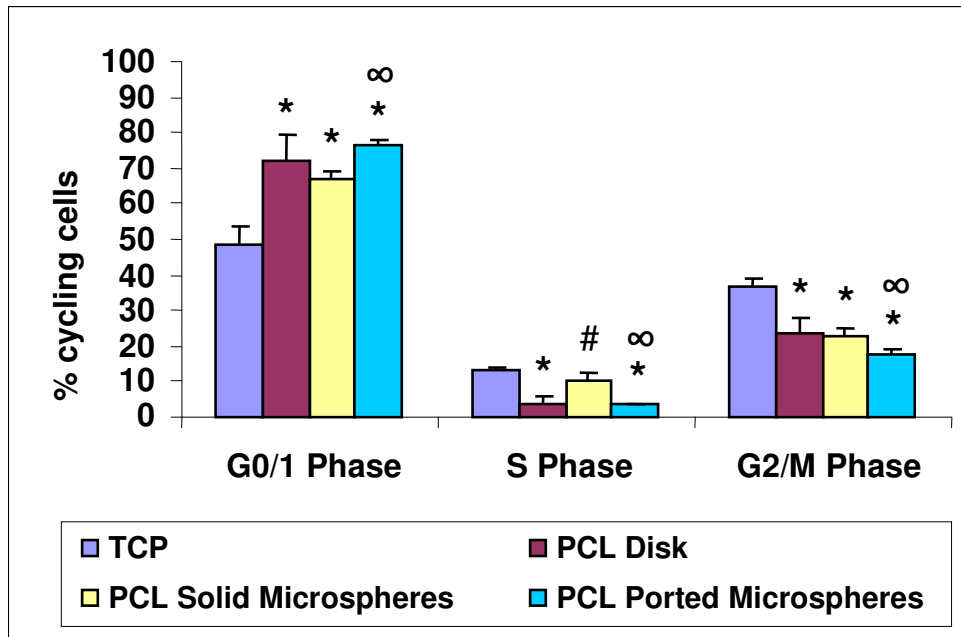


Figure 3.3.1.5: Flow cytometric analysis illustrating percentage of CRL-1701 cells after 72 hrs cycling through the G_{0/1}, S and G_{2/M} phases of the cell cycle. Cells were allowed to grow for 72 hrs on the TCP (purple bars), PCL disk (maroon bars), PCL solid microspheres (yellow bars) and PCL ported microspheres (blue bars). All experiments were conducted thrice with n=3, the results indicate the overall average. **P*<0.05, comparing PCL disk, solid microspheres and ported microspheres to TCP control, #*P*<0.05 comparing PCL solid microspheres to PCL disk, ∞*P*<0.05 comparing PCL ported microspheres to PCL solid microspheres. Error bars indicate standard deviation.

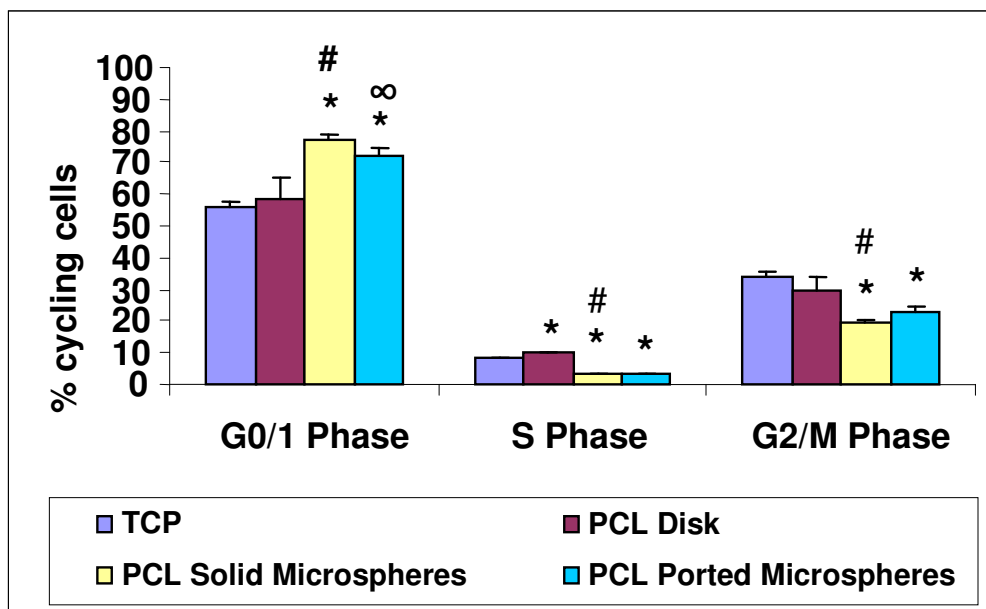


Figure 3.3.1.6: Flow cytometric analysis illustrating percentage of CRL-1701 cells cycling for 5 days through the G₀/1, S and G₂/M phases of the cell cycle. Cells were allowed to grow for 5 days on the TCP (purple bars), PCL disk (maroon bars), PCL solid microspheres (yellow bars) and PCL ported microspheres (blue bars). All experiments were conducted thrice with n=3, the results indicate the overall average. **P*<0.05, comparing PCL disk, solid microspheres and ported microspheres to TCP control, #*P*<0.05 comparing PCL solid microspheres to PCL disk, ∞*P*<0.05 comparing PCL ported microspheres to PCL solid microspheres. Error bars indicate standard deviation.

3.3.2 Quantitative analysis of SKUT and CRL-1701 cells within the S phase of the cell cycle after 5 days in culture on the PCL polymer

The incorporation of BrdU into the S phase of the of the SKUT and CRL-1701 cell lines was analyzed using Flow cytometry as illustrated in figures 3.3.2.1 and 3.3.2.2 respectively. Cells were allowed to grow for 5 days on the TCP surface (a and e), PCL disk (b and f), PCL solid microspheres (c and g) and PCL ported microspheres (d and h).

The SKUT cells grown on the TCP control (a) were concentrated within the G₀/1 phase, whereas those cells grown on the PCL disk (b) were concentrated within G₀/1 but also cycling through S and G₂ and mitosis (M). When grown on the PCL solid (c) and PCL

ported (d) microspheres, cells were observed to remain within the $G_{0/1}$ phase, with some cells cycling through to the S phase when grown on the PCL solid microspheres.

The CRL-1701 cells grown on both the TCP control (e) and PCL disk (f) were in late mitosis, proceeding through to $G_{0/1}$. The cells grown on the PCL solid microspheres (g) remained within $G_{0/1}$ whereas those cells grown on the PCL ported microspheres (h) were found to be within the G_2 phase and cycling through mitosis.

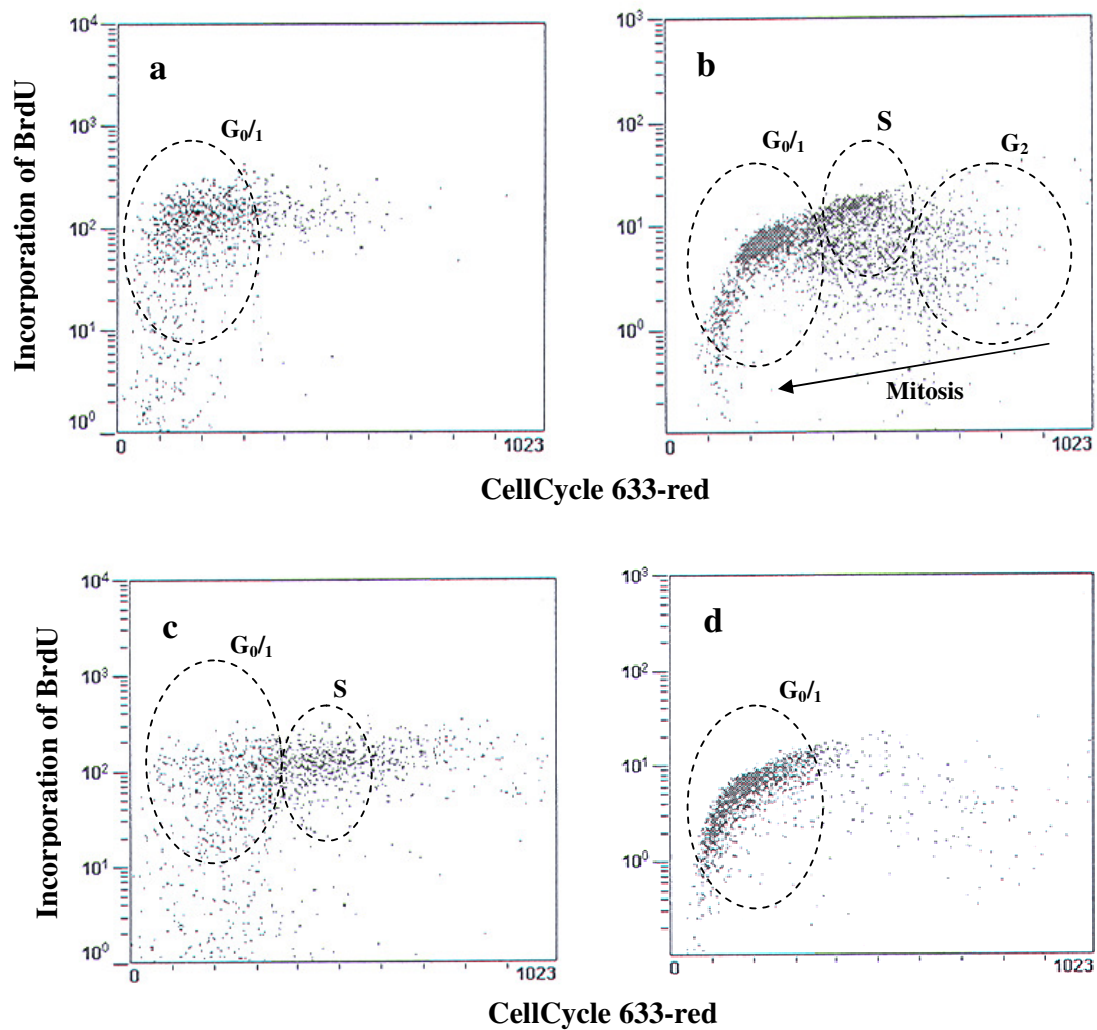


Figure 3.3.2.1: Flow cytometric analysis illustrating the incorporation of BrdU into the S phase of the SKUT cells after 5 days of proliferation: The cycling cells were stained with CellCycle 633-red in order to observe the cells through the $G_{0/1}$, S and G_2 and mitosis (M) phases of the cell cycle. Cells were allowed to grow for 5 days on the TCP (a), PCL disk (b), PCL solid microspheres (c) and PCL ported microspheres (d). All experiments were conducted in duplicate.

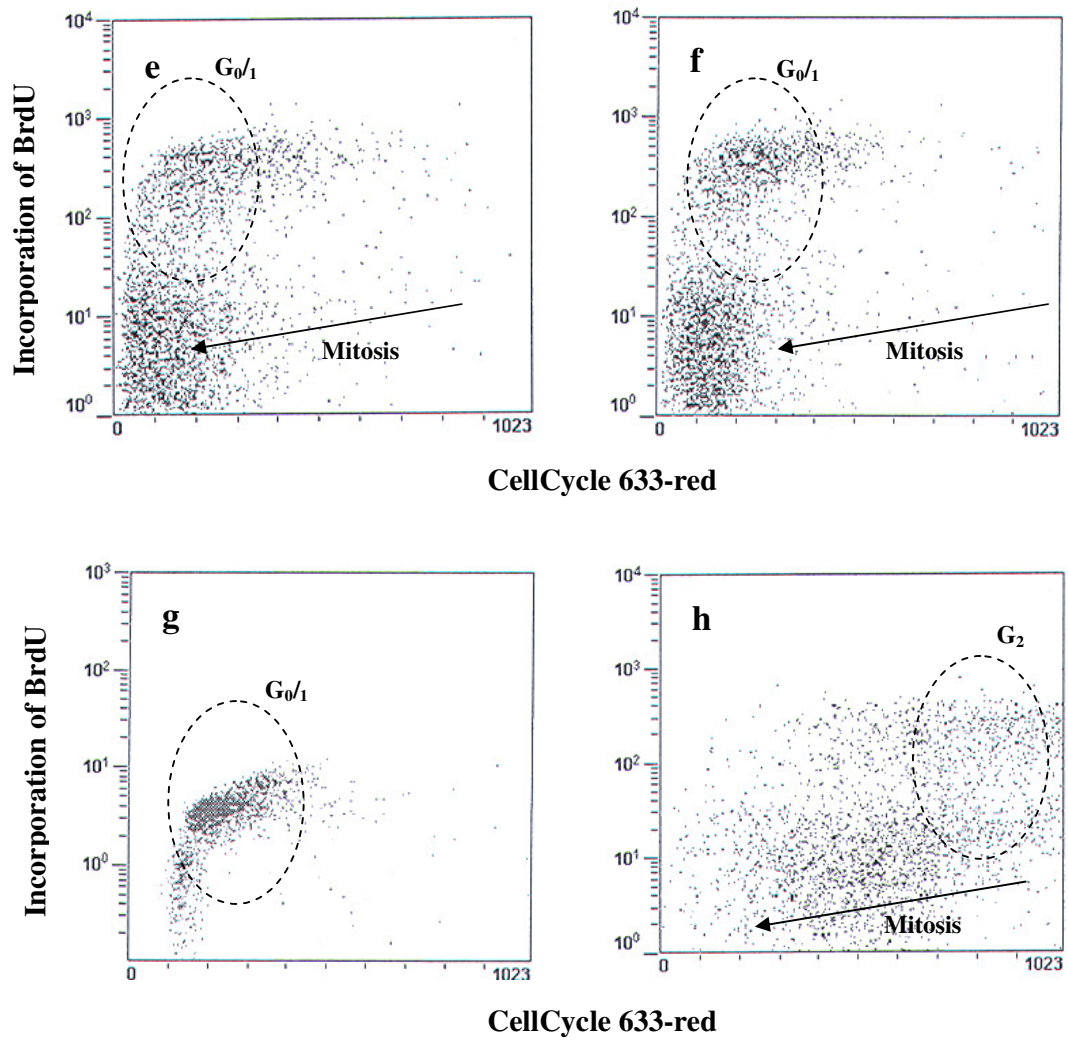


Figure 3.3.2.2: Flow cytometric analysis illustrating the incorporation of BrdU into the S phase of the CRL-1701 cells after 5 days proliferation: The cycling cells were stained with CellCycle 633-red in order to observe the cells through the G₀/1, S and G₂ and mitosis (M) phases of the cell cycle. Cells were analyzed when grown on the TCP (e), PCL disk (f), PCL solid microspheres (g) and PCL ported microspheres (h). All experiments were conducted in duplicate.

3.4 Studies to assess the cell morphology of SKUT and CRL-1701 cells grown on 2D and 3D models of the PCL polymer

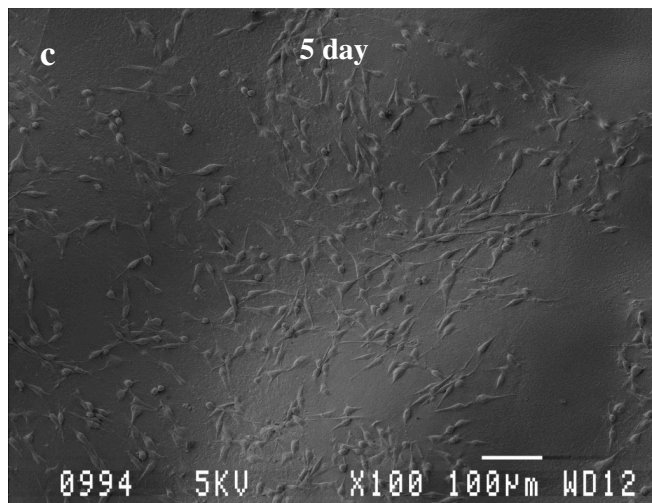
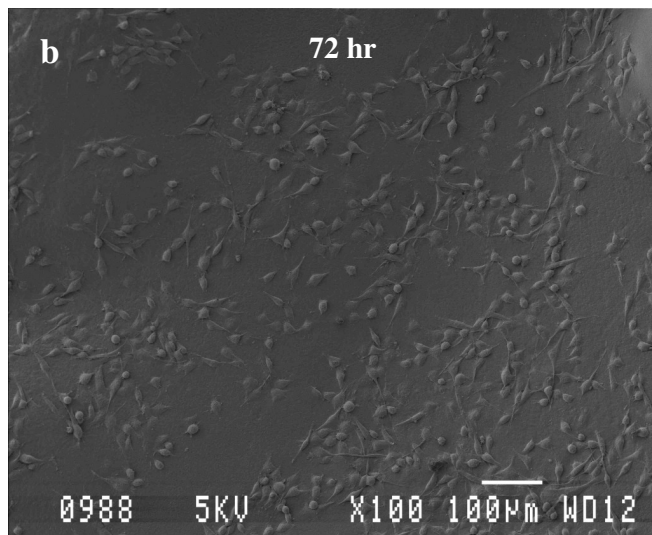
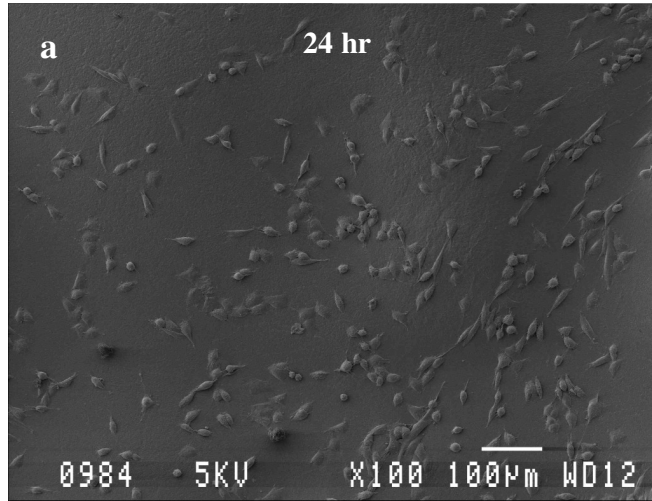
3.4.1 Cell morphology, attachment, and growth characteristics using SEM

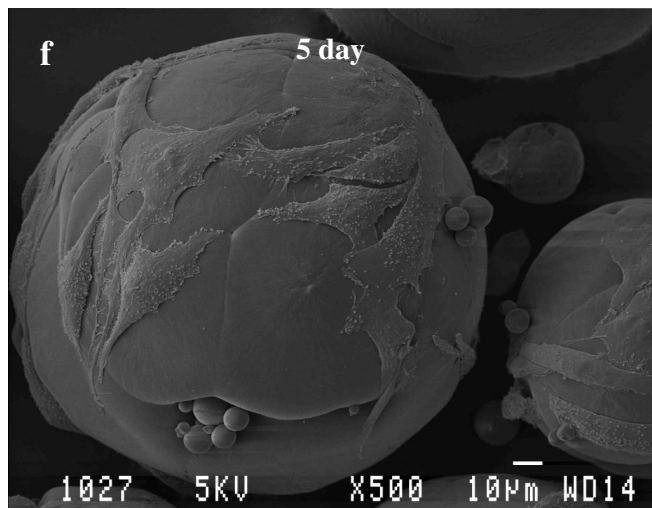
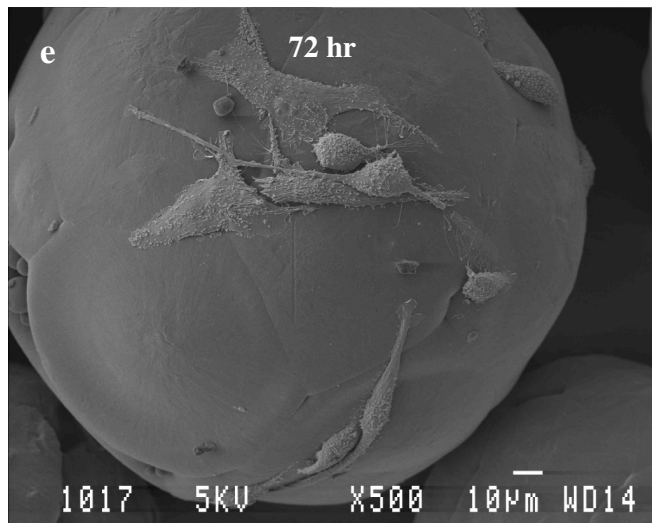
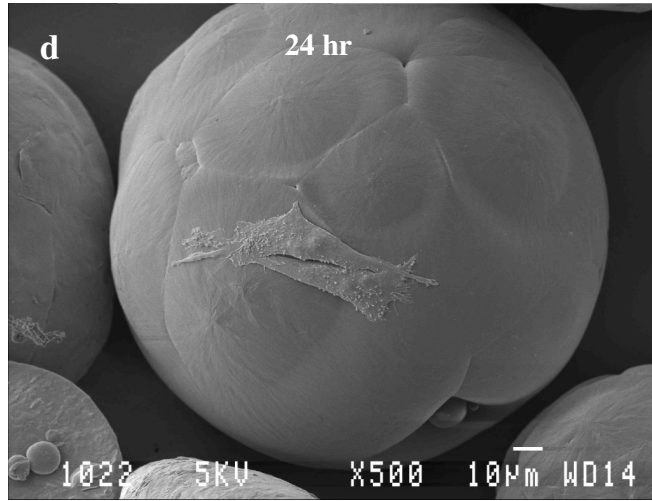
The SKUT and CRL-1701 cells were grown on the PCL polymers for the following time frames: 24 hrs, 72 hrs and 5 days. All micrographs were taken at 100x magnification.

Figure 3.4.1.1 depicts the SKUT cells grown on both the 2D (PCL disk: a, b and c) and 3D (PCL solid microspheres: d, e and f; and PCL ported microspheres: g, h and i) PCL models. Cells which have attached for 24 hrs on the PCL disk, PCL solid microspheres and PCL ported microspheres are illustrated in a, d and g respectively. Cells which have been allowed to proliferate for 72 hrs on the PCL disk, PCL solid microspheres and PCL ported microspheres are seen in b, e and f respectively; followed by the micrographs where the cells proliferated for a 5 day time period on the PCL disk, PCL solid microspheres and PCL ported microspheres are shown in c, f and i respectively. SEM illustrated the density of the SKUT cells grown on the PCL disk increased over the 5 day time period. Cells displayed spindle-like morphology and were evenly distributed throughout the entire surface. When grown on the PCL solid microspheres, once again the density of the cells increased over time, though were never as populated as they were on the disk. The morphology remained spindle-shaped with many cells undergoing mitosis. The cells were observed to wrap around the entire solid microsphere surface. The SKUT cells illustrated both mitotic, rounded cells as well as spindle-shaped, spread out when grown on the PCL ported microspheres. The cells were observed to populate around the ports of the microspheres and were noted to be migrating inside the microspheres by 72 hrs and 5 days, illustrating that they preferred the protected environment.

CRL-1701 cells depicted in figure 3.4.1.2 illustrate the cells grown on both the 2D (PCL disk: j, k and l) and 3D (PCL solid microspheres: m, n and o; and PCL ported microspheres: p, q and r) PCL models. Cells which have attached for 24 hrs on the PCL disk, PCL solid microspheres and PCL ported microspheres are illustrated in j, m and p

respectively. Cells which have been allowed to proliferate for 72 hrs on the PCL disk, PCL solid microspheres and PCL ported microspheres are seen in k, n and q respectively; followed by the micrographs where the cells proliferated for a 5 day time period on the PCL disk, PCL solid microspheres and PCL ported microspheres are shown in l, o and r respectively. The CRL-1701 cells proliferated at a faster rate than the SKUT cells and were observed to populate the entire surface of the PCL disk. The cells displayed a more fibroblast-like morphology which is characteristic of this particular cell line. Most cells were undergoing mitosis as indicated by a big, round or ovoid shaped cell. When grown on the PCL solid microsphere, the density of the cell population on the surface increased over time. The cells maintained a mainly mitotic state. Many cytoplasmic extensions were illustrated; this allowed the cells to fuse the microspheres to each other, forming larger cell/microsphere connections (micrographs not shown). Cells were well spread out on the ported PCL microspheres. It was noted that a larger population of cells seemed to occupy the inside of the microspheres as compared to the outside surface. This would be confirmed *via* confocal microscopy.





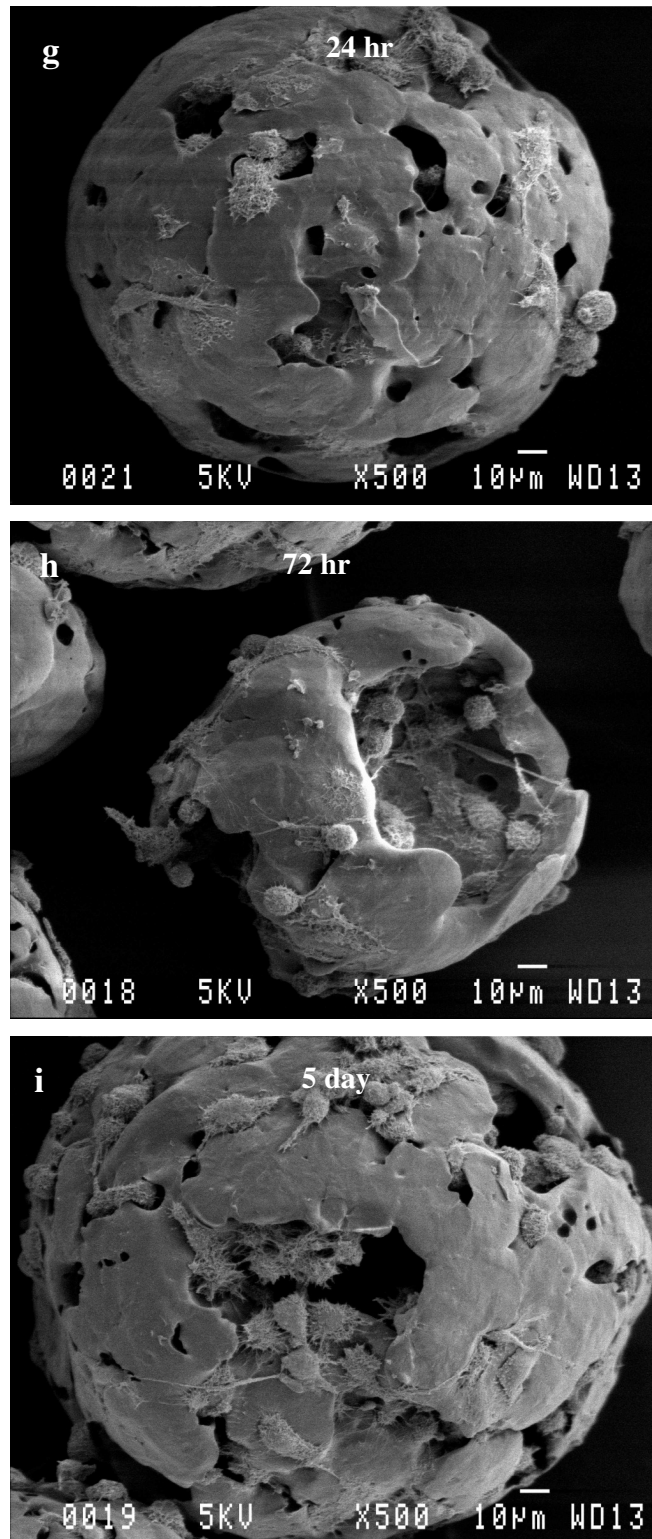
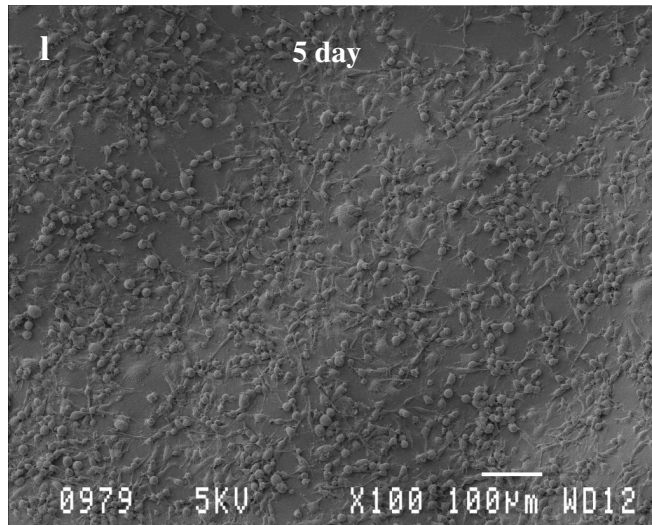
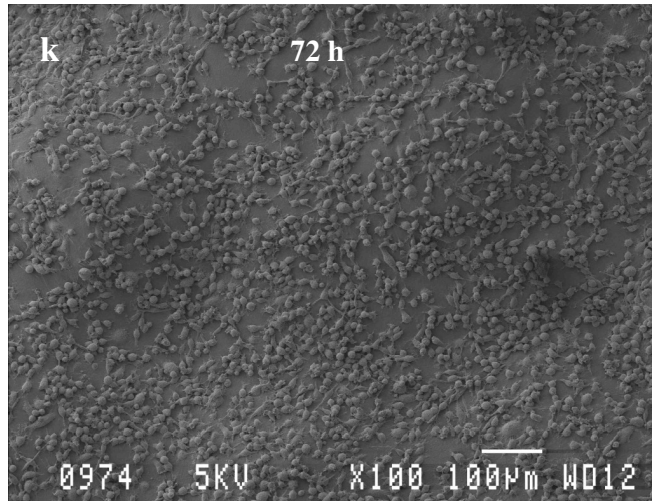
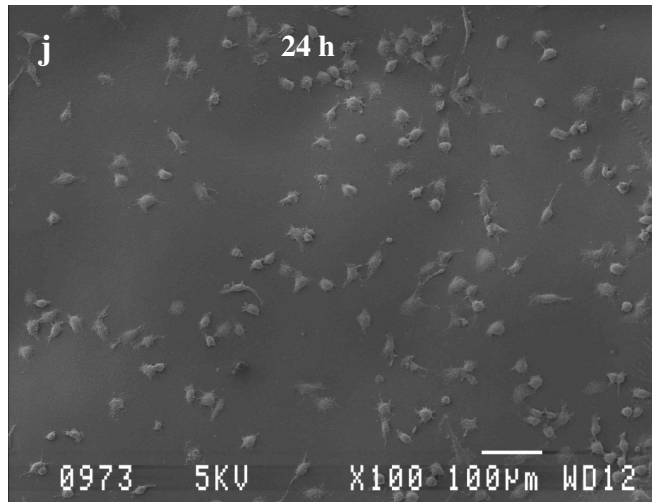
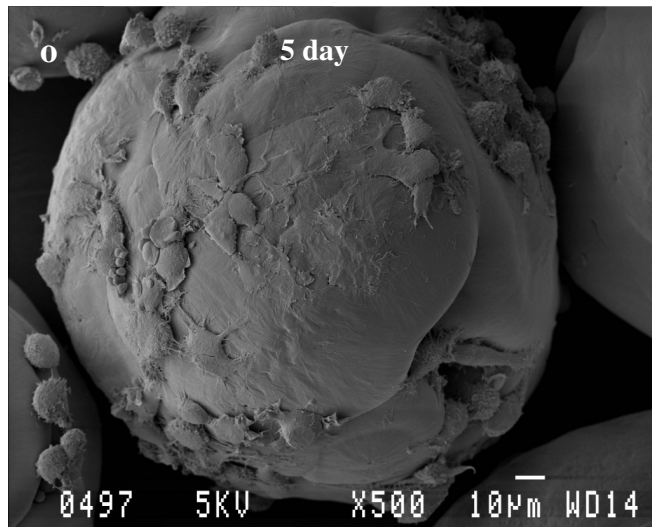
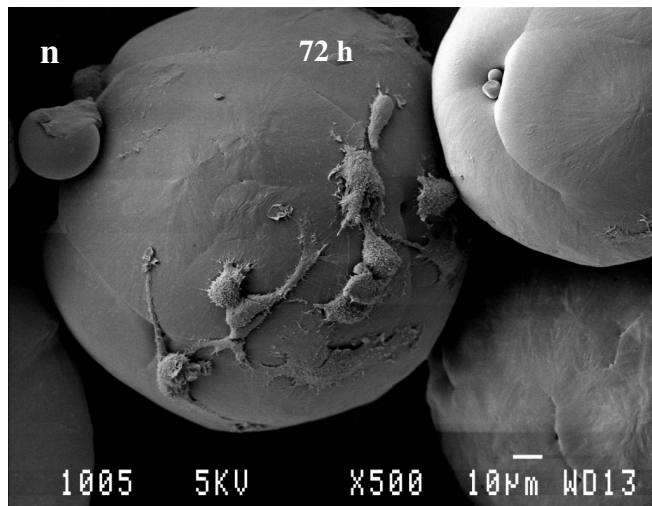
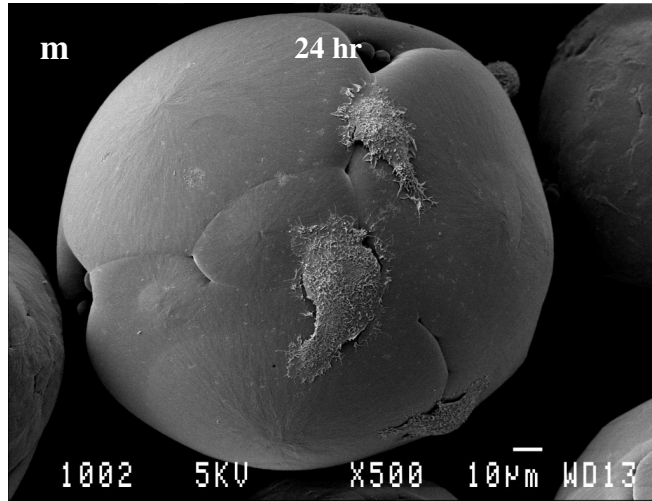


Figure 3.4.1.1: SEM micrographs illustrating SKUT cells attached for 24 hr, 72 hr, and 5 days on the 2D and 3D PCL models. PCL disk (a, b and c), the 3D PCL solid microspheres (d, e and f) and the 3D PCL ported microspheres (g, h and i) respectively. All views were taken at 100X magnification.





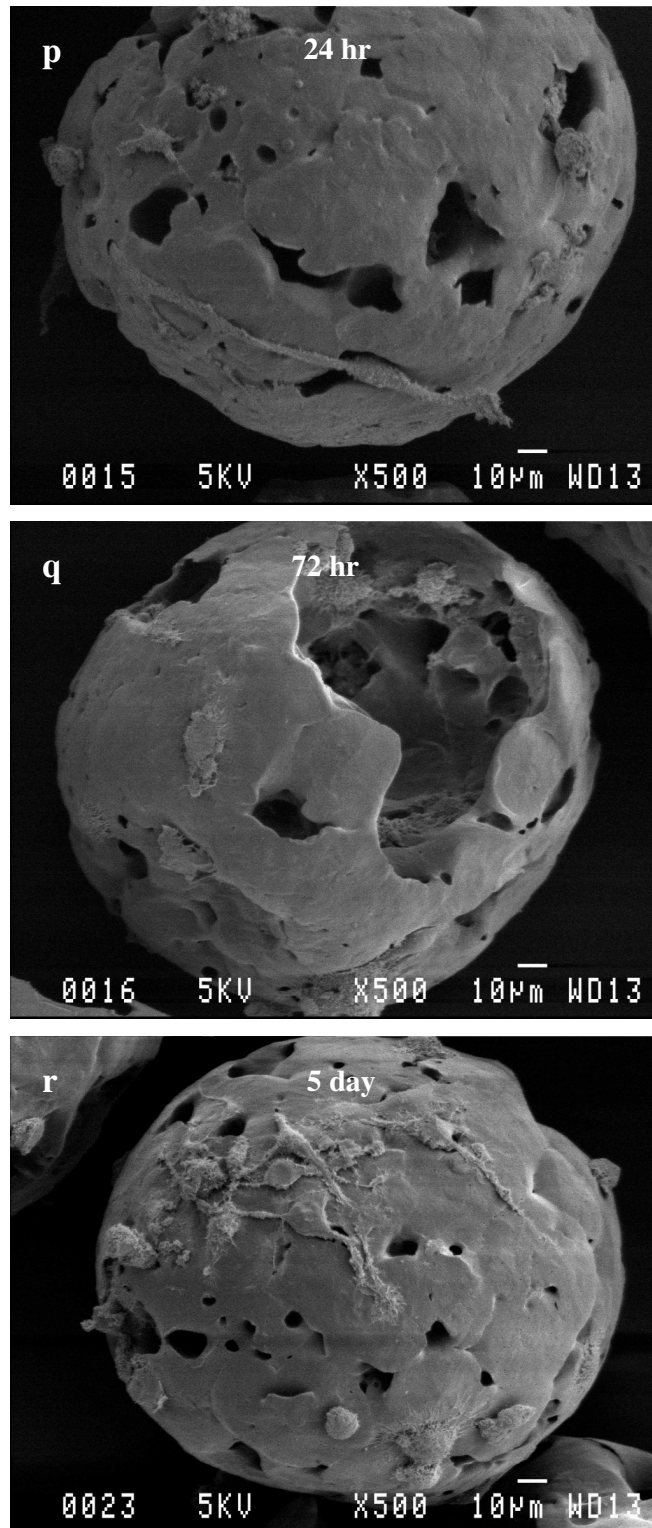


Figure 3.4.1.2: SEM micrographs illustrating the CRL-1701 cells attached for 24 hr, 72 hr, and 5 days on the 2D and 3D PCL models. PCL disk (j, k and l), the 3D PCL solid microspheres (m, n and o) and the 3D PCL ported microspheres (p, q and r) respectively. All views were taken at 100X magnification.

3.4.2 Studies to determine the morphology of the cells grown on 2D and 3D PCL models using Phalloidin staining

When viewing the cells under the fluorescent microscope, it was not possible to see the individual α -actin fibres even at a high magnification. This was attributed to the PCL background staining which could not be prevented.

Figure 3.4.2.1 illustrates the SKUT cells stained with phalloidin specific for the α -actin cytoskeleton. Cells attached for the following time periods: 24 hrs, 72 hrs and 5 days on the PCL solid microspheres (a, b and c respectively) and on the PCL ported microspheres (d, e and f respectively). Photographs were taken at 100X magnification. The SKUT cells were proliferating over the time period of 24 hrs, 72 hrs and 5 days. When focusing on different depths with the microscope, it was clear that by day 5 the SKUT cells had migrated inside the ported microspheres.

The CRL-1701 cells are seen in figure 3.4.2.2. Cells were left to attach and proliferate for the following time periods: 24 hrs, 72 hrs and 5 days on the PCL solid microspheres (h, i and j respectively) and on the PCL ported microspheres (k, l and m respectively), taken at 100X magnification.

The CRL-1701 cells increased in cell number over the time periods from 24 hrs through to 5 days. Interestingly, it was noted that the CRL-1701 cells proliferated to a greater extent when grown on the PCL ported microspheres than what they did on the PCL solid microspheres. It became evident that the cells had migrated into the ported microspheres by day 5 and that a denser population of cells existed inside these ports compared to the outside surface area.

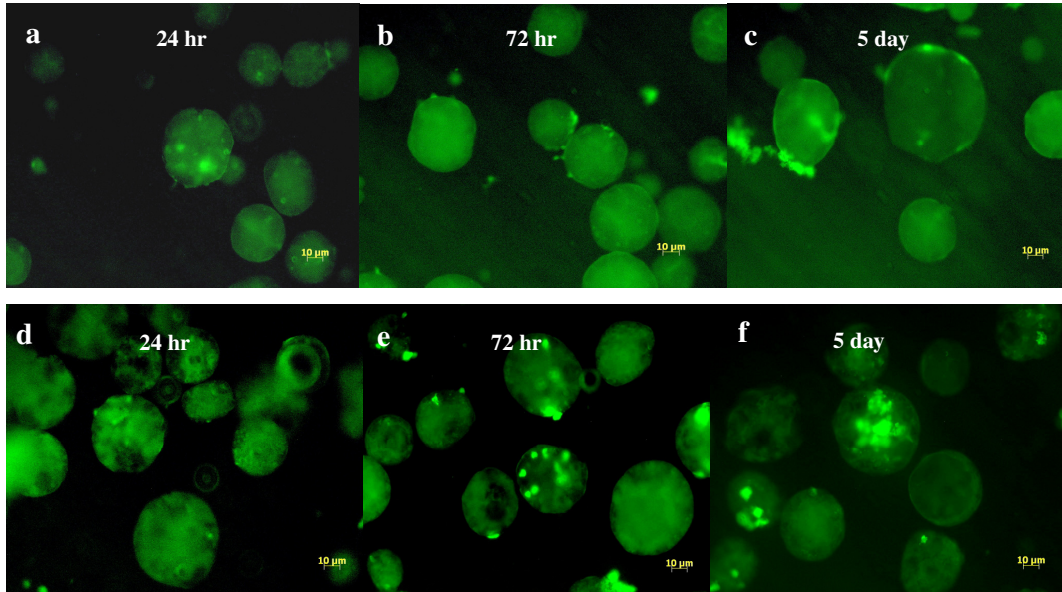


Figure 3.4.2.1: Fluorescent micrographs illustrating SKUT cells stained with phalloidin specific for the α -actin component of the SMC cytoskeleton. Cells were allowed to attach for 24 hrs, 72 hrs and 5 days on the PCL solid microspheres (a, b and c respectively) and on the PCL ported microspheres (d, e and f respectively). Photographs were taken at 100X magnification.

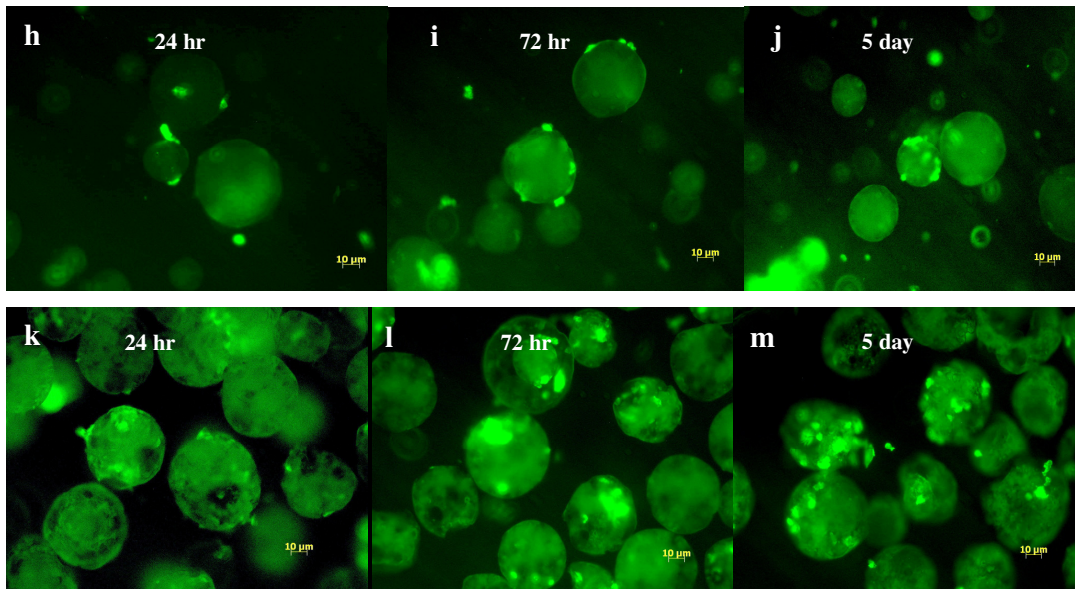


Figure 3.4.2.2: Fluorescent micrographs illustrating CRL-1701 cells stained with phalloidin specific for the α -actin component of the SMC cytoskeleton. Cells were allowed to attach for 24 hrs, 72 hrs and 5 days on the PCL solid microspheres (h, i and j respectively) and on the PCL ported microspheres (k, l and m respectively). Photographs were taken at 100X magnification.

3.5 The assessment of SKUT and CRL-1701 grown for 5 days on the 2D 3D PCL models using confocal microscopy

3.5.1 Illustration of the SKUT and CRL-1701 cells grown for 5 days on the control and PCL disk surfaces

Confocal microscopy afforded sharper images than the fluorescent microscope did. Cells were stained with phalloidin in order to view a full representation of the cell cytoskeleton.

Figures 3.5.1.1a and b illustrate the SKUT cells after 5 days of proliferation on the glass cover slip control and the PCL disk respectively. The actin cytoskeleton was visible on the control surface at 4000X magnification. When viewing the cell on the PCL disk surface, it was only possible to take pictures at a 200X magnification in order to avoid viewing the background stain of the polymer. The micrographs of the cells on the control illustrated a concentration of fibres along the perimeter of the cell cytoplasm and dense concentrations within the cytoplasmic arms. The cells grown on the PCL disk were observed to stain positively for α -actin and were stellate and polygonal in shape [94].

The CRL-1701 cells after 5 days of proliferation on the glass cover slip control and the PCL disk are illustrated in figures 3.5.1.2a and b respectively. The cells on the control and PCL disk surfaces were viewed at 4000X and 200x magnification respectively. Many of the cells allowed to proliferate on the control surface appeared spindle-shaped, with some undergoing mitosis. Once again the cells proliferating on the control surface illustrated a concentration of actin fibres along the border of the cell and within the cytoplasmic arms. The cells growing on the PCL disk surface illustrated a range of cytoplasmic shapes, from spindle to polygonal and once again stained positively for α -actin [94].

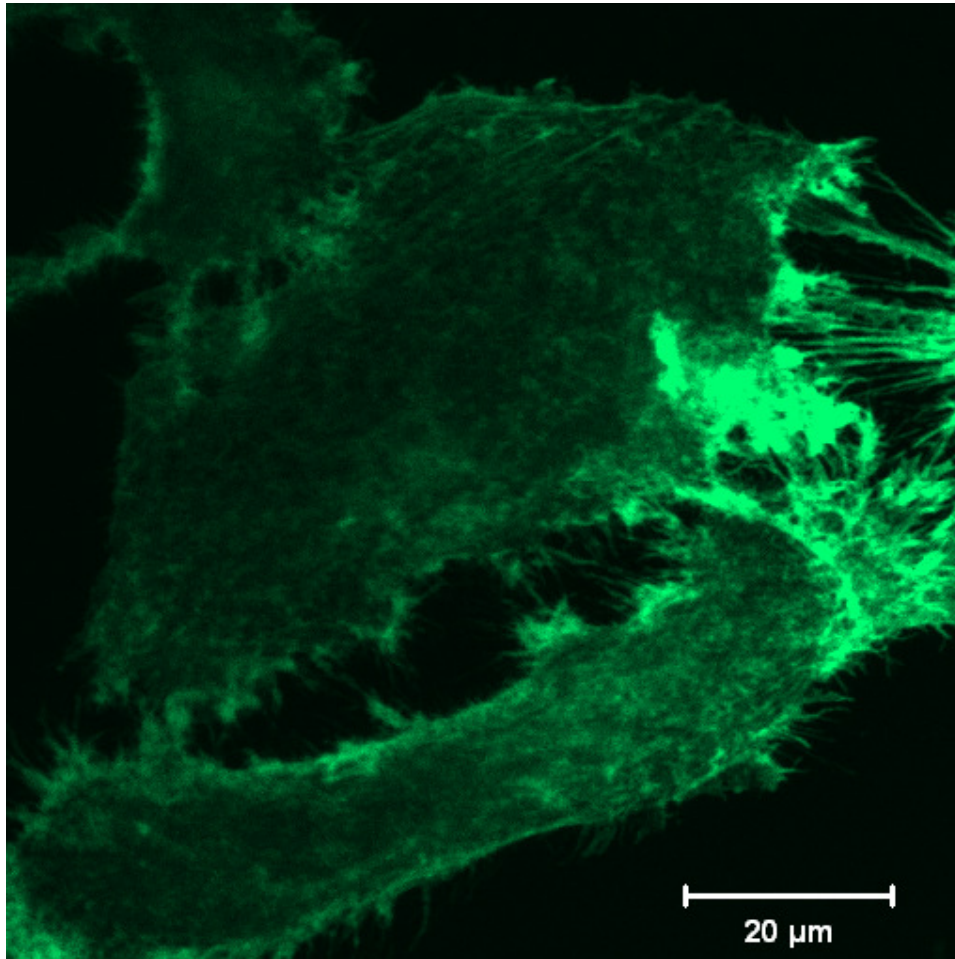


Figure 3.5.1.1a: Confocal image of SKUT cells after being allowed to proliferate on the TCP control for 5 days. Cells were stained with the α -actin fibre fluorescent stain, phalloidin. Micrograph was viewed at a 4000x magnification.

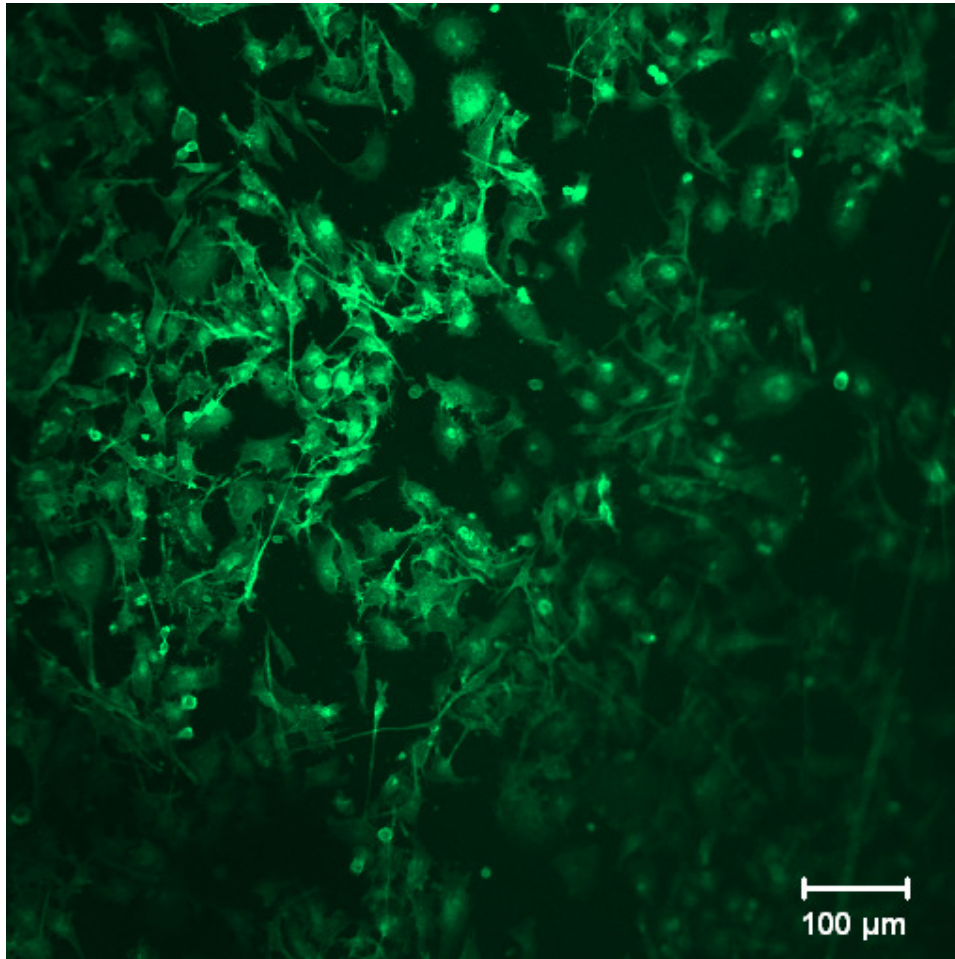


Figure 3.5.1.1b: Confocal image of SKUT cells after being allowed to proliferate on the PCL disk for 5 days. The cells were stained with phalloidin which is specific for the α -actin fibres of the cytoskeleton. Micrograph was taken at 200x magnification.

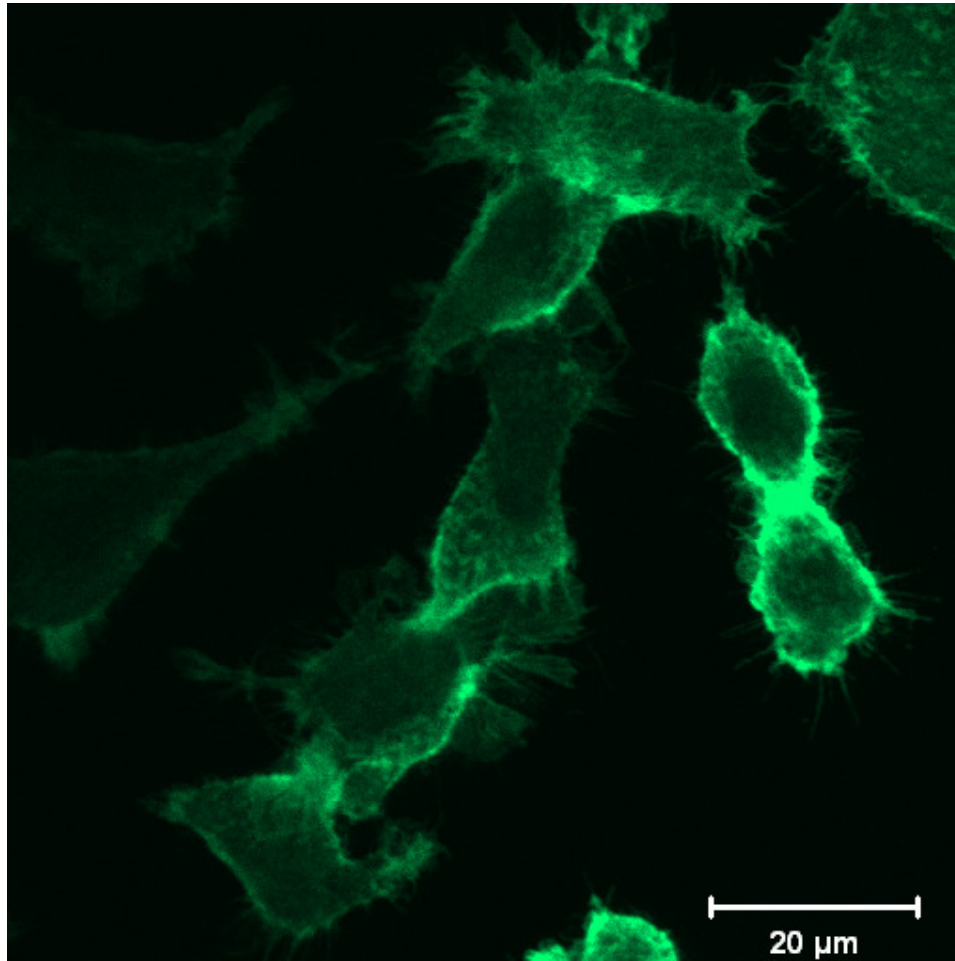


Figure 3.5.1.2a: Confocal image of CRL-1701 after being allowed to proliferate on the TCP control for 5 days. The cells were stained with the cytoskeleton fluorescent marker phalloidin, which is specific for SMC α -actin. The micrograph was taken at 4000x magnification.

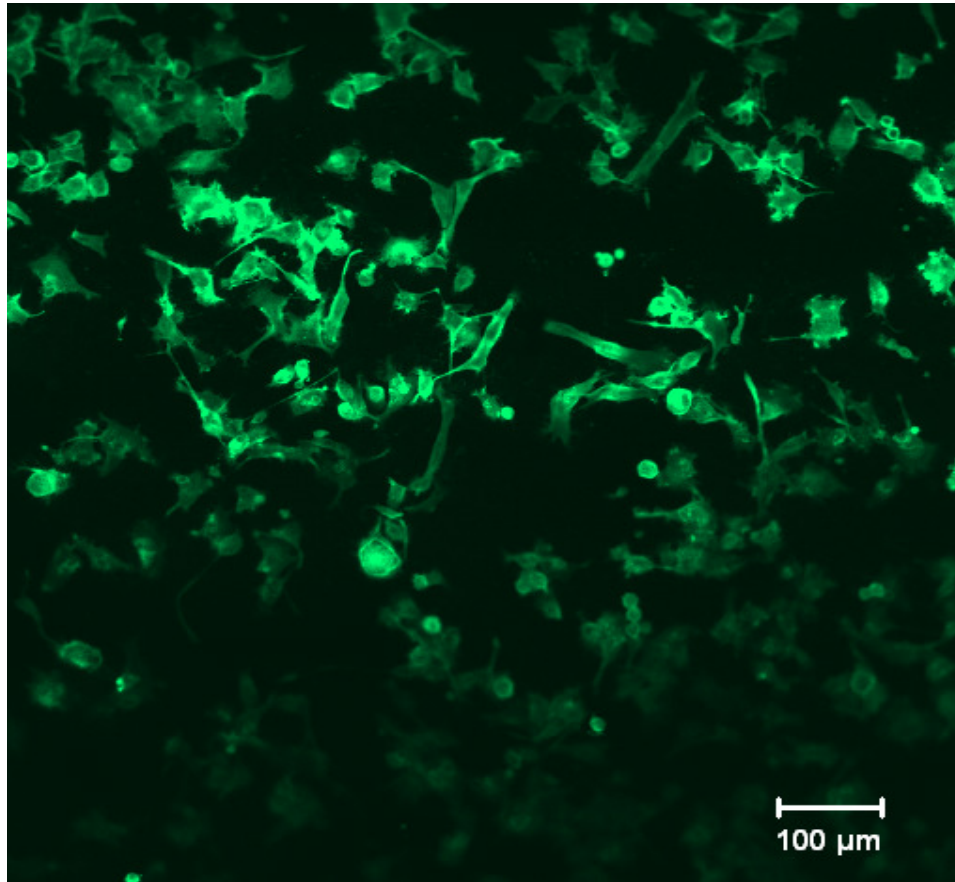


Figure 3.5.1.2b: Confocal image of CRL-1701 after being allowed to proliferate on the PCL disk for 5 days. Cells were stained with the α -actin fibre fluorescent stain, phalloidin. The micrograph taken at a 200x magnification.

3.5.2 3D video images of the SKUT and CRL-1701 cells grown for 5 days on the PCL solid microspheres and the PCL ported microspheres

The 5 day time period was the focus of this part of the study as it was wished to confirm as to whether the cells did indeed migrate inside the ported microspheres. Once again the cells were stained with the fluorescent α -actin stain, phalloidin.

The videos illustrating the SKUT (fig. 3.5.2.1a) and CRL-1701 (fig. 3.5.2.2a) cells grown for 5 days on the PCL solid microspheres confirmed that the cells did indeed attach across the entire diameter of the solid spheres. The cells were well spread out with many cells undergoing mitosis. Both cell lines illustrated long, thin cytoplasmic arms on both

sides of the cell body, illustrating a radiate, and spindle formation. Once culture time had reached the 5 day period, the cells were seen to become triangular and polygonal in shape. This was accompanied by a thickening of the cytoplasmic arms.

Confocal microscopy allowed the viewing of the cells attached inside the PCL ported microspheres. Once one orientates oneself during the rotation of the ported microspheres, it becomes evident that both the SKUT cells (fig. 3.5.2.1b) and the CRL-1701 cells (fig.3.5.2.2b) are concentrated within the ports. Long cytoplasmic arms were observed which assisted in cellular migration and invasion into the ported microspheres. Many more cells were observed on the inside surface area than the outside surface area. This confirmed that the SMCs preferred and benefited from the sheltered environment afforded by the ports.

Figure 3.5.2.1a 3D confocal image video of the SKUT cells grown for 5 days on PCL solid microspheres: Cells were stained with phalloidin and viewed under a confocal microscope with a xyz-stack which was compiled into a 3D animation using Zeiss LSM Image Browser software. Video image taken at a 200x magnification.

Figure 3.5.2.1b 3D confocal image video of the SKUT cells grown for 5 days on PCL ported microspheres: The cell cytoskeleton was stained with phalloidin and viewed under a confocal microscope with a xyz-stack which was compiled into a 3D animation using Zeiss LSM Image Browser software. Video image taken at a 200x magnification.

Figure 3.5.2.2a 3D confocal image video of the CRL-1701 cells grown for 5 days on PCL solid microspheres: Cells α -actin cytoskeleton was stained with phalloidin and viewed under a confocal microscope with a xyz-stack which was compiled into a 3D animation using Zeiss LSM Image Browser software. Video image taken at a 200x magnification.

Figure 3.5.2.2b 3D confocal image video of the CRL-1701 cells grown for 5 days on PCL ported microspheres: Cells were stained with phalloidin and viewed under a confocal microscope with a xyz-stack which was compiled into a 3D animation using Zeiss LSM Image Browser software. Video image taken at a 200x magnification.

Chapter 4

Discussion

This study was performed to evaluate the characteristics of PCL (disks, solid microspheres, and ported microspheres) and its biocompatibility for smooth muscle cells.

Metabolic activity of both the SKUT and CRL-1701 cell lines remained above 70% of the control when cultured in the 24 hr medium extracts through to 1 month old extracts. This illustrated that initial degradation products and any chemical leaching from the PCL remained non-toxic towards the cells' viability and therefore proved not to be cytotoxic. However, when both the SKUT and CRL-1701 cell lines were cultured in the 1 year PCL disk and PCL microsphere extracts. They displayed between 40% and 50% in metabolic activity, which was significantly lower than the metabolic activity of the control.

The MTT assay showed that the cell metabolism fluctuations corresponded with the pH fluctuations of the medium extracts over time. The CRL-1701 cell line appeared to be more resistant to a decrease in pH. This is illustrated by the even higher metabolic activity on both the disk and microsphere extracts compared to the control. This could be due to it being a deep ductus deferens leiomyosarcoma. Whereas, SKUT cell line is a mixed uterine leiomyosarcoma of smooth muscle and epithelial cells, thereby a surface orientated tumour, which could explain its sensitivity to a pH decrease when compared to the CRL-1701 cell line. The decline in metabolic activity may be attributed to the drop in pH caused by the degradation products of PCL. PCL degradation products are carboxylic acids (predominantly ϵ -hydroxycaproic acid or similar compounds) and alcohol groups which form when ester cleavage occurs [95]. The exact combination of degradation products will depend on the state of the sample in the PCL degradation pathway. Studies using PLLA have indicated that the metabolic activity of SMC's grown on the polymer decreased after a 1 month period. This was attributed to the release of lactic acid from the polymer as it degraded, along with the production of cellular lactic acid which occurs as cells proliferate [95]. Deep tissue sarcomas, such as the CRL-1071 cell line are more resistant to a low pH, illustrating that the hypoxic environment favors the survival of cells

which have a diminished potential to undergo apoptosis. This can be attributed to the relative lack of wild type (wt) *p53* [96].

The success of tissue engineering relies mostly on the adhesion of the relevant cells onto the scaffold. Synthetic biodegradable polymers lack the presence of proteins from the ECM and therefore of cell adhesion signals. The polymer scaffold chemistry can be modified with the addition of serum proteins. Since the PCL surface is hydrophobic, it is not suited for cell attachment [98]. The simple method of immersing the PCL polymer in sodium hydroxide (NaOH) improves the hydrophilicity of the surface [98]. This markedly improved adhesion and the proliferation rate of both primary vascular endothelial and smooth muscle cells isolated from a porcine inferior cava vein. This study was qualified by immunofluorescence and confocal microscopy of endothelial nitric oxide synthase and α -smooth muscle actin and quantified with cell counts and metabolic MTT assay [98]. Instead of radical chemical or surface modification treatments, pre-conditioning of the PCL surface with complete cell culture media has been previously illustrated to improve cell attachment density [100].

Pre-conditioning the polymers with complete cell culture medium (containing 10% FCS) has been demonstrated to coat the surface with molecules from the ECM, particularly collagen, fibronectin and laminin [99]. This pre-conditioning has been illustrated to result in a more hydrophilic surface for optimal cell adhesion [97]. The FCS specifically prepares the surface from between 5-24 hr and allows for covalent attachment of the cells [98]. The first interaction between cells and the polymer surface is cell adhesion; the surface properties of the scaffold become a key factor in governing the adhesion and subsequent growth on these polymers. Therefore pre-conditioned polymers in complete media should improve cell adhesion, thereby assisting in cell seeding efficiency, and spreading [102]. The ECM proteins in the FCS, such as fibrinogen and albumin which normally assists in cell attachment [101], could contribute to the increased attachment of cells to polymers pre-conditioned with FCS. The presence of such a protein layer also plays an important role in the subsequent growth and differentiation of cells [5]. Previous studies have illustrated polymer, polyethylene (PE), treatment with cell culture medium containing 10% FCS results in adsorption of these serum proteins on the PE surface [99].

Both the SKUT and the CRL-1701 cell lines attached with minimal density when the PCL disk was conditioned in the PBS. Density of both the cell lines, SKUT cells and the CRL-1701 cells increased when allowed to attach on the partial medium only conditioned disks. This could be due to the sugars in the partial medium increasing the hydrophilicity of the surface [100]. An increase in density of cell attachment was illustrated when cells were allowed to attach on the complete medium-treated disks, indicating that the protein present in the FCS [101] assists in initial cell density attachment. SEM micrographs illustrated that SKUT cells attach with a packed density on the PCL disk surface which had been treated with complete medium. A similar trend was observed with the CRL-1701 cell line.

Preferably the polymers should allow for cell attachment and proliferation followed by a quiescent, differentiated functional state. Studies have found where VSMC which colonize on various implanted biomaterials proliferate excessively leading to restenosis of the vascular graft [5]. Inhibition of cellular proliferation can be observed within the cell cycle as it results from inhibition of the initiation of DNA synthesis, consistent with a G₁-S transition block. Thus, cells are assumed to accumulate within the G₁ phase. This can be considered encouraging, because proliferation of the SMCs exceeds demand of regeneration it may lead to stenosis or destruction of the ported environment.

Dynamics of cell proliferation was analyzed with flow cytometry and morphological changes were analyzed under electron microscopy. When compared to the TCP control, the SKUT cells cultured on the PCL ported microspheres demonstrated significantly higher numbers of G_{0/1} phase cells and significantly lower S and G_{2/M} phase cycling cells when grown for 24 and 72 hr periods. However, after 5 days in culture the distribution of cycling cells throughout the cell cycle was comparable to that of the control cells (though with a significantly reduced G_{2/M} phase). Up to 72 hrs, this could indicate a G_{0/1} block resulting in an accumulation of cells in G₁ phase with a subsequent decrease of cells progressing through to S and G_{2/M} phases [100, 101,100]. If no DNA damage has caused this block cells should mostly be quiescent as no apoptotic cells were observed (results not shown).

After 5 days in culture, the ratio of cells on the ported microspheres was observed to recover to a G_{0/1} and S phase range comparable to the cells grown on the TCP control. This was accompanied with a recovering G_{2/M} range, illustrative of the cells regaining their proliferative phenotype.

The CRL-1701 cells proliferating on the PCL ported microspheres were consistently seen to have high percentage of G_{0/1} cycling cell numbers when compared to the control. This was accompanied by significantly low percentage of cells in S and G_{2/M} phase which were not observed to recover after the 5 day culture period. An unusually low percentage of cells in S phase were observed after the 5 day period. The declines of percentage of cells in the S phase after 5 days may be suggestive once again of a G_{0/1} block.

Available evidence, mostly derived from human tumors, has revealed frequent alterations in genes involved in the control of the G₁ restriction point and the progression from G₁ to S phase [101]. Another factor, cyclic stress, has been shown to arrest cells within the G₁ phase. This was not attributed to either apoptosis or necrosis, but rather an upregulation of p21, which in turn inhibits the phosphorylation of retinoblastoma (Rb) protein. This lack of hyperphosphorylation of Rb prevents the cell from progressing into the S phase [102]. Thus, cyclic stretch inhibits SMC proliferation due to a stretch-induced inhibition of Rb phosphorylation.

SMCs cultured *in vitro* lose their specific cell alignment which is vitally important for contractile functions [109]. Emulating the *in vivo* situation with dynamic culturing wherein cells were seeded onto very elastic three-dimensional scaffolds and subjected to a pulsatile perfusion system, Jeong *et al.* (2005) found that VSMCs aligned as they would *in vivo* [103]. Those cells cultured on the same polymer but under static conditions illustrated no particular alignment patterns [104].

SEM analysis at different time periods demonstrated that the cells were in both a state of attachment and migration along with mitotic division when grown on any of the three PCL surfaces investigated. When CRL-1701 and SKUT cells were grown on PCL disks (2D), PCL solid microspheres (3D-1) and PCL ported microspheres (3D-2) the SEM analysis indicated that both cell lines adhered and proliferated on the various PCL surfaces. Morphologically flattened adherent characteristic cells (as opposed to rounded cells) are indicative of cells attaching well to a particular surface [91]. The SKUT cells

were observed after 24 hr. These cells had adhered well and were mainly spread out and spindle-shaped (with a few cells in mitosis) when seeded on the PCL disks, solid microspheres and ported microspheres. Upon observation of these cells after 72 hr and 5 days were seen to proliferate and become more densely populated on the three surfaces. By day 5, however, cells grown on the solid PCL microspheres were flattened and seen to closely follow the contours of the spheres, suggesting high focal adhesion. These adhesions are also indicative that the cells proliferate and adhere strongly to the surface. The cells encompassed most of the surface of the spheres. We did not test for longer periods to see if they would cover the entire surface. After 72 hr and 5 days, the cells were seen to populate around the mouth of the ports on the ported microspheres with cytoplasmic arms extending into the inner surface of the spheres. The images seem to suggest that large populations of cells occupied the inner surface of the ported microspheres than the outer surface. In the study by Williamson *et al.* (2006) it was concluded that once a cell has attached and effective focal contacts are made with the substrate; this enabled forces to be transferred to the cell cytoskeleton and thereby, cell flattening [4].

The CRL-1701 cells were mainly observed to be in a cell proliferation state, *i.e.* mitosis, characterized by the rounded shape of the cells. This predominance of mitotic cells was noted after 24 hr and after 5 days of seeding of cells on the PCL disks. However, those cells on the solid microspheres and those on the ported microspheres were well flattened with many cytoplasmic extensions, indicating that the cells were migrating and spreading across the surface of both the solid and ported microspheres. Once again, the cells extended their cytoplasmic bodies into the ported microspheres' inner surface. An intact cytoskeleton as well as filopodia branching out from the cell body is considered indicative of cells that have migrated, spread, and proliferated well on the polymer surface [92].

It is primarily due to the cytoskeleton that cells are able to transport vesicles, change their shape, migrate, and contract [105]. Cell proliferation in osteoblastic and fibroblastic cells has been demonstrated to be at its' fastest not at the maximum, but only at the intermediate degree of cell adhesion [110]. Thereby, if cell spreading, adhesion strength along with the initial number adhering cells are too high, the cells usually avoid the proliferation phase and directly enter the mode of differentiation [106].

Positive immunostaining with alpha smooth muscle actin indicated the preservation of the specific cell phenotype. SMCs cultured *in vitro* dedifferentiate from a contractile phenotype to a synthetic phenotype. This results in the loss of SM-actin. Jeong *et.al* found that when VSMCs when cultured under mechanically active conditions, they retained a differentiated contractile phenotype, while VMSCs cultured statically lost their differentiated phenotype. This was quantified with the α -actin antibody *via* Western Blotting [104]. After the cells proliferated for 5 days, both the SKUT and CRL-1701 cell lines grown on the TCP control, PCL disk, and PCL solid microspheres, and PCL ported microspheres consistently stained positively for α -actin, illustrating that their contractile phenotype was maintained.

Confocal video imaging viewed on day 5 illustrated that the SKUT and CRL-1701 cells encompassed the entire perimeter of the solid microspheres. Confocal imaging confirmed the SKUT and CRL-1701 cell lines were able to infiltrate into the ported microspheres and proliferate inside the pores. The ported microspheres provided for a cell “haven” in which the cells could proliferate and form strong adhesions without the shear stress which was experienced by the cells on the surface of the solid and ported microspheres. This may explain why a higher population of cells was seen inside the ported microsphere surface when compared to the outside perimeter.

3D microspheres have several advantages over thicker cell/scaffold constructs: 1) there are fewer restrictions on diffusional flow 2) they can be injected into the patient endoscopically and 3) the operation is faster, more comfortable to the patient and is more affordable. The bioresorbability of the scaffold results in resorption within a year along with the transplanted cells having proliferated and fully intergrated the scaffold to become functional tissue [72].

Danielsson *et al.* (2006) found the pore size of DegraPol[®] being 100 to 300 μ m, allowed bladder SMCs to adhere and penetrate the scaffold [79] while Kim *et al.* (1999) found the pore sizes from 50 to 200 μ m of a polyglycolic acid and a type 1 collagen scaffold allowed infiltration of SMCs encouraged development of smooth muscle-like tissue [107]. Both studies indicated that the cells attained normal morphology and expressed α -smooth muscle actin protein. However, after 6 days in culture, the proliferation had

stopped [79]. This could be attributed to the cells undergoing contact inhibition once the cultures were confluent.

In order for engineered SM tissues to exhibit the functions of the native SM tissues, it becomes necessary to emulate the microenvironments experienced by SMCs *in vivo* during the *in vitro* tissue engineering process [104]. Dynamic culturing conditions would be optimal for SMC growth on polymer constructs, as SMC are extremely sensitive to environmental conditions [83]. The dynamic culture method increases the availability of nutrients and oxygen, allowing the cells to grow as in the *in vivo* environment [83]. It has come into view that bladder SMCs assume a dedifferentiated or proliferative phenotype when in culture. It remains unknown whether a cell can re-differentiate when placed back into the *in vivo* environment [108]. Therefore, if tissue engineering techniques with cultured SMC are to be used for human and clinical applications, one would need to know the characteristics of the cells that are to be placed back in the host.

The PCL microspheres (100 - 200 μ m) are small enough to be injected laproscopically, which makes the implantation procedure minimally invasive and represents a novel therapeutic approach to gastroesophageal reflux disease. This may also have therapeutic potential for other gastrointestinal motility disorders [109].

Chapter 5

Conclusion

In conclusion, the PCL polymers proved suitable as an environment for both smooth muscle cell lines: SKUT-1 and CRL-1701 in terms of attachment and proliferation; thus illustrating both cytocompatibility and biocompatibility of the PCL polymer with these cells. Differences of 2D and 3D polymer-cell interactions with regard to cell viability, attachment and growth indicate that the 3D polymers are favourable above the 2D polymers. Both cell lines showed spindle-shaped morphologies, closely following the contours of the microspheres, indicative of high focal adhesion after 5 days in culture. However, the porous microspheres allowed both cell lines to migrate inside the microspheres, indicating that they may benefit from the sheltered environment. This is a further indication that the cells favour a 3D environment over the 2D polymer scaffold.

Although the nature of the interactions of the cells and the polymer with respect to cell/tissue viability and growth responses when the polymer undergoes complete degradation (1 year) remains unclear, this *in vitro* study suggests that hollow microspheres allow for further cell expansion with a sheltered environment to protect cells from shear stress experienced *in vivo*.

References

1. Tissue Engineering. (2008). Retrieved May 5, 2008, from <http://www.bme.utexas.edu-faculty-schmidt-Research-TissEng.html>.
2. Vacanti CA. History of tissue engineering and a glimpse into its future. *Tissue Eng* 2006; 12(5):1137-1142.
3. Patel ZS, Mikos AG. Angiogenesis with biomaterial-based drug- and cell-delivery systems. *J Biomat Sci-Polym E* 2004; 15(6):701-726.
4. Williamson MR, Woolard KJ, Griffiths HR, Coombes AGA. Gravity spun polycaprolactone fibres for application in vascular tissue engineering: Proliferation and function of human vascular endothelial cells. *Tissue Eng* 2006; 12(1):45-51.
5. Walachová K, Vorík V, Baáková L, Hnatowicz V. Colonization of ion-modified polyethylene with vascular smooth muscle cells in vitro. *Biomaterials* 2002; 23 (14):2989-2996.
6. Garner JP. Tissue engineering in surgery. *Surg J R Coll Surg E* 2004:70-78.
7. Kaigler D, Wang Z, Horger K, Mooney DJ, Krebsbach PH. VEGF scaffolds enhance angiogenesis and bone regeneration in irradiated osseous defects. *J Bone Miner Res* 2006; 21:735-744.
8. Kazarian SG, Chan KL, Maquet V, Boccaccini AR. Characterisation of bioactive and resorbable polylactide/Bioglass composites by FTIR spectroscopic imaging. *Biomaterials* 2004; 25(18):3931-3938.
9. Lu HH, Kofron MD, El-Amin SF, Attawia MA, Laurencin CT. In vitro bone formation using muscle derived cells: a new paradigm for bone tissue engineering using polymer-bone morphogenetic protein matrices. *Biochem Bioph Res Co* 2003; 305(4):882-889.
10. Sachlos E, Czernuszka JT. Making tissue engineering scaffolds work. Review on the application of solid freeform fabrication technology to the production of tissue engineering scaffolds. *Eur Cells Mater* 2003; 5:29-40.
11. Banu N, Tsuchiya T, Sawada R. Effects of a biodegradable polymer synthesized with inorganic tin on the chondrogenesis of human articular chondrocytes. *J Biomed Mater Res A* 2006; 77A(1):84-89.
12. Trojani C, Weiss P, Michiels J-F, Vinatier C, Guicheux J, Daculsi G, Gaudray P, Carle GF, Rochet N. Three-dimensional culture of human osteogenic cells in an

-
- injectable hydroxypropylmethylcellulose hydrogel. *Biomaterials* 2005; 26:5509-5517.
13. Gogolewski S. Bioresorbable polymers in trauma and bone surgery. *Injury* 2000; 31(4):28-32.
 14. Sittinger M, Reitzel D, Dauner M, Hierlemann H, Hammer C, Kastenbauer E, Planck H, Burmester GR, Bujia J. Resorbable polyesters in cartilage engineering: affinity and biocompatibility of polymer fiber structures to chondrocytes. *J Biomed Mater Res* 1996; 33(2):57-63.
 15. Cao W, Wang A, Jing D, Gong Y, Zhao N, Zhang X. Novel biodegradable films and scaffolds of chitosan blended with poly (3-hydroxybutyrate). *J Biomat Sci-Polym E* 2005; 16(11):1379-1394.
 16. Zhu Y, Chian KS, Chan-Park MB, Mhaisalkar PS, Ratner BD. Protein bonding on biodegradable poly (L-lactide-co-caprolactone) membrane for esophageal tissue engineering. *Biomaterials* 2006; 27(1):68-78.
 17. Lin WJ, Flanagan DR, Linhardt RJ. A novel fabrication of poly (ϵ -caprolactone) microspheres from blend of poly (ϵ -caprolactone) and poly (ethylene glycol)s. *Polymer* 1999;40:1731-1735.
 18. Woodward SC, Brewer PS, Moatamed F. The intracellular degradation of poly(ϵ -caprolactone). *J Biomed Mater Res* 1985; 44:437-444.
 19. Pena J, Corrales T, Izquierdo-Barba, Serrano MC, Portoles T, Pagani R, Vallet-Regi M. Long term degradation of poly (ϵ -caprolactone) films in biologically related fluids. 19th European Conference on Biomaterials 2005 Sep 11-15, Sorrento – Italy.
 20. Lin CY, Schek RM, Mistry AS, Shi X, Mikos AG, Krebsbach PH, Hollister SJ. Functional bone engineering using ex vivo gene therapy and topology-optimized, biodegradable polymer composite scaffolds. *Tissue Eng* 2005;11(9-10):1589-1598.
 21. Jackson JK, Springate CM, Hunter WL, Burt HM. Neutrophil activation by plasma opsonized polymeric microspheres: inhibitory effect of Pluronic F127. *Biomaterials* 2000; 21:1483.
 22. Hutmacher DW, Ng KW, Kaps C, Sittinger M, Klaring S. Elastic cartilage engineering using novel scaffold architectures in combination with a biometric cell carrier. *Biomaterials* 2003; 24:4445-4458.

-
23. Saxena AK, Willital GH, Vacanti JP. Vascularized three-dimensional skeletal muscle tissue-engineering. *Biomed Mater Eng* 2001; 11 (4):275-281.
 24. Curran SJ, Chen R, Curran JM, Hunt JA. Expansion of human chondrocytes in an intermittent stirred flow bioreactor, using modified biodegradable microspheres. *Tissue Eng* 2005; 11 (9-10):1312-1322.
 25. Oh SH, Lee JY, Ghil SH, Lee SS, Yuk SH, Lee JH. PCL microparticle-dispersed PLGA solution as a potential injectable urethral bulking agent. *Biomaterials* 2006; 27:1936-1944.
 26. Vaux DL. Toward an understanding of the molecular mechanisms of physiological cell death. *Proc Natl Acad Sci USA* 1993; 90:786-789.
 27. Wyllie AH. Apoptosis and the regulation of cell numbers in normal and neoplastic tissues: An overview. *Cancer Metast Rev* 1992; 11:95-103.
 28. Halicka HD, Seiter K, Feldman RJ, Traganos F, Mittelman A, Ahmed T, Darzynkiewicz Z. Cell cycle specificity of apoptosis during treatment of leukemias. *Apoptosis* 1997; 2(1):25-39.
 29. Curtis ASG. Cell reactions with biomaterials: The microscopies. *Eur Cells Mater* 2001; 1:59-65.
 30. Tan PS, Teoh SH. Effect of stiffness of polycaprolactone (PCL) membrane on cell proliferation. *Mat Sci Eng* 2007; 27(2):304-308.
 31. Cutroneo KR. Gene therapy for tissue regeneration. *J Cell Bio* 2003; 88(2):418-25.
 32. Bond M, Sala-Newby GB, Newby AC. Focal adhesion kinase (FAK)-dependent regulation of S-phase Kinase-associated Protein-2 (Skp-2) stability. *J Biol Chem* 2004; 279:37304-37310.
 33. Baáková L, Filova E, Rypacek F, Svorcik V, Stary V. Cell adhesion on artificial materials for tissue engineering. *Physiol Res* 2004; 53(Suppl. 1):S35-S45.
 34. Giancotti FG, Ruoslahti E. Integrin signaling. *Science* 1999; 285: 1028-1032.
 35. Schwartz MA, Assoian RK. Integrin and cell proliferation: regulation of cyclin-dependant kinases. *J Cell Sci* 2001; 114: 2553-2560.
 36. Blain SW, Scher HI, Cordon-Cardo C, Koff A. p27 as a target for cancer therapeutics. *Cancer Cell* 2003; 3:111-115.

-
37. Baldassarre G, Belletti B, Nicoloso MS, Schiappacassi M, Vecchione A, Spessoto P, Morrione A, Canzonieri V, Colombatti A. p27^{kip1}-stathmin interaction influences sarcoma cell migration and invasion. *Cancer Cell* 2005; 7:51-63.
 38. Sun J, Marx SO, Chen HJ, Poon M, Marks AR, Rabbani LE. Role for p27 (Kip 1) in vascular smooth muscle cell migration. *Circulation* 2001; 103:2967-2972.
 39. Goldman J, Zhong L, Liu SQ. Degradation of α -actin filaments in venous smooth muscle cells in response to mechanical stretch. *Am J Physiol-Heart C* 2003; 284:H1839-H1847.
 40. Coriell Institute for Medical Research (1997-2008). Retrieved May 23, 2008, from <http://locus.umdj.edu/ccr/help/celltypedesc.html>
 41. Glaser R, Lu MM, Narula N, Epstein JA. Smooth muscle cells, but not myocytes, of host origin in transplanted human hearts. *Circulation* 2002; 106(1):17-19.
 42. Nagayama K, Nagano Y, Sato M, Matsumoto T. Effect of actin filament distribution on tensile properties of smooth muscle cells obtained from rat thoracic aortas. *J Biomech* 2006; 39(2):293-301.
 43. Rodriguez LV, Alfonso Z, Zhang R, Leung J, Wu B, Ignarro LJ. Clonogenic multipotent stem cells in human adipose tissue differentiate into functional smooth muscle cells. *PNAS* 2006; 103:12167-12172.
 44. McHugh KM. Molecular analysis of gastrointestinal smooth muscle development. *J Pediatr Gastr Nutr* 1996; 23:379-394.
 45. Somlyo AP, Somlyo AV. Signal transduction and regulation in smooth muscle. *Nature* 2002; 372:231-236.
 46. Brakenhielm CE, Pawliuk R, Wariaro D, Post MJ, Wahlberg E, Le Boulch P, Cao Y. Angiogenic synergism, vascular stability and improvement of hind-limb ischemia by a combination of PDGF-BB and FGF-2. *Nat Med* 2003; 9:604-613.
 47. Delafontaine P. Growth factors and vascular smooth muscle cell growth responses. *Eur Heart J* 1998; 19:G18-22.
 48. Rhoads DN, Eskin SG, McIntire LV. Fluid Flow Releases Fibroblast Growth Factor-2 From Human Aortic Smooth Muscle Cells. *Arterioscl Throm Vas* 2000; 20:416-421.
 49. Thyberg J. Differentiated properties and proliferation of arterial smooth muscle cells in culture. *Int Rev Cytol* 1996; 169: 183-265.

-
50. Hedin U, Thyberg J. Plasma fibronectin promotes modulation of arterial smooth-muscle cells from contractile to synthetic phenotype. *Differentiation* 1987; 33(3):239-46.
 51. Roy J, Kazi M, Hedin U, Thyberg J. Phenotypic modulation of arterial smooth muscle cells is associated with prolonged activation of ERK1/2. *Differentiation* 2001 Feb; 67(1-2): 50-8.
 52. Cipolla MJ, Gokina NI, Osol G. Pressure-induced actin polymerization in vascular smooth muscle as a mechanism underlying myogenic behaviour. *The FASEB Journal*. 2002; 16:72-76.
 53. Bitar KN. Aging and GI smooth muscle faecal incontinence: Is bioengineering an option. *Exp Gerontol* 2005; 40:643-649.
 54. Castell DO, Murray JA, Tutuian R, Orlando RC, Arnold R. Review article: the pathophysiology of gastro-oesophageal reflux disease - oesophageal manifestations. *Aliment Pharmacol Ther* 2004; 20(9):14-25.
 55. Richter J. Do we know the cause of reflux disease? *Eur J Gastroen Hepat* 1999; 11(1):S3-9.
 56. Van Herwaarden MA, Samsom M, Smout AJ. Excess gastroesophageal reflux in patients with hiatus hernia is caused by mechanisms other than transient LES relaxations. *Gastroenterology* 2000; 119(6):1439-46.
 57. Brittan M, Wright NA. The gastrointestinal stem cell. *Cell Proliferat* 2004; 37:35-53.
 58. Barretts Esophagus. (2006). Retrieved May 5, 2008, from <http://www.answers.com/topic/barrett-s-esophagus.html>
 59. Soll AH, Fass R. Gastroesophageal reflux disease: presentation and assessment of a common, challenging disorder. *Clin Cornerstone* 2003; 5(4):2-14.
 60. Van Rensburg CJ, Kulich KR, Carlsson J, Wiklund IK. What is the burden of illness in patients with reflux disease in South Africa? *SA Gastroenterol Rev* 2005: 16-21.
 61. Segal I. The gastro-esophageal reflux disease complex in sub-Saharan Africa. *Eur J Cancer Prev* 2001; 10:209-212.
 62. Berardi RR, Kroon L, McDermott JH and Newton GD. *Handbook of Nonprescription Drugs*. 15th edition. Acid-Peptic Products. American Pharmaceutical Association; Washington DC. pp 12-26. 2006.

-
63. Quigley EM. New developments in the pathophysiology of gastro-oesophageal reflux disease (GERD): implications for patient management. *Aliment Pharmacol Ther* 2003; 17(2):43-51.
 64. Tam WC, Holloway RH, Dent J, Rigda R, Schoeman MN. Impact of endoscopic suturing of the gastroesophageal junction on lower esophageal sphincter function and gastroesophageal reflux in patients with reflux disease. *Am J Gastroenterol* 2004; 99(2):95-202.
 65. Metz DC. Managing gastroesophageal reflux disease for the lifetime of the patient: evaluating the long-term options. *Am J Med* 2004; 117(5A):49S-55S.
 66. Clarke JO, Jagannath SB, Kalloo AN, Long VR, Beitler DM, Kantsevov SV. An endoscopically implantable device stimulates the lower esophageal sphincter on demand by remote control: a study using a canine model. *Endoscopy* 2007; 39(1):72-76.
 67. Von der Mark K, Gauss V, von der Mark H, Muller P. Relationship between cell shape and type of collagen synthesized as chondrocytes lose their cartilage phenotype in culture. *Nature* 1977; 267:531-532.
 68. Xiao YL, Riesle J, van Blitterswijk CA. Static and dynamic fibroblast seeding and cultivation in porous PEO/PBT scaffolds. *J Mater Sci-Mater M* 1999; 10:773-777.
 69. Kim B-S, Putnam AJ, Kulik TJ, Mooney DJ. Optimizing seeding and culture methods to engineer smooth muscle tissue on biodegradable polymer matrices. *Biotechnol Bioeng* 1998;57(1):46-54.
 70. Sahai E, Marshall CJ. Differing modes of tumour cell invasion have distinct requirements for Rho/ROCK signalling and extracellular proteolysis. *Nat Cell Biol* 2003; 5:711-719.
 71. Kang SW, Jeon O, Kim BS. Poly (lactic-co-glycolic acid) microspheres as an injectable scaffold for cartilage tissue engineering. *Tissue Eng* 2005; 11(3-4):438-447.
 72. Senuma Y, Franceschin S, Hilborn JG, Tissieres P, Bisson I, Frey P. Bioresorbable microspheres by spinning disk atomization as injectable cell carrier: from preparation to in vitro evaluation. *Biomaterials* 2000; 21:1135-1144.
 73. Hong Y, Gao C, Xie Y, Gong Y, Shen J. Collagen-coated polylactide microspheres as chondrocyte carriers. *Biomaterials* 2005; 26:6305-6313.

-
74. Jeong SI, Kim SH, Kim YH, Jung Y, Kwon JH, Kim B-S, Lee YM. Manufacture of elastic biodegradable PLCL scaffolds for mechano-active vascular tissue engineering. *J Biomat Sci-Polym E* 2004; 5(16):645-660.
 75. Plaat BEC, Hollema H, Molenaar WM, Torn Broers GH, Pijpe J, Mastik MF, Hoekstra HJ, van den Berg E, Scheper RJ, van der Graaf WTA. Soft tissue leiomyosarcomas and malignant gastrointestinal stromal tumors: Differences in clinical outcome and expression of multidrug resistance proteins. *J Clin Oncol* 2000; 18(18):3211-3220.
 76. Lai J-Y, Yoon CY, Yoo JJ, Wulf T, Atala A. Phenotypic and functional characterization of in vivo tissue engineered smooth muscle from normal and pathological bladders. *J Urology* 2002; 168(4) Suppl. 1:1853-1858.
 77. Sigma Aldrich. Coated plates – Cell culture. (2006). Retrieved May 19, 2006, from <http://www.sigma-aldrich.com/ttechmfb>
 78. Protocol online. (n.d). Retrieved May 18, 2007, from <http://www.protocol-online.org/cgi-bin/prot.html>
 79. Danielsson C, Ruault S, Simonet M, Neuenschwande P, Frey P. Polyesterurethane foam scaffold for smooth muscle cell tissue engineering. *Biomaterials* 2006; 27(8):1410-1415.
 80. Van de Loosdrecht AA, Beelen RH, Ossenkoppele GJ, Broekhoven MG, Langenhuijsen MM. A tetrazolium-based colorimetric MTT assay to quantitate human monocyte mediated cytotoxicity against leukaemia cells from cell lines and patients with acute myeloid leukaemia. *J Immunol Methods* 1994; 174:311-320.
 81. Ruffa MJ, Ferraro G, Wagner ML, Calcagno ML, Campos RH, Cavallaro L. Cytotoxic effect of Argentine medicinal plant extracts on human hepatocellular carcinoma cell line. *J Ethnopharmacol* 2002; 79:335-339.
 82. Sharifah Sakinah SA, Tri Handayani S, Azimahtol Hawariah LP. Zerumbone induced apoptosis in liver cancer cells via modulation of Bax/Bcl-2 ratio. *Cancer Cell* 2007, 7:4.
 83. Cohen JJ. Apoptosis. *Immunol Today* 1993; 14:126-130.
 84. Compton MM. A biochemical hallmark of apoptosis: Internucleosomal degradation of the genome. *Cancer Metast Rev* 1992; 11:105-119.

-
85. Kerr JFR, Wyllie AH, Curie AR. Apoptosis: a basic biological phenomenon with wide-ranging implications in tissue kinetics. *Brit J Cancer* 1972; 26:239-257.
 86. Mazzini G, Ferrari C, Erba E. Dual excitation multi- fluorescence flow cytometry for detailed analyses of viability and apoptotic cell transition. *Eur J Histochem* 2003; 47(4):289-298.
 87. Hayes TL, Pease RF. The scanning electron microscope: principles and applications in biology and medicine. *Adv Biol Med Phys* 1968; 12:85-137.
 88. The John Curtin School for Medical Research. JCSMR Flow Cytometry “An Introduction.” Internet: <http://jcsmr.anu.edu.au/facslab/intro.html>. [Cited: 23 May 2006].
 89. Salzman GC, Singham SB, Johnston RG, Bohren CF: Light scattering and cytometry. In: *Flow Cytometry and Sorting*. Melamed MR, Lindmo T, Mendelsohn ML (eds): Wiley- Liss, New York, pp 81-107, 1990.
 90. Molecular Probes®. Invitrogen detection technologies. Click-iT™ EdU flow cytometry kit product insert. Revised 10 Sept 2007.
 91. Hunter A, Archer CW, Walker PS, Blunn GW. Attachment and proliferation of osteoblasts and fibroblasts on biomaterials for orthopaedic use. *Biomaterials* 1995; 16:287-295.
 92. Baxter LC, Frauchiger V, Textor M, ap Gwynn I, Richards RG. Fibroblast and osteoblast adhesion and morphology on calcium phosphate surfaces. *Eur Cell Mater* 2002; 4:1-17.
 93. Pawley JB (editor) (2006). *Handbook of Biological Confocal Microscopy*, 3rd ed., Berlin: Springer. Pp 22-68, 2006.
 94. Kropp BP, Zhang Y, Tomasek JJ, Cowan R, Furness III PD, Vaughan MB, Parizi M, Cheng EY. Characterization of cultured smooth muscle cells: assessment of in vitro contractility. *J. Urology* 1999; 162(5):1779-17784.
 95. McGlohorn JB, Holder WD, Grimes LW, Thomas CB, Burg KJL. Evaluation of smooth muscle response using two types of porous polylactide scaffolds with differing pore topography. *Tissue Eng* 2004; 10(3/4):505-514.
 96. Graeber TG, Osmanian C, Jacks T, Houseman DE, Koch CJ, Lower SW, Giaccia AJ. Hypoxia-mediated selection of cells with diminished apoptotic potential in solid tumors. *Nature (Lond.)* 1996; 379:88-91.

-
97. Huang ZM, Zhang YZ, Kotaki M, Ramakrishna S. A review on polymer nanofibres by electrospinning and their applications in nanocomposites. *Compos Sci Technol* 2003; 63:2223-2253.
 98. Raja RH, Herzig M, Grissom M, Weigel PH. Preparation and use of synthetic cell culture surfaces. *J Biol Chem* 1986; 261 (18); 8505-8513.
 99. Baáková L, Walachová K, vorík V, Hnatowicz V. Adhesion and proliferation of rat vascular smooth muscle cells on polyethylene implanted with O⁺ and C⁺ ions. *J Biomater Sci-Polym* 2001; 12: 817-834.
 100. Pollock R, Lang A, Ge T, Sun D, Tan M, Yu D. Wild-type *p53* and a *p53* temperature-sensitive mutant suppress human soft tissue carcinoma by enhancing cell cycle control. *Clin Cancer Res* 1998; 4:1985-1994.
 101. Ortega S, Malumbres M, Barbacid M. Cell Cycle and Cancer: The G₁ Restriction Point and the G₁ / S Transition. *Curr Genomics* 2002; 3(4):245-263.
 102. Chapman GB, Durante W, Hellums JD, Schafer AI. Physiological cyclic stretch causes cell cycle arrest in cultured vascular smooth muscle cells. *Am J Physiol-Heart C* 2000; 278:H748-H754.
 103. Jeong SI, Kwon JH, Lim JI, Cho S-W, Jung Y, Sung WJ, Kim SH, Kim YH, Lee YM, Kim B-S, Choi CY, Kim S-J. Mechano-active tissue engineering of vascular smooth muscle using pulsatile perfusion bioreactors and elastic PLCL scaffolds. *Biomaterials* 2005; 26(12):1405-1411.
 104. Jeong SI, Kwon JH, Lim JI, Cho S-W, Jung Y, Sung WJ, Kim SH, Kim YH, Lee YM, Kim B-S, Choi CY, Kim S-J. Mechano-active tissue engineering of vascular smooth muscle using pulsatile perfusion bioreactors and elastic PLCL scaffolds. *Biomaterials* 2005; 26 (12):1405-1411.
 105. Yu JT, Lopez Bernal A. The cytoskeleton of human myometrial cells. *J Reprod Fertil* 1998; 112(1):185-98.
 106. Baáková L, Pellicciari C, Bottone MG, Lisá L, Mare V. A sex-related difference in the hypertrophic Versus hyperplastic response of vascular smooth muscle cells to repeated passaging in culture. *Histol Histopathol* 2001; 16:675-684.
 107. Kim BS, Nikolovski J, Bonadio J, Smiley E, Mooney DJ. Engineered smooth muscle tissues: regulating cell phenotype with the scaffold. *Exp Cell Res* 1999; 15:318-328.

-
108. Kropp BP, Zhang Y, Tomasek JJ, Cowan R, Furness III PD, Vaughan MB, Parizi M, Cheng EY. Characterization of cultured smooth muscle cells: assessment of in vitro contractility. *J Urology* 1999; 162(5):1779-1784.
109. Clarke JO, Jagannath SB, Kalloo AN, Long VR, Beitler DM, Kantsevoy SV. An endoscopically implantable device stimulates the lower esophageal sphincter on demand by remote control: a study using a canine model. *Endoscopy* 2007; 39(1):72-76.